Cloning and Characterization of β-site APP cleaving enzyme (BACE)-Type I

By

Chung Wilson
B.Sc. (Hons.), HKUST

A Thesis Submitted in Partial Fulfillment of the Requirement for the Degree of Master of Philosophy in Biochemistry

July 2002
Department of Biochemistry
The Chinese University of Hong Kong

The Chinese University of Hong Kong holds the copyright of this thesis. Any person(s) intending to use a part or whole of the materials in the thesis in a proposed publication must seek copyright release from the Dean of the Graduate School

香港中文大學
圖書館系統
28 MAR 2003
UNIVERSITY
LIBRARY SYSTEM
THE CHINESE UNIVERSITY OF HONG KONG

Acknowledgements

I would like to express my sincere gratitude to my supervisors, Dr. David C. C. Wan for his kind guidance and advice in the preparation of this thesis.

I would like to thank Mr. Xiang Zhang and Mr. Dennis Ip for their technical assistance and useful discussion.

Abstract

Alzheimer's disease (AD) is a neurodengerative disease that causes progessive cognitive and behavior deterioration. This disease is characterized by two histopathological hallmarks: the presence of neurofibrillary tangles (NFTs) and senile plaques. Formation of senile plaques is by deposition of amyloid β protein (Aβ), which is proteolytic cleavage of the amyloid precursor protein (APP) by two unknown proteases: β- and γ-secretase. These proteases are prime therapeutic targets. In 1999, β-secretase was independently cloned by four different research groups, and was named as beta-site APP-cleaving enzyme (BACE), memapsin 2 and membrane-bound aspartyl protease (Asp2).

The present study was aimed at developing reliable screening assays for inhibitor of BACE. This involved the cloning of mouse and human BACE cDNAs with complete amino acid coding sequences, the soluble form of human BACE with deletion of transmembrane region and pre region which was designated as prohBACE, and the human BACE with deletion of transmembrane region as well as pre and pro region which was designed as nohBACE by polymerase chain reaction (PCR). These cDNAs were subcloned into appropriate expression vectors. The proteins of mouse and human BACE containing the full coding sequences were successfully expressed in Chinese hamster ovary (CHO) cells transiently and stable cell lines overexpressed with mouse and human BACE in CHO cells have been established. The soluble form

of BACE, the prohBACE and nohBACE were also successfully expressed in *E.coli.*, BL21(DE3)LysS cells. Bioactive recombinant BACE was purified by metal chelating chromatography.

For assaying BACE activity, two methods were developed. The high performance liquid chromatography (HPLC) and the fluorescence resonance energy transfer (FRET). For HPLC analysis, two different peptide substrates were synthesized in-house. One was derived from Swedish mutation of APP with cleavage site of β-secretase which was demonstrated a better substrate for β-secretase, the other was derived from sequence of the wild type APP with the cleavage site of β-secretase. The proteolytic cleavage of these substrates by membrane extracts of CHO cells overexpressed with BACE or by purified recombinant BACE was measured by analytical reverse-phase high performance liquid chromatography (RP-HPLC). The activity of recombinant enzyme was also measured by a novel fluorometric assay with custom-made fluorogenic substrates. The fluorometric method was demonstrated to be suitable for high throughput screening of BACE inhibitors.

Specific antibody against BACE was used as primary antibody in immunohistochemistry. Immunohistochemical characterization of this antibody demonstrated that specific immunoreactive staining was found in CHO cells stably over-expressed with mouse and human BACE but not with non-transfected CHO cells.

The BACE immunohistochemistry was found concentrated in the cytoplasm and in cell membrane but not in the nucleus.

摘要

老年痴呆症 (AD) 是一種進行性的認知和行爲衰退的神經退化疾病。根據組織病理學, 疾病有以下兩個特徵 : 神經元纖維纏結 (NFTs) 和老年斑。老年斑的形成是由於 β 澱粉樣蛋白 (Aβ) 的沉積, β-澱粉樣蛋白是由兩種尚不清楚的蛋白酶 (β- and γ-蛋白酶) 對於澱粉樣蛋白前體 (APP) 的剪切而形成。 這些蛋白酶是治療老年痴呆症的主要目標。 在 1999 年, β-蛋白酶由四個不同的研究小組分別克隆出來, 並取名 BACE、memapsin 2 和 Asp2。

本研究主要在發展一個可靠的分析篩選方法以找尋 (BACE) 的抑制劑。 以聚合酶鏈反應 (PCR) 完成編碼完整氨基酸序列的老鼠、 人類 BACE 互補脫氧核糖核酸 (cDNA)、 無轉膜結構域及前體部分的可溶性的人類 BACE cDNA 而命名爲 prohBACE 和無轉膜結構域、前體及原體的人類 BACE cDNA 而命名爲 nohBACE 的克隆。 這些 cDNAs 被插入適當的表達載體。 編碼完整氨基酸序列的老鼠、 人類 BACE 蛋白在中國倉鼠卵巢 (CHO) 細胞被成功瞬時以及篩選的穩定轉染 CHO 細胞株表達出來。 可溶性的 BACE, prohBACE 和 nohBACE 在大腸杆菌 BL21(DE3)LysS 成功表達。 有活性的重組 BACE 由金屬螯合色譜純化出來。

兩個分析方法用來分析 BACE 活性: 高壓液相色譜 (HPLC) 和螢光共振能量轉移 (FRET)。 以 HPLC 來分析, 兩個不同肽底物被製出: 一個底物是由有 β-剪切位置的 Swedish 突變的 APP 衍生出來, 對於 β-蛋白酶是一個較好的底

物, 而另一個底物是由有 β-剪切位置的原型的 APP 衍生出來。 這些底物被提取的有 BACE 表達的 CHO 細胞膜和純化的重組 BACE 的剪切是由 HPLC 測定。 重組酶的活性由新的螢光分析方法以螢光底物測定。 實驗証明螢光分析方法比較適合篩選 BACE 的抑制劑。

以高滴度的抗 BACE 抗體在免疫組織化學作爲一抗。 免疫組織化學測出抗體能在表達老鼠、人類 BACE 的 CHO 細胞表現出高滴定度的免疫反應顏色, 但卻不能在沒有轉染的 CHO 細胞內測出。 BACE 的陽性反應部位集中在細胞質和細胞膜而不是在細胞核。

Content

Acknowledgements.....i

Abstract (English).....ii

Abstract (Chinese).....v

Content.....vii

Abbreviations.....xii

List of Figures.....xv

Chapter 1 Introduction.....1

1.1 Alzheimer's disease.....1

1.1.1 History of Alzheimer's disease.....1

1.1.2 Definition of Alzheimer's disease.....2

1.1.3 Symptoms of Alzheimer's disease.....6

1.1.3.1 Memory deficit.....6

1.1.3.2 Difficulty in learning.....6

1.1.3.3 Language difficulties.....7

1.1.3.4 Decline in ability to perform routine tasks.....7

1.1.4 Prevalence of Alzheimer's disease.....8

1.2 Present treatment of Alzheimer's disease.....9

1.2.1 Acetylcholine and dementia.....9

1.2.2 Tacrine as first drug approved by US Food and Drug Administration..9

1.3 Proposed theory of Alzheimer's disease formation.....10

1.3.1 The amyloid cascade hypothesis.....10

1.3.1.1 The amyloid precursor protein.....10

1.3.1.2 The processing of amyloid precursor protein.....12

1.3.1.3 Neurotoxic effect of amyloid plaque.....15

1.3.1.4 Genetic factors.....15
1.3.1.4.1 The amyloid precursor protein.....15
1.3.1.4.2 Apolipoprotein E (ApoE).....16
1.3.1.4.3 Presenilin genes.....17
1.3.2 Tau and tangle hypothesis.....19
1.3.2.1 Tau protein.....19
1.3.2.2 Paired helical filaments (PHF).....20
1.3.2.3 Tau protein kinase.....20
1.3.2.3.1 Glycogen synthase kinase-3 (GSK-3).....21
1.3.2.3.2 Cyclin-dependent kinase 5 (CDK5).....21
1.3.2.4 Tangle leads to dementia.....22
1.4 Cross-talk between the two hypotheses.....24
1.5 β-secretase (BACE).....24
1.5.1 Discovery of β-secretase (BACE).....24
1.5.2 Detailed structure of BACE.....25
1.5.3 Comparsion of human and mouse BACE.....27
1.5.4 Comparsion of BACE-1 with BACE-2.....27
1.5.5 Properties of BACE-1.....28
1.5.6 Expression of BACE in *E.coli*.....29
1.5.7 Expression of BACE in mammalian cells.....30
1.6 Objectives of the present study.....32

Chapter 2 Materials and Methods.....34

2.1 Recombinant DNA techniques.....34
2.1.1 Amplification of genes by PCR techniques.....34
2.1.2 Agarose gel electrophoresis.....34

2.1.3 Extraction of DNA from agarose gel.....35
2.1.4 Digestion of various vectors and inserts.....36
2.1.5 Ligation of DNA fragments.....36
2.1.6 Preparation of *Escherichia coli* competent cells.....37
2.1.7 Bacterial transformation.....38
2.1.8 Minipreparation of plasmid DNA.....38
2.1.9 Large scale preparation of plasmid DNA.....39
2.1.10 Strain storage and revival.....40
2.1.11 Plasma DNA purification by High Pure plasmid isolation kit.....41
2.1.12 DNA sequencing.....42
2.1.13 Quantitation of DNA by spectrophotometric method.....43
2.2 Prokaryotic protein expression.....43
2.2.1 Selection of appropriate clones for recombinant protein expression using conventional method.....43
2.2.2 Selection of appropriate clones for recombinant protein expression using modified method.....44
2.2.3 Large –scale expression of recombinant human BACE protein using modified method.....45
2.2.4 Preparation of inclusion body from the bacterial expression culture..46
2.2.5 Refolding of human BACE.....47
2.2.6 Purification of recombinant human BACE by immobilized metal ion affinity chromatography (IMAC).....47
2.2.7 Protein concentration determination.....48
2.2.8 Sodium dodecyl sulfate polyacrylamide gel electrophoresis (SDS-PAGE).....48
2.2.9 Western blotting.....50
2.2.10 Plasmid stability test.....50
2.3 Mammalian cell expression.....51

2.3.1 Transient transfection.....51
2.3.2 Measuring transfection efficiency.....52
2.3.3 Stable transfection.....52
2.3.4 Preparation of membrane extracts from CHO cells.....53
2.4 HPLC analysis.....53
2.4.1 Preparation of samples.....53
2.4.2 Reverse phase HPLC.....54
2.5 Fluorometric assay.....54
2.6 Immunohistochemistry.....55
2.7 Reagents and buffers.....55
2.7.1 Medium for bacterial culture.....56
2.7.2 Reagents for preparation of plasmid DNA.....56
2.7.3 Buffers for agarose gel electrophoresis.....57
2.7.4 Buffers for SDS-PAGE.....58
2.7.5 Buffer for purification of protein.....60
2.7.6 Buffer for Western Blotting.....61
2.7.7 Culturing medium of CHO cells.....62
2.7.8 Solutions for estimating transfection efficiency.....63
2.7.9 Reagents for HPLC.....64
2.7.10 Reagents for fluorometric assays.....65
2.7.11 Reagents for Immunohistochemistry.....66

Chapter 3 Results.....67

3.1 Expression of BACE in *E.coli*.....67
3.1.1Cloning of truncated human and mouse BACE into pRSET.....67
3.1.2 Expression of BACE in BL21(DE3)LysS cells.....70
3.1.2.1 Expression of truncated mouse and human BACE in

BL21(DE3)LysS cells using conventional method.....70
3.1.2.2 Expression of truncated mouse and human BACE in BL21(DE3)LysS cells using modified method.....72
3.1.3 Analysis of BACE activity of purified recombinant proteins.....76
3.1.3.1 Fluorometric analysis.....76
3.2 Expression of BACE in mammalian cells.....81
3.2.1 Cloning of full length mouse and human BACE into pCDNA3, pCDNA4HisMax.....81
3.2.2 Transient transfection.....84
3.2.2.1 Western blot analysis.....86
3.2.2.2 Fluorometric analysis.....88
3.2.2.3 HPLC.....91
3.2.3 Stable transfection.....100
3.2.3.1 Western blot analysis.....101
3.2.3.2 Fluorometric analysis.....103
3.2.3.3 HPLC.....105
3.2.3.4 Immunohistochemistry.....112
Chapter 4 Discussion.....115
References.....126
Appendix.....i
A1 Vector circle map.....i
A1-1 Vector circle map of pBluescript II-.....i
A1-2 Vector circle map of pCDNA3.....ii
A1-3 Vector circle map of pCDNA4HisMax.....iii
A1-4 Vector circle map of pRSET.....iv
A2 Primer lists.....v
A3 Chemical structure of fluorophore and quench used in fluorometric assay...vi

Abbreviations

Aβ	β-amyloid
ACh	acetylcholine
AChE	acetylcholinesterase
AD	Alzheimer's disease
AP	alkaline phosphatase
ApoE	Apolipoprotein E
APP	Amyloid precursor protein
APS	ammonium persulfate
BACE	beta-site APP-cleaving enzyme
BCIP	5-Bromo-4-Chloro-3-Indolyl phosphate
BLAST	Basic Local Alignment Search Tool
BSA	bovine serum albumin
bp	base pair
cDNA	complementary deoxyribonucleic acid
CDK-5	cyclin-dependent kinase-5
ChAT	Choline acetyltransferase
CMV	cytomegalovirus
CTF	Carboxyl-terminal fragment
DABCYL	4-dimethylaminophenylazo benzoic acid
ddH_2O	double distilled water
DMEM	Dulbecco's Modified Eagle Medium
DMSO	dimethylsulfoxide
DNA	deoxyribonucleic acid
dNTP	deoxynucleotide triphosphate
DTT	dithiothreitol
E.coli	*Escherichia coli*
EB	ethidium bromide

EDANS	2-aminoethyl amino-naphthalene-1-sulfonic acid
EDTA	ethylenediamine tetraacetic acid
ER	endoplasmic reticulum
FAD	familial Alzheimer's disease
FBS	Fetal bovine serum
FITC	fluorescein isothiocyanate
FRET	fluorescence resonance energy transfer
FTP	fronto temporal degeneration
GSK-3	glycogen synthase kinase 3
HPLC	high performance liquid chromatography
IMAC	immobilized metal ion affinity chromatography
IPTG	isopropylthio-β-D-galactoside
kb	kilobase
LB	Luria Bertani
MAP	microtubule associated protein
NBT	nitro blue tetrazolium
NEAA	non-essential amino acid
NFT	neurofibrillary tangles
PAGE	polyacrylamide gel electrophoresis
PBS	Phosphate buffered saline
PC	proprotein convertase
PCR	polymerase chain reaction
PEG	polyethylene glycol
PHF	paired helical filament
PMSF	Phenylmethylsulfonyl fluoride
PS1	presenilin 1
PS2	presenilin 2
PVDF	polyvinylidene difluoride

RNase	ribonuclease
RP	reverse phase
SDS	sodium dodecyl sulfate
TAE	tris acetate EDTA
TEMED	N,N,N,N-tetramethyl ethylene diamine
TFA	trifluoroacetic acid
TGN	*trans*-Golgi network
TPK	tau protein kinase

List of Figures

Chapter 1

Fig. 1-1 (A) Aβ deposited as diffuse and neuritic plaques in brain parenchyma; (B) neurofibrillary tangles within neuronal cell bodies.

Fig. 1-2 Chemical structure of tacrine.

Fig. 1-3. Schematic diagram of APP and its alternate transcripts.

Fig. 1-4 Schematic diagram of cleavage of APP by α-, β- and γ-secretase.

Fig. 1-5 Summary of the amyloid cascade hypothesis.

Fig. 1-6 Summary of tau and tangle hypothesis.

Fig. 1-7 (A) Schematic diagram of human BACE precursor protein and its domain structure as deduced from its cDNA sequence; (B) Schematic diagram of mouse BACE precursor protein and its domain structure as deduced from its cDNA sequence.

Chapter 3

Fig. 3-1 (A) Agarose gel of insert (nohBACE and prohBACE) and vector (pRSETA) digested by restriction enzyme EcoRI and XhoI; (B) Agarose gel of insert (nomBACE) and vector (pRSETB) digested by restriction enzyme EcoRI and NheI.

Fig. 3-2 (A) SDS-PAGE of the expression of the nomBACE by conventional method; (B) SDS-PAGE of the expression of the nohBACE and prohBACE by conventional method.

Fig. 3-3 SDS-PAGE of the expression of the nomBACE by modified method.

Fig. 3-4 SDS-PAGE of the expression of the nohBACE and prohBACE by modified method.

Fig. 3-5 SDS-PAGE of purified inclusion bodies from BL21(DE3)LysS cell lysates overexpressed with nohBACE and prohBACE.

Fig. 3-6 Standard curve of fluorophore, EDANS.

Fig. 3-7 (A) Fluorometric analysis of activity of nohBACE and prohBACE protein towards FS-1 in terms of number of mole of fluorophore released; (B) Fluorometric analysis of activity of nohBACE and prohBACE protein towards FS-2 in terms of number of mole of fluorophore released.

Fig. 3-8 (A) Agarose gel of insert (mBACE) and vector (pBluescript II KS-) digested by EcoRI and XhoI; (B) Agarose gel of insert (hBACE) and vector (pBluescript II KS-) digested by EcoRI and XhoI.

Fig. 3-9 CHO cells transfected with pCDNA4HisMax*lacZ* gene viewed under light microscope (200x) to estimate transfection efficiency.

Fig. 3-10 (A) SDS-PAGE of membrane extracts from cells transiently transfected with mBACE-pCDNA3, mBACE-pCDNA4HisMaxC, hBACE-pCDNA3 and hBACE-pCDNA4HisMaxA; (B) Western blot analysis of membrane extracts from cells transiently transfected with mBACE-pCDNA3, mBACE-pCDNA4HisMaxC, hBACE-pCDNA3 and hBACE-pCDNA4HisMaxA using antibody hBACE 485.

Fig. 3-11 (A) Fluorometric analysis of activity of membrane extracts from cells transiently transfected with mBACE-pCDNA3, mBACE-pCDNA4HisMaxC, hBACE-pCDNA3 and hBACE-pCDNA4HisMaxA towards FS-1 in terms of number of mole of fluorophore released; (B) Fluorometric analysis of activity of membrane extracts from cells transiently transfected with mBACE-pCDNA3, mBACE-pCDNA4HisMaxC, hBACE-pCDNA3 and hBACE-pCDNA4HisMaxA towards FS-2 in terms of number of mole of fluorophore released.

Fig. 3-12 Standard curve of synthetic peptides, SEVNLDAEFR, EVKMDAEFR and DAEFR in HPLC.

Fig. 3-13 HPLC of membrane extracts (A) preboiled from untransfected cells

using substrate EVKMDAEFR; (B) from untransfected cells using substrate EVKMDAEFR; (C) preboiled from untransfected cells using substrate SEVNLDAEFR; (D) from untransfected cells using substrate SEVNLDAEFR; (E) preboiled from cells transiently transfected with mBACE-pCDNA3 using substrate EVKMDAEFR; (F) from cells transiently transfected with mBACE-pCDNA3 using substrate EVKMDAEFR; (G) preboiled from cells transiently transfected with mBACE-pCDNA3 using substrate SEVNLDAEFR; (H) from cells transiently transfected with mBACE-pCDNA3 using substrate SEVNLDAEFR; (I) preboiled from cells transiently transfected with mBACE-pCDNA4HisMaxC using substrate EVKMDAEFR; (J) from cells transiently transfected with mBACE-pCDNA4HisMaxC using substrate EVKMDAEFR; (K) preboiled from cells transiently transfected with mBACE-pCDNA4HisMaxC using substrate SEVNLDAEFR; (L) from cells transiently transfected with mBACE-pCDNA4HisMaxC using substrate SEVNLDAEFR.

Fig. 3-14 (A) SDS-PAGE of membrane extracts from cells stably transfected with mBACE-pCDNA3 and hBACE-pCDNA3; (B) Western blot analysis of membrane extracts from cells stably transfected with mBACE-pCDNA3 and hBACE-pCDNA3 using antibody hBACE 485.

Fig. 3-15 (A) Fluorometric analysis of activity of membrane extracts from cells stably transfected with mBACE-pCDNA3 and hBACE-pCDNA3 towards FS-1 in terms of number of mole of fluorophore released; (B) Fluorometric analysis of activity of membrane extracts from cells stably transfected with mBACE-pCDNA3 and hBACE-pCDNA3 towards FS-2 in terms of number of mole of fluorophore released.

Fig. 3-16 HPLC of membrane extracts (A) preboiled from untransfected cells using substrate EVKMDAEFR; (B) from untransfected cells using

substrate EVKMDAEFR; (C) preboiled from untransfected cells using substrate SEVNLDAEFR; (D) from untransfected cells using substrate SEVNLDAEFR; (E) preboiled from cells stably transfected with mBACE-pCDNA3 using substrate EVKMDAEFR; (F) from cells stably transfected with mBACE-pCDNA3 using substrate EVKMDAEFR; (G) preboiled from cells stably transfected with mBACE-pCDNA3 using substrate SEVNLDAEFR; (H) from cells stably transfected with mBACE-pCDNA3 using substrate SEVNLDAEFR; (I) preboiled from cells stably transfected with hBACE-pCDNA3 using substrate EVKMDAEFR; (J) from cells stably transfected with hBACE-pCDNA3 using substrate EVKMDAEFR; (K) preboiled from cells stably transfected with hBACE-pCDNA3 using substrate SEVNLDAEFR; (L) from cells stably transfected with hBACE-pCDNA3 using substrate

Fig. 3-17 (A) Immunohistochemistry of unpermelised untransfected cells using hBACE 485; (B) Immunohistochemistry of unpermelised cells stably transfected with mBACE-pCDNA3 using hBACE485; (C) Immunohistochemistry of unpermelised cells stably transfected with hBACE-pCDNA3 using hBACE485.

Chapter 4

Fig. 4-1 (A) Models of BACE with wild type APP substrate; (B) Models of BACE with Swedish mutation APP substrate.

Appendix

Fig. A1-1 Vector circle maps of pBluescript II-

Fig. A1-2 Vector circle maps of pCDNA3

Fig. A1-3 Vector circle maps of pCDNA4HisMax

Fig. A1-4 Vector circle maps of pRSET

Fig. A3 (A) Chemical structure of DABCYL; (B) Chemical structure of EDANS.

List of Tables

Chapter 2

Table 1 Flow rate and different composition of buffer used in HPLC assay

Chapter 4

Table 2 Summary of results of different assays using different vectors transformed and transfected into *E.coli* cells, BL21(DE3)LysS and mammalian cells, CHO cells.

Chapter 1 Introduction

Chapter 1

Introduction

1.1 Alzheimer's disease

1.1.1 History of Alzheimer's disease

Senile dementia, the loss of memory and other intellectual properties that commonly occur in the elderly, was first recognized in the time of Hippocrates (B.C. 460-B.C. 370). The dementia begins at age 65 or older and progresses slowly and was considered as an inevitable accompaniment of aging.

In 1906, a German psychiatrist named Alois Alzheimer (1864-1915) presented his findings on what was first called presenile dementia. One of his patients died at the age of 56 because of complete dementia. By examination of the autopsy of the brain of this woman, Alzheimer found not only the deposition of senile plaques that were commonly found in the brains of people with senile dementia but also the presence of neurofibrillary tangles – the thick, coiled fibers within the cytoplasm of the cerebral cortical neurons. This case was different from classical pathology of senile dementia because of the occurrence at relative young age, the rapid deterioration of the disease's progression, and the neuropathological findings. The

disease was subsequently named Alzheimer's disease in honor of his contribution. (Alzheimer, 1907)

Alzheimer's disease was initially thought to be a rare condition affecting only young people, and was referred to as presenile dementia. Today late-onset Alzheimer's disease is recognized as the most common cause of the loss of mental function in those aged 65 and over. Alzheimer's diseases occur in people in their 30s, 40s, and 50s, are called early-onset Alzheimer's disease. It occurs much less frequently, accounting for less than 10 percent of the estimated 4 million Alzheimer's cases in the United States.

1.1.2 Definition of Alzheimer's disease

Alzheimer's disease is the most common cause of dementia, characterized by a decline in intellectual functioning severe enough to interfere with a person's normal daily activities and social relationships. It is marked by progressive, irreversible declines in memory, performance of routine tasks, time and space orientation, language and communication skills, abstract thinking, and the ability to learn and carry out mathematical calculations (Esiri and Morris, 1997). Other symptoms of Alzheimer's disease include personality changes and impairment of judgment. The brains of patients with Alzheimer's have distinctive formations—abnormally shaped

proteins called tangles and plaques—that are recognized as the hallmark of the disease. Not all brain regions show these characteristic formations. The areas most prominently affected are those related to memory.

As shown in Fig. 1-1A, plaques, or clumps of fibers, are formed outside the neurons in the adjacent brain tissue. A long-established plaque may be several hundred micrometers in diameter. The major component of senile plaques is now characterized as β-amyloid (Aβ), a peptide of 39-43 amino acids, derived from proteolytic breakdown of a larger protein called the amyloid precursor protein. When Aβ deposits are surrounded by abnormal neuronal processes called dystrophic neuritis, they form neuritic plaques. Aβ also appears in diffuse plaques, which lack a central core and the corona of dystrophic neuritis. Diffuse and neuritic plaques are sometimes called senile plaques. Some authors think the diffuse plaque is the premature form of neuritic plaque (Esiri and Morris, 1997). In almost all cases of Alzheimer's disease, there is a mixture of diffuse and neuritic plaques, and in severe cases very large numbers of plaques are present. It is widely believed that the Aβ plaque is central to the pathogenesis of Alzheimer's disease, but the mechanism of Aβ deposition is still unclear (Hardy and Higgins, 1992). In most cases, not only is amyloid deposited inside the plaque, but also along the walls of arteries in the cerebral cortex (congophilic angiopathy) (Esiri and Morris, 1997).

As shown in Fig.1-1B, tangles are long, slender tendrils found inside nerve cells, or neurons. Scientists have learned that the tangles are mainly composed of a protein called tau that becomes structurally altered. The abnormal tau formation is now known to cause the characteristic tangles in the brain of Alzheimer's patients. In healthy brains, the tau protein provides structural support for neurons, but in Alzheimer's patients this structural support collapses.

Scientists have found that tangles and plaques cause neurons in the brains of Alzheimer's patients to shrink and eventually die, first in the memory and language centers and finally throughout the brain. This widespread neuron degeneration leaves gaps in the brain's messaging network that may interfere with communication between cells, causing some of the symptoms of Alzheimer's disease.

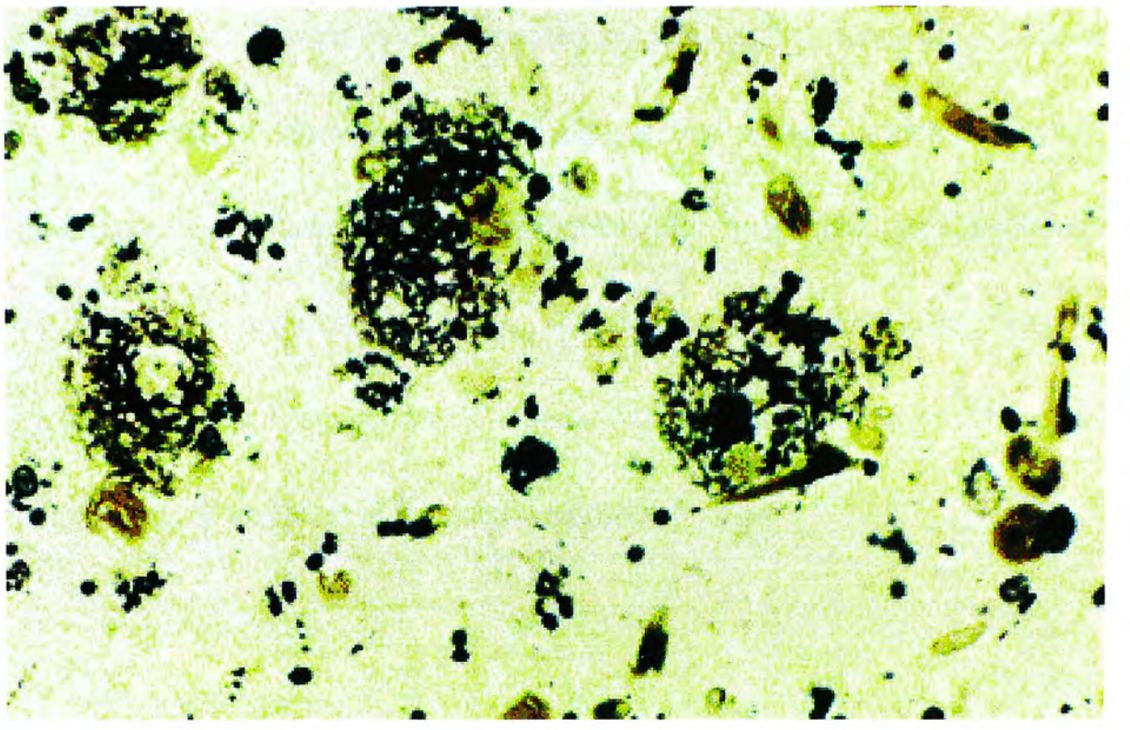

A

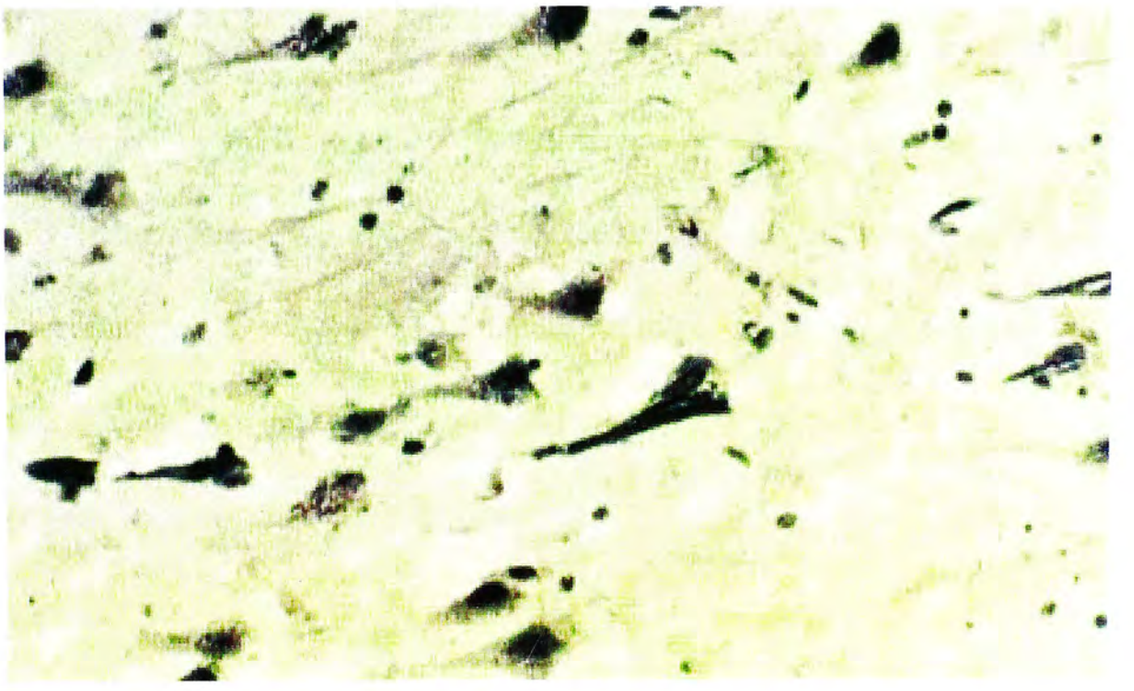

B

Fig. 1-1 The major histopathological hallmarks of Alzheimer's disease seen on light microscopy. (A) Aβ deposited as diffuse and neuritic plaques in brain parenchyma. (B) neurofibrillary tangles within neuronal cell bodies (Bayer *et al.*, 1999).

1.1.3 Symptoms of Alzheimer's disease

Alzheimer's disease is characterized by damages of nerve cells in several regions of the brain. These regions include cerebral cortex, which involved in conscious thought and language; the basal forebrain, which has large numbers of neurons containing acetylcholine (ACh), a chemical important in memory and learning and the hippocampus, which is essential to memory storage. The earliest signs of Alzheimer's are found in the nearby entorhinal cortex

1.1.3.1 Memory deficit

AD is characterized by destroys of neurons in parts of the brain controlling memory, especially the hippocampus. There are two types of memory, the short-term memory (remembering for a few minutes or hours), and the long-term memory (remembering for a few years). In the early stage in Alzheimer's disease, the short-term memory is impaired but long-term memory is preserved. However, in the later stages, long-term memory is impaired.

1.1.3.2 Difficulty in learning

One of the earliest manifestations of Alzheimer's disease is the inability to acquire and retain new information and to integrate it with previously acquired

knowledge. This problem is partly the result of short-term memory impairment and can be readily observed in the difficulty the patient has in keeping abreast of recent developments in his or her profession and an inability to discuss current events.

1.1.3.3 Language difficulties

Alzheimer's disease's patient has damaged neurons in the cerebral cortex. The greatest damage occurs in areas of the cerebral cortex responsible for functions such as language and reasoning. At the early stage of disease, anomia occurs. Anomia, the inability to find the right word. The patient is aware of this deficit and may try to make up for them by using sentences to describe the object he cannot name (paraphrasia). As the disease progresses, agnosia sets in. Agnosia is more serious than anomia because, in addition to being unable to name an object, the person cannot identify it. For instance, he may not recognize a key; he may think it is a spoon and try to eat soup with it.

1.1.3.4 Decline in ability to perform routine tasks

Apraxia, the inability to carry out purposeful movements and actions despite intact motor and sensory systems, is evident early in the course of Alzheimer's disease. The more complex or technical skills, particularly those recently acquired or

requiring integration of various stimuli, are lost early in the process. The less complex actions, such as eating, walking, dressing, and undressing, tend to be reserved until the late stages.

1.1.4 Prevalence of Alzheimer's disease

Alzheimer's disease is the fourth leading cause of death of adults in USA, after heart disease, cancer and stroke (Lendon *et al.*, 1997). However, the cost of treatment of Alzheimer's disease is much higher than the above-mentioned diseases. It is because it is a chronic disease, the duration of the disease is about 8 years after the diagnosis (Lendon *et al.*, 1997) and huge amount of money is spent on residential and hospital care. AD is the most common cause of dementia among people age 65 and older. Four million Americans currently suffer from the AD, and experts estimate that 22 million people around the world will be so afflicted by 2025 (Alzheimer's Disease Research Center, ADRC, 2002). The prevalence of AD doubles every 5 years beyond age 65. Prevalence is the number of people in a population with a disease at a given time. In fact, some studies indicate that nearly half of all people age 85 and older have symptoms of AD.

AD is becoming a major public health concern. This is because life expectancy has increased dramatically since the turn of the century. More than 34

million people--13 percent of the total population of the United States--are age 65 and older. According to the U.S. Bureau of the Census, this percentage will climb to 18 percent by the year 2025.

1.2 Present treatment of Alzheimer's disease

1.2.1 Acetylcholine and dementia

Alzheimer's disease has been associated with loss of cholinergic nervous activity in the brain. Cholinergic nerves are so named because they use acetylcholine as their neurotransmitter. There is a dramatic loss of cholinergic cells within both the nucleus basalis and the medial septum of the AD brain as compared to aged matched controls (Whitehouse *et al.*, 1982). Choline acetyltransferase (ChAT), the synthetic enzyme for acetylcholine, has been reported to be decreased 60-90% in the cerebral cortex and hippocampus of AD brains, (Davies and Maloney, 1976), and there is a correlation between the extent to which cholinergic markers are decreased in cortical areas of the AD brain and the degree of cognitive impairments observed (Perry *et al.*, 1978). Acetylcholine is a critical neurotransmitter in the process of forming memories. Moreover, it is the neurotransmitter used commonly by neurons in the hippocampus and cerebral cortex--regions devastated by Alzheimer's disease.

1.2.2 Tacrine as first drug approved by US Food and Drug Administration

Various drugs have been designed to inhibit acetylcholinestese (AChE), so as to increase the levels of ACh in the brain of AD patients, tacrine (9-amine-1,2,3,4-tetrahydroacridine) was the first drug approved for treatment. Tacrine is a centrally active noncompetitive AChE and butryl-ChE inhibitor that prevents the degradation of endogenously released ACh. The chemical structure of tacrine is shown in Fig. 1-2.

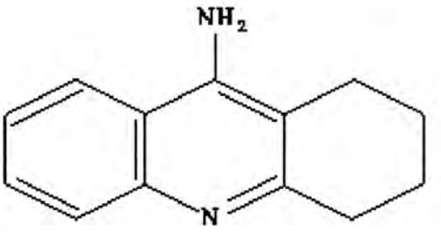

Fig. 1-2 Chemical structure of tacrine

However, drugs inhibit AChE can only treat the symptoms of AD, but not the cure of it. Scientists investigated the biochemistry of two main hallmarks of AD brains, the senile plaques and neruofibrillary tangles that led to the development of two theories of AD pathophysiology.

1.3 Proposed theory of Alzheimer's disease formation

1.3.1 The amyloid cascade hypothesis

1.3.1.1 The amyloid precursor protein

Cleavage of amyloid precursor protein (APP) by α-, β- and γ-secretase produced amyloid protein (Aβ), which is responsible for the formation of amyloid plaques. (Glenner and Wong, 1984; Masters *et al.*, 1985; Castano *et al.*, 1986). APP is composed of 770 amino acids, and the gene of APP is on chromosome 21. It is a transmembrane protein.

As shown in Fig. 1-3, the APP consists of a 17-residue signal peptide at the amino terminus (box with vertical lines). Two alternatively spliced exons of 56 and 19 amino acids are inserted at residue 289; the first contains a serine protease inhibitor domain of the Kunitz type (KPI). A single membrane-spanning domain at amino acids 700-723 (vertical hatched bar). The amyloid β-protein (Aβ) fragment (white box) includes 28 residues just outside the membrane plus the first 12-14 residues of the transmembrane domain.

APP is a glycoprotein and there are two potential glycosylation sites located at amino acid residues 542 and 571.

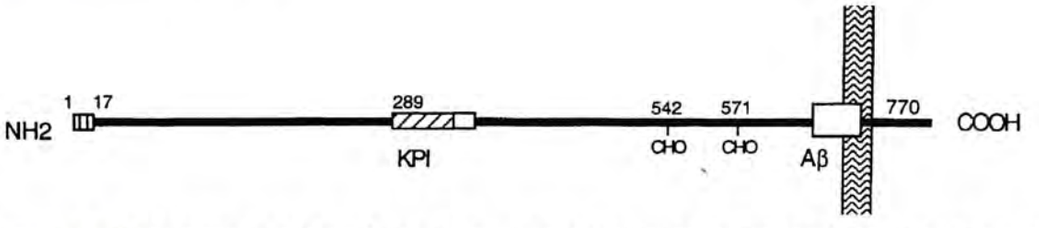

Fig. 1-3. The largest APP of the known APP alternate transcripts. Regions of interest are indicated at their correct relative positions.

The APP is encoded by a single copy gene located at chromosome 21. Multiple transcripts of APP are formed by alternatively sliced transcripts, which, in its longest isoform, encode a single transmembrane spanning polypeptide of 695-770 amino acids (Goldgaber *et al.*, 1987; Kang *et al.*, 1987; Tanzi *et al.*, 1987; Robakis *et al.*, 1988). It has been implicated in a variety of cellular processes and events. Secreted isoforms of APP (sAPP) containing a Kunitz-type protease inhibitor (KPI) consensus sequence that have a role in regulation of extracellular protease activity (Oltersdorf *et al.*, 1989) and as inhibitors of protease involved in the regulation of the coagulation cascade (Smith *et al.*, 1990). The carboxyl-terminus of sAPP has been shown to be involved in regulating intracellular calcium levels and thus exerting neuroprotective activities (Mattson *et al.*, 1993).

1.3.1.2 The processing of amyloid precursor protein

As schematically illustrated in Fig. 1-4, it is now becoming clear that the APP is processed through site-specific cleavages by at least three proteases, the α-, β-, and γ-secretase. During the normal processing of APP, α-secretase cleaves within the sequence of Lys687 and Leu688 of APP that enables secretion of the large, soluble ectodomain of APP (α-APP_s) into the medium and retention of the 83 residue carboxyl-terminal fragment (~10 kDa) in the membrane. The 10 kDa fragment can undergo cleavage by γ-secretase at residue 711 or residue 713 to release the p3

peptides.

It is hypothesized that AD is caused by abnormal processing of APP, which involves proteolytic cleavages, by β- and γ-secretase. β-secretase cleaves within sequence of Met671 and Asp672 of APP that results in the secretion of a truncated APP_s (β-APP_s) molecule and the retention of a 99 residue (~12kD) carboxyl-terminal fragment. The 12 kDa fragment undergoes cleavage by γ-secretase at residue 711 or residue 713 to release the Aβ40 or Aβ42 peptides.

Aβ is a 4kD fragment of APP that constitutes the major component of plaques. It is 39-43 amino acids in length in AD brain (Glenner and Wong, 1984). Soluble Aβ from normal cells is composed chiefly of Aβ40 and insoluble Aβ is composed mainly of Aβ42 (Dovey *et al.*, 1993). *In vitro* study has shown that free Aβ peptides cleaved from APP easily self-aggregate into highly neurotoxic amyloid fibrils (Pike *et al.*, 1993). Aβ42 aggregates much more rapidly than the most common form of Aβ40 (Barrow and Zagorski, 1991; Jarrett *et al.*,1993).

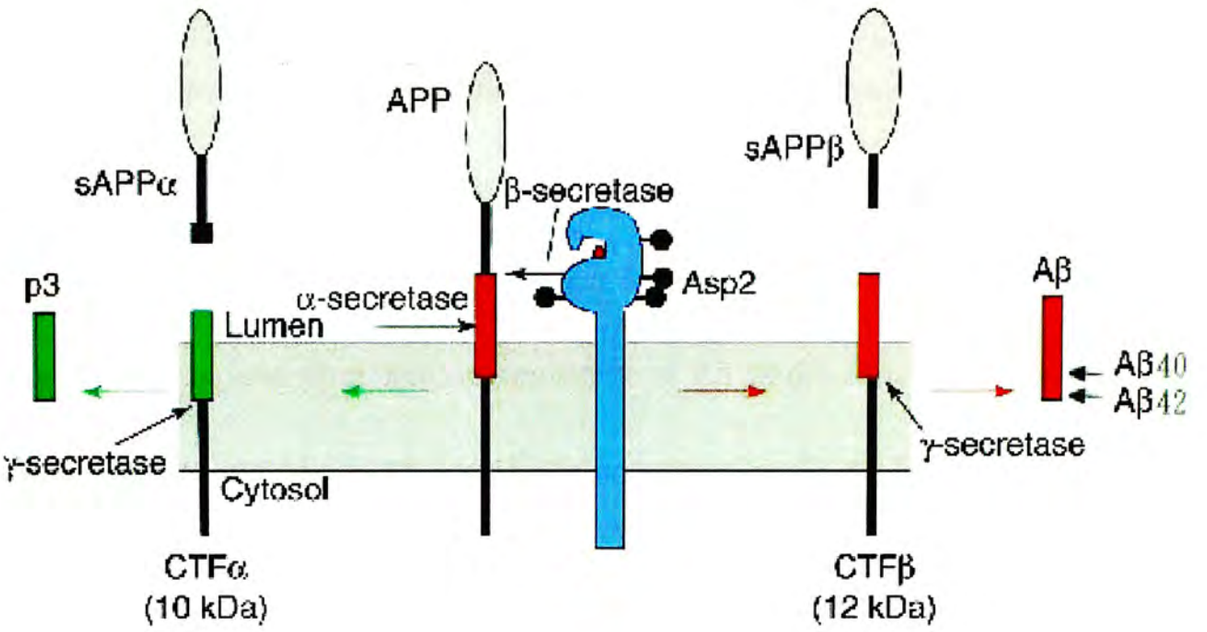

Fig. 1-4 Processing of APP by α-, β- and γ-secretase. Cleavage of APP by α- and γ-secretase to produce soluble APPα protein, a cytoplasmic protein, CTFα and a soluble protein, p3. Cleavage by β- and γ-secretase to produce soluble APPβ protein , a cytoplasmic protein, CTFβ, Aβ peptide. Abbreviation: CTF, carboxyl-terminal fragment (Hussain *et al.*, 1999).

1.3.1.3 Neurotoxic effect of amyloid plaque

The length of the C-terminal tail of Aβ is an important determinant of its readiness to aggregate into the amyloid fibrils (Yanker, 1996). It was found that the higher the ratio of Aβ42 to Aβ40, the higher the risk of developing amyloid fibrils. The accumulation and presumed neurotoxicity of Aβ fibrils forms the basis of the amyloid cascade hypothesis of AD (Neve and Robakis, 1998; Hardy and Allsop, 1991). According to the hypothesis, increased production of Aβ42 leads to progressive extracellular deposition of fibrillar Aβ42 around blood vessels and as diffuse and neuritic plaques, which in turn leads to disruption of neuronal homeostasis and progressive neuronal injury. This accumulation of neuritic plaques has two consequences: the first is inflammatory response (microglial activation and cytokine release, activation of complete cascade) and oxidative injury. The second is altered phosphatase activities, which leads to hyperphosphorylated tau protein, which leads to neurofibrillary tangles. Both consequences cause neuronal dysfunction and degeneration, with progressive cholinergic and other neurotransmitter deficits, which leads to dementia (Nagy *et al.*, 1995).

1.3.1.4 Genetic factors

1.3.1.4.1 The amyloid precursor protein

There are substantial evidences that mutation of APP causes some forms familial Alzheimer's disease (FAD). The autosomal dominant mutations in APP that are associated with FAD cluster around the β- and γ- cleavage sites. A two-point mutation (the Swedish mutation) at amino acids 670 and 671 from Lys-Met to Asp-Leu is upstream of the β-cleavage site (Mullan, 1992) and results in a five- to eightfold increase in the formation of both $A\beta_{40}$ and $A\beta_{42}$ (Citron *et al.*, 1992). The most simple explanation is that the Swedish mutation results in the over-production of the Aβ peptide and in particular, overproduction of long-tailed isoforms ending at residue 42 (Haass *et al.*, 1994; Susuki *et al.*, 1994). Studies from a variety of groups suggested that Aβ, like several other amyloids, exhibits neurotoxicity when aggregated as a fibril, and implied that a conformational change is necessary to change the inert (or even marginally neurotrophic) soluble Aβ into toxic Aβ (Lorenzo and Yanker, 1994).

1.3.1.4.2 Apolipoprotein E (ApoE)

ApoE is the major serum protein involved in cholesterol metabolism, transport and storage (Weisgraber *et al.*, 1994). It is polymorphic and encoded by three alleles (ApoE-2, -3, -4), of which the ApoE-3 allele is the most common. Analysis of these polymorphisms in normal control populations and in patients with

AD has consistently shown that there is an increase in the frequency of the ε4 allele in patients with AD (allele frequency in AD is approximately 40%) (Saunders *et al.*, 1993) There is no correlation between the presence of NFTs and a particular ApoE allele, whereas there is dose-dependent relationship between Aβ and ApoE4 (Price and Sisodia, 1998).

1.3.1.4.3 Presenilin genes

St. George-Hyslop *et al.*(1992), Van Broeckhoven *et al.* (1992) and Mullan (1992) presented evidence of location of a mutation responsible for early-onset familial Alzheimer disease on 14q, and was named as presenilins. Presenilins are transmembrane proteins. Presenilin-1 and presenilin-2 are encoded by genes on chromosome 14 and 1, respectively (Levy-Lahad *et al.*,1995; Sherrington *et al.*, 1995), and are predominantly present in neurons (and to a lesser extent in glia) and its expression is closely associated with APP (Lee *et al.*, 1996). One consequence of PS1 mutations is the enhanced production of $A\beta_{42}$ (Borchelt *et al.*, 1996), suggesting that PS1 mutations influence processing at the γ-secretase site. Recent evidence suggests that activity of γ-secretase require PS1 and PS1 could itself be the γ-secretase (Strooper *et al.*, 1998, Wolfe *et al.*, 1999).

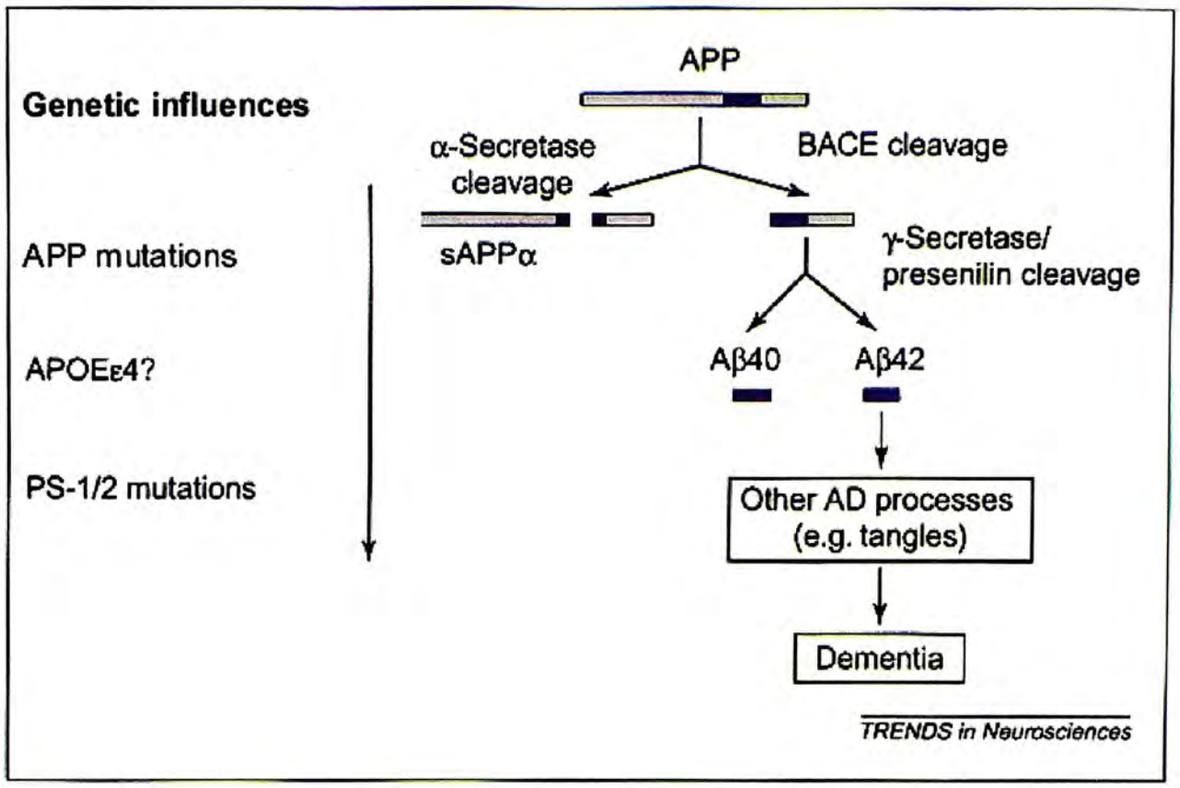

Fig.1-5 Summary of the amyloid cascade hypothesis. Amyloid precursor protein (APP) is cleaved either by α-secretase resulting in the production of sAPPα, which might have a neuroprotective role, or by β-amyloid cleaving enzyme (BACE) and then γ-secretase to yield Aβ. The larger Aβ42 peptides are more prone to self-aggregate and are thought to be more pathogenic (Mudher and Lovestone, 1999).

1.3.2 Tau and tangle hypothesis

1.3.2.1 Tau protein

Tangles are comprised of the microtubule associated protein called tau that is normally expressed in axons. In AD brain, the tau proteins become highly phosphorylated and aggregated into abnormal filaments in the cell body, known as paired helical filament (PHF). Tau protein belongs to a group of proteins known as microtubule-associated proteins (MAPs) with the function of modulating microtubule assembly, dynamic behavior and spatial organization (reviewed by Lee, 1993; Mandelkow and Mandelkow, 1995). Tau protein from adult human brain consists of six isoforms which all are phosphoproteins (Grundke-Iqbal *et al.*, 1986 ; Wood *et al.*, 1986). The degree of phosphorylation of tau protein regulates its biological activity. These proteins are expressed predominantly in axons and are brain-specific microtubule-associated proteins. The function of tau is presumably to stabilize the microtubule that serves as tracks for cytoplasmic transport (Tucker, 1990).

Mutations in tau were found in various fronto-temporal degeneration (FTD) disorders (Heutink *et al.*, 2000). Missense mutations in tau have been shown both to increase self-aggregation and to reduce microtubule binding (Rizzu *et al.*, 2000; Arrasate *et al.*, 1999; Perez *et al.*, 2000). Other intronic mutations alter splicing and hence the ratio of isoforms with either three or four microtubule binding domains

(D'Souza *et al.*, 1999; Grover *et al.*, 1995). As there is competition for microtubule binding between the different isoforms (Lu and Kosik, 2001). Both the intronic and exonic mutations have been shown to decrease binding of tau to microtubules. Hence, increases in free, unbound tau, also enchance the possibility of tau aggregation.

1.3.2.2 Paired helical filaments (PHF)

PHF are mainly composed of hyperphosphorylated tau protein. Tau protein isolated from normal adult brain contains 2-3 moles of phosphate per mole of tau protein whereas form AD brain, it contains 5-12 moles (Selden and Pollard, 1983). About half of the known phosphorylation sites in PHF are serine or threonine residues followed by a proline (reviewed by Goedert *et al.*, 1997).

1.3.2.3 Tau protein kinase (TPK)

Protein phosphorylation is one of the major mechanisms for the regulation of many biological functions. One of the key events in the formation of PHF-tau involves the hyperphosphorylation of normal adult brain tau, which renders the abnormal proteins incapable of binding to microtubules and a loss of tau-induced microtubule stabilization (Goedert *et al.*, 1993; Bramblett *et al.*, 1993). At present, it is not known which kinase involved in the initial stages or how such protein kinases

interact to bring about the final phosphorylation state of tau. TPKI and II were found as candidate enzymes responsible for hyperphosphorylation of tau to induce the formation of PHF. TPKI and TPKII were identified as glycogen synthase kinase(GSK)-3 β and cyclin-dependent kinase 5 (CDK5). The phosphorylation sites on tau by TPKI and TPKII account for most, but not all of the major phosphorylation sites of fetal tau and PHF-tau (reviewed by Imahori and Uchida, 1997).

1.3.2.3.1 Glycogen synthase kinase-3 (GSK-3)

GSK-3 is a serine/threonine-specific kinase, which was initially found to be able to phosphorylate and thereby inactivate glycogen synthase (Embi *et al.*, 1980; Hemmings *et al.*, 1981; Hughes *et al.*, 1993). It is identified as TPKI and is crucially involved in the hyper-phosphorylation of tau in AD (Lovestone and Reynolds, 1997). GSK-3, especially the β-isoform, is associated with the paired helical filaments (PHF) found in the AD brains (Shiruba *et al.*, 1996; Yamaguchi *et al.*, 1996; Pei *et al.*, 1997). GSK-3β has been shown to phosphorylate tau *in vitro* on several serine and threonine residues known to be phosphorylated in PHF-tau (Lovestone *et al.*, 1994; Mulot *et al.*, 1994; Anderton *et al.*, 1995).

1.3.2.3.2 Cyclin-dependent kinase 5 (CDK5)

CDK5 is a proline-directed kinase that phosphorylates serine and threonines immediately upstream of a proline residue. Like other CDKs, monomeric CDK5 shows no enzymatic activity and requires association with a regulatory partner for activation. Two activators of CDK5, p35 and p39 have been identified (Lew *et al.*, 1994; Tsai *et al.*, 1994; Ishiguro *et al.*, 1994). Deregulation of CDK5 through the proteolytic cleavage of p35 to generate p25 is associated with Alzheimer's disease (reviewed by Dhavan and Tsai, 2001). In transfected cells and cultured neurons, p35-CDK poorly phosphorylates tau, whereas tau is potently phosphorylated by p25-CDK5 (Patrick et al., 1999). TPKII/p25-CDK5 was shown to be associated with neurofibrillary tangles in vivo (Pei et al., 1998), and phosphorylated tau on sites found in PHF-tau (Paudel et al., 1993).

1.3.2.4 Tangle leads to dementia

There were substantial attempts to ascertain which pathological lesion was responsible for the clinical features of AD that showed good correlation between cognitive state and the numbers of tangles (Nagy *et al.*, 1995). The process of tangle formation starts with increased phosphorylation and then aggregation of tau in those areas known to be critical for memory (Braak *et al*, 1994; Braak and Braak, 1998).

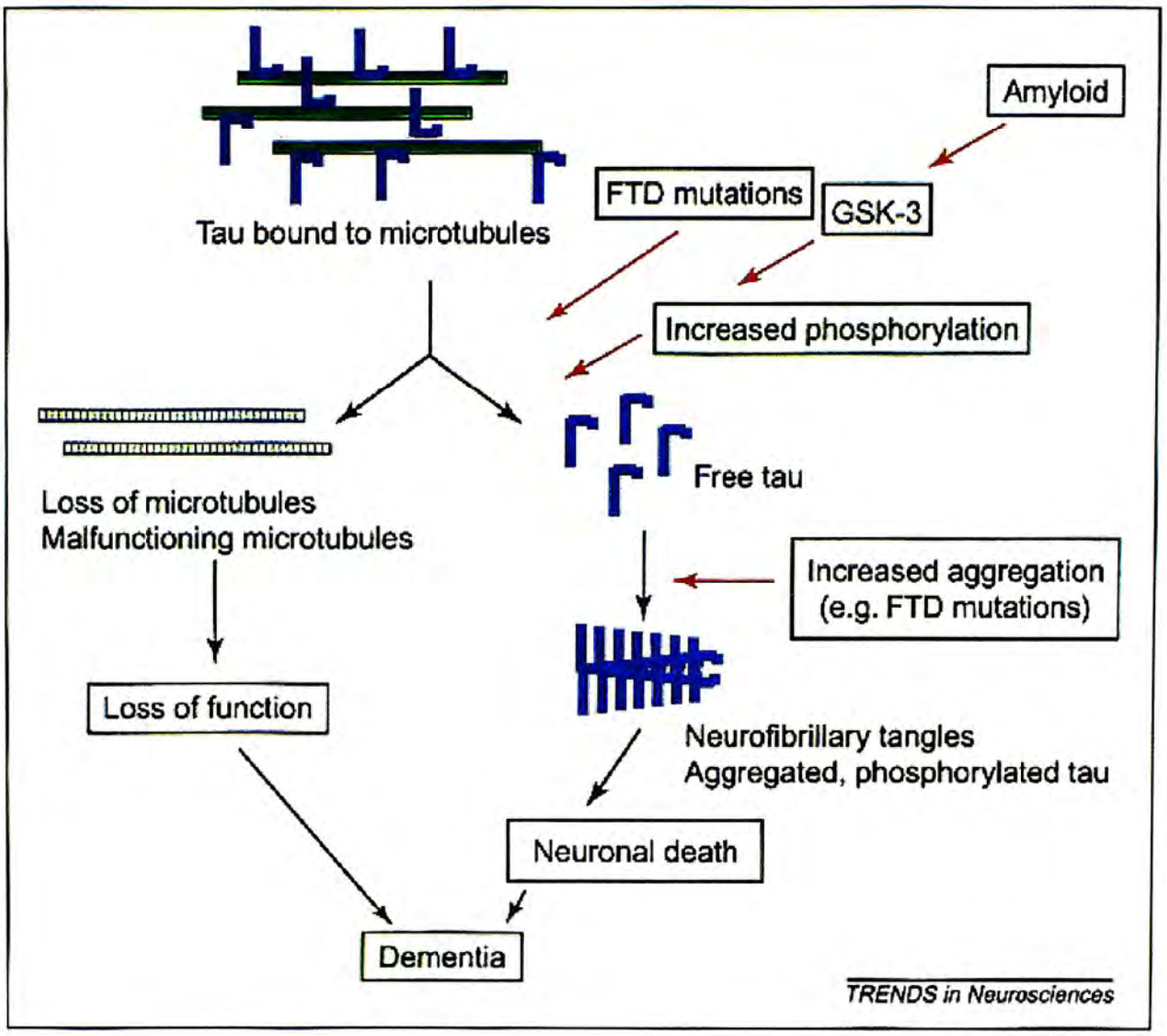

Fig. 1-6 Summary of tau and tangle hypothesis. Tau binding to microtubules is disrupted by phosphorylation, directly by mutations that alter function, and by mutations that alter isoform expression. Decreased tau binding to microtubules might result in increased free tau, which under the appropriate conditions, will self-aggregate to form insoluble paired helical filaments. Loss of tau binding is predicted to result in loss of microtubule function. The process of tau aggregation in the absence of mutations is not known but might result from increased phosphorylation, protease action or exposure to polyanions, such as glycosaminoglycans (Mudher and Lovestone, 1999).

1.4 Cross-talk between the two hypotheses

There had been many arguments supporting each hypothesis as the sole cause of AD. However, recent researches have shown that both hypotheses may harmonize together. A transgenic mouse overexpressing both APP and mutant tau had more tangles than tau-mutant mice alone and tangles appear in areas of the brain that are unaffected in single mutant-tau transgenic mice (Levis *et al.*, 2001). In a parallel experiment another group showed that injection of amyloid into the cerebrum of mutant tau transgenic mice exacerbated tangle pathology in another brain region from where neurons project to the injection site (Gotz *et al.*, 2001)

1.5 Detail description of β-secretase (BACE)

1.5.1 Discovery of β-secretase (BACE)

In late 1999, β-secretase was identified as a novel membrane-bound protease of 501 amino acids in length belonging to the pepsin family of aspartyl protease. The enzyme has been named as β-site cleaving enzyme (BACE), Asp2 and memapsin 2 by four different groups (Hussain *et al.*, 1999; Sinha *et al.*, 1999; Vassar *et al.*, 1999; Yan *et al.*, 1999). The targeting of this protease for specific inhibitors of β-amyloid production has opened a new therapeutic approach in treating Alzheimer's

disease. At the amino acid level, BACE shows less than 30% sequence identity with human pepsin family members, with most similarity to cathepsin E (30% identity, 37% similarity). The homology to other pepsins is highest in the central portion of BACE, while the NH_2- and COOH-termini are more divergent. The low sequence similarity of BACE to pepsins together with the putative transmembrane domain indicate that BACE may define a new subclass of membrane-bound aspartic proteases.

It has previously been reported that BACE mRNA is expressed widely at low levels, at moderate levels in the brain and at higher levels in the pancreas (Vassar *et al.*, 1999; Yan *et al.*, 1999). However, β-secretase activity is low in pancreas and highest in brain (Sinha *et al.*, 1999). This discrepancy between mRNA and activity is probably due to a slice variant lacking two-thirds of exon 3 being the predominant BACE transcript in pancreas, resulting in a protein that is incompletely processed and retained in the endoplasmic reticulum (Bodendorf *et al.*, 2001). In the brain, BACE mRNA is widely expressed only in neurons, with most pronounced expression in the cerebellum, cortex and hippocampus observed by *in situ* hybridization (Vassar *et al.*, 1999). BACE is co-localized with its substrate, APP, in the trans-Golgi network of cells (Hussain *et al.*,1999; Vassar *et al.*, 1999).

1.5.2 Detailed structure of BACE

As commonly found in other aspartyl proteases, BACE was synthesised as zymogen with a pre- and pro-domain which are proteolytically cleaved by signal enzymes. The BACE protein has an NH_2-terminal signal peptide of 21 amino acids followed by a proprotein domain spanning amino acid 22 to 45. The lumenal domain of the protein extends from residues 46 to 460, and is followed by one predicted transmembrane domain of 17 residues and a short cytosolic COOH-terminal tail of 24 amino acids (Vassar *et al.*, 1999).

BACE contains two active site motifs at amino acids 93 to 96 and 289 to 292 in the lumenal domain. Each motif contains the highly conserved signature sequence of aspartic proteases, $D^T/_SG^T/_S$, within which the aspartic acid residue is essential for catalytic activity (reviewed by Rawlings and Barrett, 1995). BACE also has four putative N-linked glycosylation sites and six lumenal cysteines, which would allow the formation of up to three intramolecular disulfide bonds. Thus, BACE is predicted to be a type I transmembrane protein with the active site on the lumenal side of the membrane, where it catalyses the cleavage of APP. A schematic presentation of human BACE is shown in Fig. 3-1A.

The pro-domains are commonly found in protease precursors where they have been shown to virtually abolish catalytic activity (Khan and James, 1998) and to

assist in protein folding (Baker *et al.*, 1993; Shi *et al.*, 2001). The pro-domain is typically cleaved from the protease precursor to generate the mature active protease. Edman degradation of purified human brain BACE revealed a single N-terminal protein sequence that began at the protease domain (Sinha *et al.*, 1999) (this species was designated as mature BACE).

1.5.3 Comparsion of human and mouse BACE

The mouse homolog of BACE was identified through a computer search of an Amgen expressed sequence tag database. The mouse BACE (GenBank Accession number AF190726) has 93% sequence identity with the cDNA of human BACE. Both the mouse cDNAs encode proteins of 501 amino acids that have 96% identity with the human BACE protein (Vassar *et al.*, 1999). Fig. 3-1B shows the schematic diagram of mouse BACE structure.

1.5.4 Comparsion of BACE-1 with BACE-2

A close homologue was also identified and termed as BACE-2, Asp1, DRAP, or memapsin 1 (Hussain *et al.*, 1999; Acquati *et al.*, 2000; Farzan *et al.*, 2000; Lin *et al.*, 2000). Both enzymes are type I membrane proteins sharing significant homology with other members of the aspartyl protease family (Sinha *et al.*, 1999; Vassar *et al.*,

1999; Yan *et al.*, 1999; Lin *et al.*, 2000). The role of BACE-2 in the pathogenesis of Alzheimer's is presently unclear as BACE-2 is predominantly expressed in peripherial tissues.

1.5.5 Properties of BACE

According to the current hypothesis, BACE and APP are both membrane proteins present in human brain and are co-localized in the same neuronal cells (Vassar *et al.*, 1999; Hussain *et al.*, 1999; Lin *et al.*, 2000). BACE specifically cleaves the β-secretase site of APP in cells and preferentially cleaves the β-secretase site from the Swedish mutation over the wild-type APP (Vassar *et al.*, 1999; Yan *et al.*, 1999; Ermolieff *et al.*, 2000; Lin *et al.*, 2000). The acidic pH optimum for BACE activity (Ermolieff *et al.*, 2000; Lin *et al.*, 2000) is consistent with the previous observations that β-secretase cleavage occurs in acidic vesicles (Knops *et al.*, 1995). BACE is not inhibited by many protease inhibitors, such as leupeptin (serine/cysteine proteinase inhibitor), 3,4-DCIC (serine proteinase inhibitor), PMSF (serine/cysteine proteinase inhibitor) and the classical aspartyl protease inhibitor pepstatin (pepsin inhibitor) in *vitro*, though BACE is structurally related to the pepsin aspartic protease family (Vassar *et al.*, 1999; Bennett *et al.*, 2000; Mallender *et al.*, 2001). BACE may be a new class of protease because of its broad spectrum inhibitor insensitivity despite its sequence classification as an aspartyl protease (Yamazaki and Ihara, 1998; Vassar *et*

al., 1999).

Swedish mutation is associated with family early onset of Alzheimer's disease (Mullan *et al.*, 1992; Cai *et al.*, 1993). Overproduction of the 42-amino acid form of Aβ, Aβ42, has been suggested to be the cause of all known cases of familial early onset AD (Younkin, 1998). This is correlated with the results that BACE showed higher preference of cleavage towards Swedish mutation peptide than wild type peptide (Vassar *et al.*, 1999; Yan *et al.*, 1999; Lin *et al.*, 2000) and much greater release of Aβ from cells stably transfected with Swedish mutation APP than those with wild type APP (Citron *et al.*, 1992; Hussain *et al.*, 1999; Vassar *et al.*, 1999).

1.5.6 Expression of BACE in *E.coli*

In this study, both the cDNAs for human and mouse BACE were cloned by reverse-transcription polymerase chain reaction (RT-PCR). The cDNAs of human and mouse BACE with the deletion of transmembrane region and pro-domain were also amplified by PCR approach and then subcloned into prokaryotic expression vectors. The objective was to provide recombinant BACE expressed in *E.coli*. The human BACE cDNA with deletion of transmembrane and pre-region was named as prohBACE. The human BACE cDNA with deletion of transmembrane, pre- and

pro-region was named as nohBACE, where 'h' means human. Similarly, the mouse BACE cDNA with deletion of transmembrane, pre and pro region was named as nomBACE gene, where 'm' means mouse. Fig 3-1A and 3-1B shows the schematic diagram of human and mouse BACE and their domain organisation.

1.5.7 Expression of BACE in mammalian cells

In this study, stably transfected cell lines over-expressed with human and mouse BACEs were developed. The reason for expression of protein in mammalian cells was to compare with those in *E.coli*. Although the expression of protein in *E.coli*, can allow us to obtain larger amount of protein in relatively short time, however, due to incorrect folding in inclusion body, most of proteins are inactive unless they refold correctly under special conditions. The expression of protein in mammalian cells, on the other hand, can allow us to obtain a more correctly refolding protein, and is more close to cells that produced in *vivo*. The stably transfected cell lines are also an excellent model system to investigate the intracellular trafficking and location of BACE in the cells.

In this study, both the full coding sequences of mouse and human BACE were subcloned into mammalian expression vectors pCDNA3 and pCDNA4HisMax. These vectors were used to transfect Chinese hamster ovary (CHO) cells.

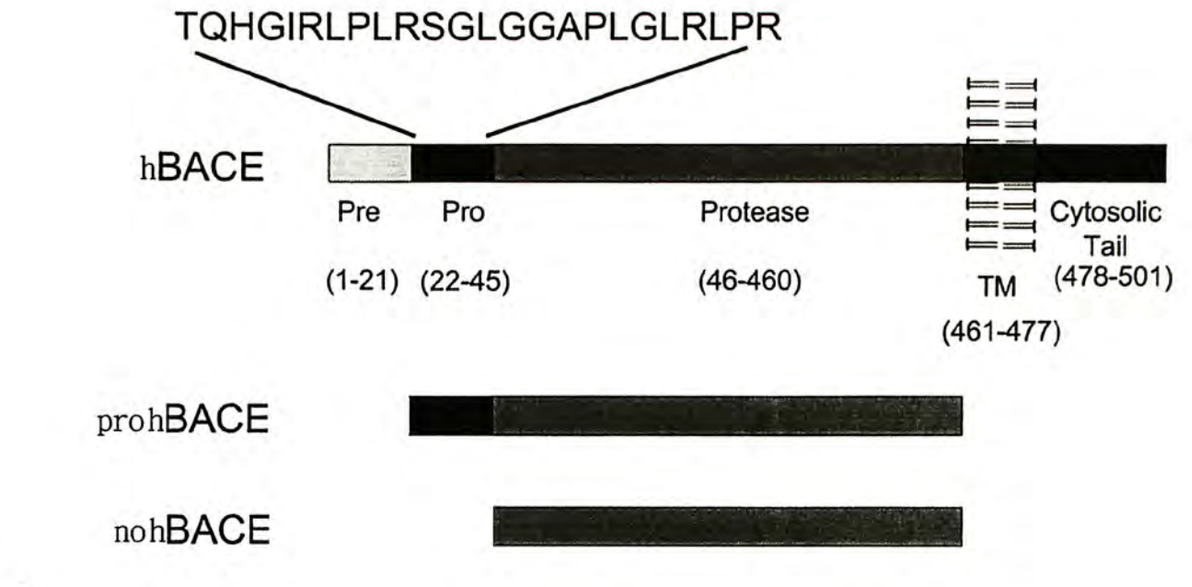

A

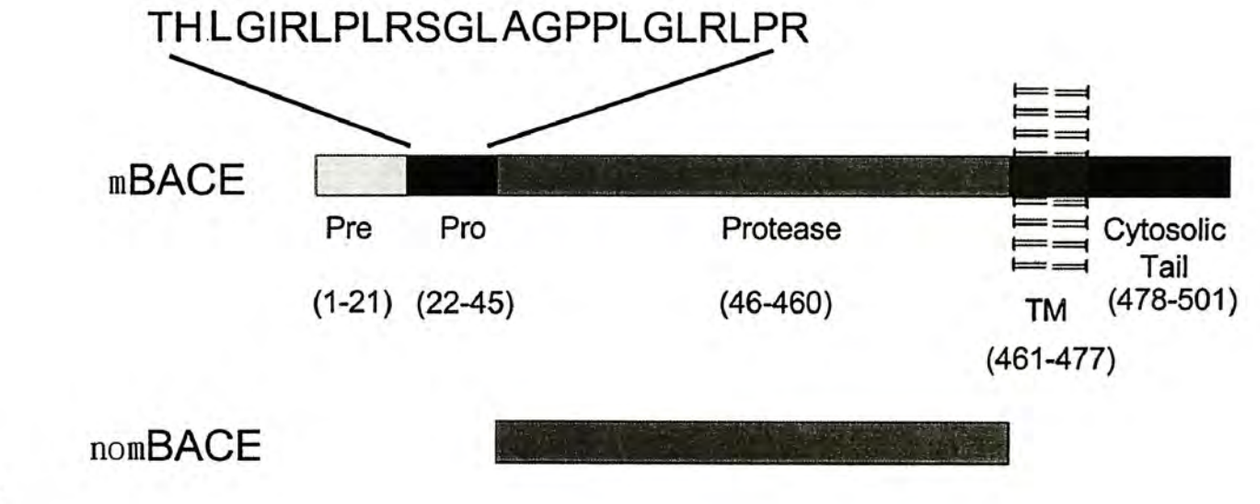

B

Fig. 3-1 Schematic representation of the protein structure of the human (A) and mouse (B) BACE precursor protein and its domain structure as deduced from its cDNA sequence. Full length BACE is composed of several domains that include the Pre(residues 1-21), Pro (residues 22-45), protease (residues 46-460), transmembrane (TM; residues 461-477) and cytosolic tail (residues 478-501) regions. The amino acid sequence of the putative pro-region is shown (Shi *et al.*, 2001).

1.6 Objectives of the present study

At the beginning of my thesis, much of work has already been done to investigate the protease that functions as β-secretase. However, not much progress has been made until four different research groups independently cloned the then elusive β-secretase by genetic screening, direct enzyme purification and sequencing approaches (Vassar *et al.*, 1999; Yan *et al.*, 1999, Sinha *et al.*, 1999; Hussain *et al.*, 1999). The β-secretase was named as beta-site APP-cleaving enzyme (BACE) and membrane-bound aspartyl protease (Asp2). BACE possesses many of the features of β-secretase. BACE can cleave full-length APP at Asp1 of the Aβ sequence and also at Glu11, which is an alternative cleavage site (Vassar *et al.*,1999). The Swedish mutation, which is known to enhance β-secretase cleavage (Forman *et al.*, 1997), also promotes cleavage of APP at Asp1 by BACE (Vassar *et al.*, 1999). BACE is expressed coordinately with APP in many regions of the brain, particularly in neurons, and has a subcellular distribution similar to that of β-secretase (Vassar *et al.*, 1999). Cell biology studies suggest three potential sites of intracellular BACE activity: endosomal/lysosomal compartments, Golgi apparatus and endoplasmic reticulum/intermediate compartments in postmitotic neurons (Chyung *et al.*, 1997). BACE has an acidic pH optimum(Vassar *et al.*, 1999; Ermolieff *et al.*, 2000).

After the elucidation of BACE, the BACE has become a potential drug target for AD drug treatment. My study is thus aimed at setting up reliable assay systems for BACE. This involved the cloning of mouse and human BACE by PCR and subcloning of these cDNAs into appropriate expression vectors. The expression of BACE protein from *E.coli.* and mammalian cells. The stable cell lines overexpressed with mouse BACE and human BACE were established. Enzymatic assays were established by the synthesis of model peptide substrates for proteolyic cleavage by recombinant BACE by analytical reverse-phase high performance liquid chromatography (RP-HPLC). The activity of recombinant enzyme was also measured by a fluorometric assay with a custom-made fluorogenic substrate. .

Besides, the intracellular location of BACE was studied by immunofluorescence. Polyclonal antibody, hBACE485, purchased from ALEXIS was used as primary antibody. Immunohistochemistry was conducted to the mammalian cell line stably expressing BACE using the polyclonal antibody to determine intracellular location of BACE.

Chapter 2 Materials and Methods

Chapter 2

Materials and Methods

2.1 Recombinant DNA techniques

2.1.1 Amplification of genes by PCR techniques

Polymerase chain reaction (PCR) was performed with 5 μ g/ml template in 2 μ l of 10 μ M forward primer, 10 μ M backward primer, 0.2mM dNTPs, 1.5 mM $MgCl_2$, 1 x PCR buffer (20 mM Tris-HCl, pH 8.4 and 50 mM KCl), 5% DMSO and Tag DNA polymerase (Invitrogen) of 2.5 U. Thirty-five cycles were done at the following temperatures: 94°C for 1 minute, 58 °C for 30 seconds, and 72 °C for 2.5 minutes and 7 minutes final extension at 72 °C.

2.1.2 Agarose gel electrophoresis

DNA was usually separated by 1 % (w/v) TAE agarose gel. Agarose was weighed at 1% (w/v) according to the gel volume. It was then dissolved by heating in 1xTAE buffer. The gel solution was cooled to luke-warm before ethidium bromide (EB) (at a final concentration of 0.5 μg/ml) was added. The gel solution was poured to the gel tray with comb inserted near the top margin. After 30 minutes hardened gel was formed. DNA sample was mixed with 6x gel loading buffer to obtain 1x final

concentration. After the gel was formed, it was put into the gel-tank pre-filled with TAE buffer at the level just covering the gel. Then the sample was loaded into the sample slots of the gel. The setup was operated at a rate of 8V/cm until the bromophenol blue dye was migrated to the desired distance. The separated DNA band(s) in the gel could be examined under UV illumination. The gel photo was taken by Polaroid MP-4 instant camera on Polaroid film.

2.1.3 Extraction of DNA from agarose gel

The extraction was done according to QIAquick Gel Extraction Kit (Qiagen, USA). The DNA fragment was excised from agarose gel with a clean, sharp scalpel. After weighing the gel slice in a colorless tube. 3 volumes of Buffer QG was added to 1 volume of gel. The gel buffer solution was incubated at 50 °C for 10 minutes. To help dissolve the gel, the solution was vigorously mixed by vortexing the tube every 2 minutes during the incubation. After the gel slice was dissolved completely that that the color of the mixture became yellow, the gel solution was loaded on a QIAquick spin column in a provided 2 ml collection tube. The column was then centrifuged at 10,000 x g for 1 minute to remove unbounded materials. The column was then washed by adding 0.75 ml of buffer PE to the column followed by centrifugation for 1 minute. The flow through was discarded and the column was washed once more with 0.75 ml buffer PE. An amount of 30 µl elution buffer was added and after incubation

for 1 minute, the bound DNA was eluted from the column by centrifugation at 10,000 x g for 1 minute to a 1.5 ml microfuge tube.

2.1.4 Digestion of various vectors and insert

Restriction digestion of DNA was carried out in a reaction volume of 20 µl for small amount of DNA (0.5 to 5 µg). The reaction mixture consisted of DNA sample, appropriate restriction digestion buffer, double distilled water, bovine serum albumin (BSA) (optional) and restriction enzyme(s). The selection of restriction digestion buffer was based on the type of restriction enzyme in use and was according to the manufacturer's suggestion. The amount of restriction enzyme added was usually in activity units 5-fold or higher of the DNA amount in microgram. The reaction was incubated at the optimal temperature of the enzyme in use for 2 hours or longer. After digestion, the products were analyzed by agarose gel electrophoresis.

2.1.5 Ligation of DNA fragments

The following procedure describes the general condition for ligation of foreign DNA to a linearized vector. 100 ng of the vector and 3-fold molar amount of foreign DNA were mixed together. Then 10x ligation buffer was added to the reaction mixture to a final concentration of 1x. 1 unit of T4 DNA ligase (Promega) was added

and the mixture was incubated at 16°C for 16 hours.

2.1.6 Preparation of Escherichia coli competent cells

An appropriate strain of *Escherichia coli (E.coli)* was streaked directly from a –70°C frozen stock onto the surface of a LB agar plate and incubated for 16 hours at 37°C. A single bacterial colony was picked by a sterile toothpick and inoculated into 50 ml LB medium. Bacteria cultures were allowed to grow overnight at 37°C with constant shaking at 250 rpm. An aliquot of 4-ml culture was inoculated into 400 ml LB medium in a sterile 2-liter flask. The cells were allowed to grow at 37°C until OD_{600} reaching 0.4, which represents a cell density of $4\text{-}7 \times 10^7$ cells/ml. Then the culture was chilled in ice for 15 minutes. The cells were harvested by centrifugation at 1600 x g for 10 minutes at 4 °C. The supernatant was discarded and the pellet was resuspended in 10 ml of ice-cold $CaCl_2$ solution. The cells were collected by centrifugation at 1100xg at 4 °C for 5 minutes. The supernatant was discarded and the pellet was resuspended in 10 ml ice-cold $CaCl_2$ solution and was incubated on ice for 30 minutes. The cells were then collected by centrifugation at 1100xg at 4 °C for 5 minutes. The supernatant was discarded and the pellet was resuspended in 2 ml ice-cold $CaCl_2$ solution. The cells were dispensed in aliquots of 250 µl into 1.5 ml tubes and kept frozen immediately at –70°C until use.

2.1.7 Bacterial transformation

A frozen tube of competent cells was thawed in an ice bath. An appropriate amount of plasmid (1-10 ng) or ligation mixture was added to the competent cells, followed by mixing moderately and kept chilling on ice for 30 minutes. The mixture tube was then heat-shocked at 42°C by incubating the tube in water bath for 90 seconds. Then the tube was again chilled in ice rapidly for 10 minutes. An amount of 500 µl of 37°C pre-warmed LB medium was added to the tube in sterile condition. The tube was incubated in 37°C for 45 minutes and appropriate fraction of the cells was spread evenly onto a LB plate with antibiotic according to the resistance conferred by the transformed plasmid. The plate was placed in an inverted position in an incubator at 37°C for 16 hours to obtain plasmid-containing colonies.

2.1.8 Minipreparation of plasmid DNA

A single bacterial colony was inoculated into 2.0 ml LB medium containing the containing the appropriate antibiotic in a capped sterile tube. The culture was incubated overnight at 37°C with vigorous shaking. The bacterial cells were collected by centrifugation at 12,000 x g for one minute at room temperature in a microcentrifuge. The bacterial pellet was suspended in 200 µl solution I. Then 100 µl solution II was added and the mixture was kept on ice for 5 minutes. After 150 µl

solution III was added, the mixture was centrifuged at 12,000xg for 10 minutes at 4°C. The supernatant was transferred to fresh tube containing 800 µl 95% ethanol and was allowed to sit at room temperature for 2 minutes. Plasmid DNA and RNA were collected by centrifugation at 12,000g for 1 minute. After removing the supernatant, the pellet was washed with 1 ml of 70% ethanol and dried under vacuum. The pellet was resuspended in 30 µl TE buffer and RNase (at final concentration of 100 µg/ml) was added to digest the RNA remained in the solution.

2.1.9 Large scale preparation of plasmids

A single colony of bacteria containing cloning plasmid was inoculated into 2 ml LB medium containing 100 µg/ml ampicillin or appropriate antibiotic. After an overnight incubation at 37°C with constant shaking, a 1-ml aliqot of the bacterial culture was inoculated to 100ml LB medium containing 100 µg/ml ampicillin in a 500-ml flask and incubated at 37°C with constant shaking until the culture reached saturated condition (OD_{600}=4). The cells were collected by centrifuging for 12 minutes at 6000 x g at 4°C and the resulting cell pellet was resuspended in 4 ml solution I, followed by an addition of 8ml solution II to the mixture. After an incubation on ice for 10 minutes. 6 ml solution III was added to the mixture and allowed to stand on ice for 15 minutes. The mixture was then centrifuged for 20,000g for 10 minutes at 4°C and the resulting supernatant was collected. A 0.6 volume of

isopropanol was added to the supernatant and incubated room temperature for 20 minutes. The solution was centrifuged at 20,000g for 15 minutes. The resulting DNA pellet was then washed with 75% ethanol and dried under vacuum. The DNA pellet was resuspended in 1 ml TE buffer and stand at $4^{O}C$ overnight. The insoluble material was removed by centrifugation at 20,000 x g for 5 minutes. The clear supernatant was transferred to a clean tube. The plasmid DNA was further extracted with 1 volume of buffered phenol, then with 1 volume of chloroform/isoamyl alcohol (24:1v/v). After transferring the aqueous phase to a clean tube, an amount of 1/4 volume 10 M ammonium acetate (2M final concentration) and 2 volumes of 100% ethanol were added and mixed thoroughly. The plasmid DNA was recovered by centrifuging for 10 minutes at 10,000 x g at $4^{o}C$. After washing the pellet with 70% ethanol and dried briefly under vacuum. The DNA pellet was resuspended in 2 ml TE buffer followed by an addition of 0.8 ml polyethylene glycol (PEG) solution. After an incubation for 1 to 15 hours at $0\,^{o}C$, the plasmid DNA was recovered by centrifuging for 20 minutes at 10,000g x g at $4^{O}C$. The purified plasmid DNA was finally re-dissolved in 1 ml TE buffer. If necessary, the plasmid DNA was ethanol precipitated by acidifying the solution with 3M sodium acetate, pH 5.5 followed by an addition of 2 volumes of ethanol.

2.1.10 Strain storage and revival

After successful transformation, the bacteria strain was kept for long-term storage by making glycerol stock for future use. Briefly, a single bacterial colony was picked on sterile toothpick and inoculated by dipping the toothpick in 2 ml LB medium in a sterile Falcon tube. After growing the bacteria culture at 37°C with constant shaking at 250 rpm until the optical density of the bacteria culture reached OD_{600} of approximately 0.6. An amount of 1-ml bacteria culture were taken and mixed with 1ml of 30% glycerol and stored at –70°C.

Upon retrieval of bacterial clone, the cell stock in frozen glycerol-LB culture was picked by scraping with a flame-sterile, cooled inoculating loop and inoculated in LB medium with or without antibiotic according the properties of the bacteria.

2.1.11 Plasmid DNA purification by High Pure plasmid isolation kit

The purification of plasmid DNA was done by high pure plasmid isolation kit (Roche). A single bacterial colony was grown in 2 ml LB medium containing appropriate antibiotics until the optical density of the culture reached OD_{600} at 2.0. The bacterial cells were then recovered by centrifugation at 9,000 rpm for 30 seconds. After carefully removing the supernatant, the pellet was resuspended in 250 µl Suspension Buffer and RNase and mixed well. The solution was mixed gently with

250 µl Lysis Buffer by inverting the tube 3 to 6 times and then incubated at room temperature for 5 minutes. 350 µl of Binding Buffer was added and mixed gently by inverting the tube 3 to 6 times and incubated on ice for 5 minutes. The solution was then centrifuged on a microcentrifuge at 14,000 rpm for 10 minutes and the supernatant was transferred to the upper reservoir of each of the High pure filter tube (Roche) connected to an collection tube. The tube was centrifuged at 14,000 rpm for 60 seconds and the flow-through solution was discarded. After connecting the filter tube to the same collection tube, an amount of 700 µl Wash Buffer II was added to the upper reservoir and centrifuged at 14,000 rpm for 60 seconds. The flow-through solution was discarded and another 700 µl Wash buffer was added to the filter tube and the washing procedure was repeated two times. After the washing steps, the filter tube was connected into a clean 1.5 ml microcentrifuge tube. An amount of 100 µl Elution Buffer was added to the upper reservoir of the filter tube and the bounded DNA was eluted from the filter tube by centrifugation at 14,000 rpm for 30 seconds.

2.1.12 DNA sequencing

The cloned plasmid DNA was sequenced to confirm identity of the cDNAs and to ensure proper open reading frame of the cDNAs was obtained. Sequencing reactions were boiled at 95°C for 5 minutes and cycled for 40 times at 94°C for 36 seconds, 50°C for 36 seconds, 72°C for 2 minutes and a 10 minutes final extension at

72°C using T7 or T3 universal sequencing primers. The sequencing products were run and analyzed in LI-COR 4200 DNA sequencer or MegaBACE 1000 system.

2.1.13 Quantitation of DNA by spectrophotometric method

The DNA concentration was calculated by spectrophotometric method based on the following relationship: $OD_{260\ nm}$ =1 is equivalent to to 50 μg/ml double-stranded DNA. A small volume (1-10 μl) of DNA sample was diluted in 500 μl TE buffer and the diluted DNA sample was transferred to a quartz curvette. The absorbance was measured at $OD_{260\ nm}$ so that the reading was in the range 0.1-1 by adjusting the dilution of sample. TE was used as blank to correct for background absorbance. The purity of DNA sample could be determined by the ratio of its absorbance at $OD_{260\ nm}$ and $OD_{280\ nm}$. If the ratio of the former data to the latter data is 1.8 or above, the DNA sample was considered to be pure.

2.2 Prokaryotic protein expression

2.2.1 Selection of appropriate clones for recombinant protein expression using conventional method

The bacterial colonies harboring expression vectors suitable for recombinant protein expression (i.e. BL21(DE3)LysS strain of *E. coli*) were screened

for proper induction of recombinant protein expression. It was done by streaking the frozen bacterial stocks on LB agar plates with appropriate antibiotics. After an overnight incubation at 37°C, selected bacterial colonies were grown in 2 ml LB medium with 100 µg/ml ampicillin and 37 µg/ml chloramphenical at 37°C overnight with orbital shaking at 240 rpm. 10 µl of cell culture was added to 2 ml freshly prepared LB medium with 100 µg/ml ampicillin and 37 µg/ml chloramphenical. Cells were collected when cell density reached OD_{600} of 0.2-0.6. Afterwards, an aliquot of 0.5 ml of bacterial culture was taken and kept for SDS-PAGE analysis and an aliquot of 0.5 ml for preparing 15 % glycerol stock. The remaining bacterial culture was used for induction of expression of recombinant protein by 0.4 mM IPTG and the culture was allowed to grow for 3 hours at 37°C with orbital shaking at 240 rpm for optimal recombinant protein expression.

2.2.2 Selection of appropriate clones for recombinant protein expression using modified method

Modified expression method was performed according to (Studier *et al.*, 1990). The bacterial colonies harboring expression vectors suitable for recombinant protein expression were screened for proper induction of recombinant protein expression. It was done by streaking the frozen bacterial stocks on LB agar plates with appropriate antibiotics. After an overnight incubation at 37°C, selected bacterial

colonies were grown in 2 ml LB medium with 100 μg/ml ampicillin and 37 μg/ml chloramphenical at 37°C until OD_{600} reach 0.2-0.6 with orbital shaking at 240 rpm. The cells were pelleted at 10,000 x g for 2 minutes. After removing the supernatant, the cells were resuspended in 2 ml fresh LB. An aliquot of 100 μl culture was added to 8 ml LB containing 100 μg/ml ampicillin and 37 μg/ml chloramphenical. Bacterial culture was allowed to grow until OD_{600} reach 0.2-0.6 with orbital shaking at 240 rpm. The cells were collected at 6,000 x g for 6 minutes and resuspended in 2 ml LB containing 100 μg/ml ampicillin and 37 μg/ml chloramphenical. Afterwards, an aliquot of 0.5 ml of bacterial culture was taken and kept for SDS-PAGE analysis and an aliquot of 0.5 ml for preparing 15 % glycerol stock. The remaining bacterial culture was used for induction of expression of recombinant protein by 0.4 mM IPTG and the culture was allowed to grow for 3 hours at 37°C with orbital shaking at 240 rpm for optimal recombinant protein expression.

2.2.3 Large –scale expression of recombinant human BACE protein using modified method

The clone that was demonstrated to express human BACE protein as indicated by SDS-PAGE analysis was used for a large-scale culture. The streaking of the 15% glycerol bacterial stock of that clone was added into 2 ml LB broth with 100 μg/ml ampicillin and 37 μg/ml chloramphenical, and grown in 100 ml LB broth with

100 μg/ml ampicillin and 37 μg/ml chloramphenical at 37°C until OD_{600} reach 0.2-0.6 with orbital shaking at 240 rpm. The cells were centrifuged at 10,000 x g for 2 minutes. After removing the supernatant, the cells were resuspended in 100 ml LB. An aliquot of 5 ml culture was added to 400 ml LB containing 100 μg/ml ampicillin and 37 μg/ml chloramphenical. Bacterial culture was allowed to grow until OD_{600} reach 0.2-0.6 with orbital shaking at 240 rpm. The cells were collected at 6,000 x g for 6 minutes and resuspended in 100 ml LB containing 100 μg/ml ampicillin and 37 μg/ml chloramphenical. An aliquot of 1 ml of bacterial culture was taken and kept for SDS-PAGE analysis. The induction of expression of recombinant protein was then initiated by the addition of 0.4 mM IPTG into the remaining bacterial culture and the culture was allowed to grow for 3 hours at 37°C with orbital shaking at 240 rpm.

2.2.4 Preparation of inclusion body from the bacterial expression culture

After induction of bacterial cells with IPTG, the cells were centrifuged at 5,000 x g for 5 minutes. After decanting the LB broth, the pellet was dried as much as possible. The cells were dispersed by the addition of 40 ml binding buffer, followed by a brief sonication on ice. The cell solution was centrifuged at 16,000g for 15 minutes to collect inclusion body. The pellet, which consisted of inclusion body, was resuspended in 20 ml binding buffer and then centrifuged at 16,000 x g for 15 minutes. After removing the supernatant, the pellet was resuspended in 20 ml buffer B with 8

M urea or in 2 ml buffer D with 6 M guanidine hydrochloride and incubated at room temperature for 1 hour to dissolve protein completely. Insoluble debris was removed by centrifugation at 16,000 x g for 30 minutes.

2.2.5 Refolding of human BACE

The protein was renatured by rapid dilution the protein solution in binding buffer B or buffer D to yield a final concentration of 0.8 M urea or 0.1 M guanidine HCl and incubated at room temperature for 2 and 6 hours respectively. The solution was then centrifuged at 10,000 x g for 20 minutes. The recombinant human BACE solution was concentrated by Centriprep 30 (Centricon) and stored in aliquots at –80°C.

2.2.6 Purification of recombinant human BACE by immobilized metal ion affinity chromatography (IMAC)

As the recombinant protein contained poly histidine residues at the N-terminus as a fusion tag, the protein can easily be purified by immobilized metal ion affinity chromatography (IMAC). The Chelating Sepharose Fast Flow (Pharmacia Biotech) consists of iminodiacetic acid groups coupled to Sepharose Fast Flow by stable ether linkages via a 7-atom spacer. The gel was washed with 3 columns of

double distilled water. Then, it is charged with nickel, Ni^{2+} ions by adding one column of 0.1 M $NiSO_4$. After washing the column with 2 columns of double distilled water and was equilibrated with 2 columns of buffer B with 0.8 M urea or buffer D with 0.1 M guanidine HCl. The human BACE solution in buffer B with 0.8 M urea or buffer D with 0.1 M guanidine HCl was then applied to the column. Unbounded proteins were washed from the column by the addition of 2 column-volumes of buffer B with 0.8 M urea or buffer D with 0.1 M guanidine HCl containing 50 mM imidazole. The histidine-tagged recombinant protein was finally eluted by eluting the column with 1 column-volume of buffer B with 0.8 M urea or buffer D with 0.1 M guanidine HCl with 200 mM imidazole.

2.2.7 Protein concentration determination

The protein concentration was determined by Bradford method (1976) (Bradford, 1976) and bovine serum albumin (BSA) was used as protein standard.

2.2.8 Sodium dodecyl sulfate polyacrylamide gel electrophoresis (SDS-PAGE)

The Mini-PROTEAN II electrophoresis cell (Bio-Rad) was used for SDS-PAGE. The gel-mould was assembled according to the manufacturer's instruction. Before casting the gel, small amount of distilled water was added to fill up

the gel-mould to check if leaking occurred. After draining the last bit of water by inserting filter paper strip between the two glass plates, 5 ml of 12% separating gel solution was then mixed according to section 2.7.4. The solution was pipetted into the gel-mould to two-third of total gel volume for preparation of the running gel. After the gel solution was pipetted to the gel gap at one side, a thin layer (approximately 1 cm) of isopropanol was then added on the top of the solution surface to remove air bubbles and to keep the solution away from air. The gel was allowed to polymerize for more than 30 minutes. After polymerization, isopropanol was removed from the gel top. The stacking-gel mix was prepared according to section 2.7.4, and was pipetted on top of the running gel. A sample comb for sample slots was inserted into the stacking-gel layer immediately. The gel was ready to use after 15 minutes. The gel set up was assembled in the Bio-Rad gel-tank. Freshly prepared SDS-PAGE running buffer was poured to the cavity formed by electrode-unit and to the surrounding space. Protein samples were mixed with SDS sample loading buffer and boiled at 100°C for 10 minutes. An amount of 40 µl of each denatured sample was loaded into the sample slot. The system was operated at a constant voltage of 120 V for 2 hours or until the blue front-dye just reaching the gel-end.

Proteins on the gel was stained by immersing the gel in a staining solution. Staining could be done faster by staining at 42°C for 30 minutes. Excess stain was removed by gentle agitation in a destaining solution.

2.2.9 Western blotting

After running SDS-PAGE as described previously, the gel used in Western blotting was immersed in transfer buffer for 30 minutes and transferred with a Mini Trans-Blot Electrophoretic Transfer Cell (Bio-Rad) onto a PVDF membrane (Millipore) at 15 V for 1 hour. Non-specific binding sites of the PVDF membrane with bound protein was blocked with immunoblotting buffer for 45 minutes at room temperature. The membrane was probed with suitable antibodies (1:5000) in immunoblotting buffer and incubated at 4°C overnight. Alkaline phosphatase (AP) labeled goat anti-rabbit IgG antibodies (ZYMED) was used as the secondary antibodies (1:2500) and the membrane was incubated at room temperature for 1 hour with secondary antibodies. After washing with immunoblotting buffer, followed by buffer 3, signal was detected by incubating with 5-Bromo-4-Chloro-3-Indolyl phosphate (BCIP) and nitroblue tetrazolium (NBT) in buffer 3 (at a final concentration of 0.01% and 0.02% respectively). The reaction was stopped until signal was detected by washing with distilled water.

2.2.10 Plasmid stability test

Plasmid stability test was performed according to (Studier *et al.*, 1990) to

determine the fraction of cells that carry the target plasmid. The test was done as follows. Just before induction in section 2.2.1, when the bacterial culture had reached OD_{600}=0.2-0.6, the culture were diluted into 10^5 fold and spread on LB plates with IPTG and with antibiotics and IPTG. The culture was diluted into $2x10^6$ fold and spread on LB plates only and LB plates with antibiotics. The cells were allowed to grow overnight at 37°C. For stable plasmids, almost all the cells will form colonies both on LB plates only and on LB plates containing antibiotics, less than 2% of cells will grow on LB plates containing IPTG, and less than 0.01% of cells will grow on LB plates containing antibiotics and IPTG.

2.3 Mammalian Cell Expression

2.3.1 Transient transfection

Chinese Hamster Ovary (CHO) cells were transfected with various plasmid constructs using Lipofectamine Plus Reagent (Life Technologies, Inc.). The CHO cells at the density of 1 x 10^5 cells were grown on 35 mm dishes, until the cells were 60-80% confluent. An amount (1 μg) of purified mammalian expression plasmid DNA and 6 μl of the Plus reagent (BRL) were added to 100 μl DMEM medium lacking serum and antibiotics and incubated for 15 minutes at room temperature. An amount of 4 μl of lipofectamine reagent was added to 100 μl DMEM medium lacking serum and antibiotics to another tube and incubated for 15 minutes at room

temperature. The two solutions were mixed and incubated for another 15 minutes at room temperature. The cells were washed in PBS twice and then 1 ml of DMEM medium lacking serum and antibiotics was added to the cells. The DNA-lipofectamine plus mixture was added directly to the cells and incubated for 4 hours at 37°C. After 4 hours incubation, the cells were rinsed in PBS and fresh DMEM medium supplemented with 10% FBS and 0.1 mM non essential amino acid (NEAA) was added followed by incubation for another 24 hours before harvesting the cells.

2.3.2 Measuring transfection efficiency

Cells transfected with plasmid containing *lacZ* gene were collected. The cells were washed twice with PBS. PBS was removed and the cells were fixed with 0.2% glutaraldehyde in PBS for 5 minutes at room temperature. The cells were washed with PBS for 3 times. PBS was removed and the cells were stained with X-gal solution and incubated in humidified incubator of 37°C until signals had been detected.

2.3.3 Stable transfection

Various mammalian expression plasmid constructs were transfected into CHO cells as described in section 2.3.1. Transfected cells were grown in a 25 cm^2

culture flask for 24 hours. The culture medium was then replaced by fresh complete medium containing of 1 mg/ml of Geneticin® (G418 sulfate) (Gibco, BRL) for the cultures were kept for 3 weeks with subculturing of cells when necessary. The stably transfected cells were maintained in complete medium containing of 1.2 mg/ml G418 .

2.3.4 Preparation of membrane extracts from CHO cells

After the culturing medium was removed, and the CHO cells were washed with sterile PBS twice. The cells were then lysed by incubation with lysis buffer for 30 minutes at 4°C. Cells were removed by centrifugation of 500 x g for 5 minutes. The supernatant was collected and centrifuged at 26,000 rpm for 10 minutes in an ultracentrifuge (Beckman). The pellet was dissolved in assay buffer.

2.4 HPLC analysis

2.4.1 Preparation of samples

The proteolytic activity of enzymes was analyzed by high performance liquid chromatography (HPLC). Two synthetic peptide substrates and one product peptide were synthesized in-house and used for the present study, which were shown in section 2.7.9. The amount of samples added were adjusted to 2 μg. The samples

were mixed according to section 2.7.9. and incubated for 2 hours at 37°C. The reaction was stopped by boiling and stored at –20°C. The supernatant were collected by centrifuging at 10,000 x g for 5 minutes and analyzed by HPLC.

2.4.2 Reverse phase HPLC

Samples were analyzed by reverse phase HPLC separation on a C_{18} Protein/peptide reverse phase column (Vydac C_{18} 218TP) using Waters HPLC system. The Vydac C_{18} reverse phase was first pre-equilibrated with buffer A at a flow rate 0.1 ml/min. An amount of 50 µl of sample mix, as shown in section 2.7.9, was loaded into the HPLC. The eluate was monitored at UV 214 nm at a flow rate of 1 ml/min. The column was eluted with a gradient according to the following table.

Table 1 Flow rate and different composition of buffer used in HPLC assay

Time (minutes)	Flow rate (ml/min)	% of Buffer A	% of Buffer B
0	1.00	100	0
2	1.00	100	0
32	1.00	0	100
40	1.00	0	100
45	1.00	100	0
50	1.00	100	0
51	0.10	100	0

2.5 Fluorometric assay

The BACE activity was also monitored by a fluorometric assay based on the

principle of fluorescence resonance energy transfer (FRET). Two fluorogenic substrates, FS-1 and FS-2 were shown in section 2.7.10. 2 μg of samples were added in each assay. The reaction mixture was prepared as described in section 2.7.10 and the enzyme activity was monitored by the release of quenched fluorescence. The mixture was incubated at 37°C for the fluorescence intensity was measured in a spectrofluorometer (SpectraMax Gemini) with an excitation wavelength of 350 nm and an emission wavelength of 490 nm at each hour interval.

2.6 Immunohistochemistry

The specimen were fixed in 4% paraformaldehyde solution at room temperature for 20 minutes, and further fixed with 100% methanol at room temperature for 5 minutes. The specimen were blocked with 2% normal goat serum in PBS and incubated at 37°C for 1 hour. It was then labeled by incubating for 3 hours with the hBACE485 antibody (1:50) in 2% normal goat serum in PBS, was then incubated at room temperature for 1 hour with fluorescein isothiocyanate (FITC)-conjugated goat anti-rabbit IgG (1:100) in PBS. The immunolabeled section was viewed in a Zeiss Axiophot microscope equipped with epifluorescence optics or examined in a Leica laser confocal microscope.

2.7 Reagents and buffers

2.7.1 Medium for bacterial culture

Luria-Bertani (LB) medium

Tryptone	10 g
Yeast extract	5 g
NaCl	10 g

The solution was made up to 1L with double distilled water and autoclaved at 121°C for 20 minutes

LB agar plate

The powder mixture in preparing LB medium was supplemented with 1.5% (w/v) bactoagar. 20 ml solution was poured to a 100 mm plate and cooled at room temperature until it was hardened. The plates were inverted and stored at 4°C.

LB agar plate with antibiotics

The procedures were the same as preparing LB agar plate except ampicillin (at a final concentration of 100 μg/ml) and/or chloramphenicol (at a final concentration of 37 μg/ml) was supplemented to the luke-hot LB agar solution before pouring onto plates.

2.7.2 Reagents for preparation of plasmid DNA

Solution I

Tris-base	6.06g/l
Na_2EDTA	3.36g/l
RNase	100 μg/ml of solution I

Solution II

NaOH	8g/l
SDS	1%

Solution III

Potassium acetate(pH4.8)	250.6 g/l

TE buffer

Tris-Cl, pH7.4	10 mM
EDTA, pH 8.0	1mM

PEG solution

PEG 8000	13%

Desired volume was made by filling with 1.6 M NaCl.

2.7.3 Buffers for agarose gel electrophoresis

TAE (Tris-acetate), 1x

Tris-base	4.84 g/l
Na_2EDTA	0.34 g/l
Acetic acid	20 mM

6x agarose gel loading buffer

Sucrose	40% (w/v)
Bromophenol blue	0.25% (w/v)

2.7.4 Buffers for SDS-PAGE

30% Acrylamide mix

Acrylamide	29 g/100ml
N, N'-Methylenebisacrylamide	1 g/100ml

The solution was dissolved by warming at 37 °C, filtered sterile and stored in darkness at 4 °C.

12% separating gel solution

ddH_2O	3.3 ml
30% acrylamide solution	4 ml

1.5 M Tris-HCL, pH 8.8	2.5 ml
10% SDS	100 µl
10% w/v ammonium persulfate (APS)	100 µl
TEMED	4 µl

5% stacking gel solution

ddH_2O	3.4 ml
30% acrylamide solution	0.83 ml
1.0 M Tris-HCl (pH 6.8)	0.63 ml
10% SDS	50 µl
10% APS	50 µl
TEMED	5 µl

SDS sample loading buffer 6x

Tris-HCl (1M, pH 6.8)	3.5 ml
SDS	1 g
DTT	0.93 g
Bromophenol blue	1.2 mg
Glycerol (99%)	3 ml

The solution was made up to 10 ml by ddH_2O and stored as 0.5 ml aliquots at $-70^{\circ}C$.

Running buffer

Tris-base	3.02 g/l
Glycine	18.8 g/l
10% SDS	10 ml/l

2.7.5 Buffer for purification of protein

Binding buffer 1 x

imidazole	5 mM
NaCl	0.5 M
Tris-HCl	20 mM

The pH was adjusted to 7.8.

Buffer B

Tris-HCL (pH7.5)	10 mM
dithiothreitol , DTT	10 mM

Buffer D

NaCl	125 mM
Tris-HCl	20mM

The pH was adjusted to 7.2.

2.7.6 Buffer for Western Blotting

Transfer buffer

Tris-HCl	25mM
Glycine	192 mM
Methanol	10% (v/v)

Immunoblotting buffer

Skimmed dry milk	5%
NaN_3	0.02%
Tris-HCl	50 mM
$CaCl_2$	2 mM
NaCl	80 mM

The pH was adjusted to 7.4 and prepared freshly.

Buffer 3

Tris-HCl (pH 9.5)	0.1M
NaCl	0.1M
$MgCl_2$	0.05m

Antibodies against BACE

hBACE122 (ALEXIS)

A rabbit polyclonal antibody raised against a 10-residue synthetic peptide (RDLRKGVYVP) corresponding to the human BACE gene (residues 122-131).

hBACE485 (ALEXIS)

A rabbit polyclonal antibody raised against a 17-residue synthetic peptide (C_{485}LRQQHDDFADDISLLK$_{501}$) corresponding to the human BACE gene C-terminal region (residues 485-501).

2.7.7 Culturing medium of CHO cells

DMEM medium

DMEM powder	10g
$NaHCO_3$	3.7g

The solution was made up to 10 ml by ddH_2O, pH was adjusted to 7.4 by 1M HCl or NAOH, and solution was filtered and stored at 4°C.

DMEM with 0.1 mM NEAA

10 mM NEAA solution was added to DMEM medium (final concentration of 0.1 mM)

DMEM medium with 0.1 mM NEAA and ampicillin

10,000 μg/ml penicillin-streptomycin was added to DMEM medium with 0.1 mM NEAA (final concentration of 100 μg/ml).

Lysis buffer

Tris-HCl, pH 7.4	50 mM
Triton X-100	1%
PMSF	1 mM
Leupeptin	0.5 μg/ml

Assay buffer

Sodium acetate, pH4.8	20 mM
Trition X-100	0.06%
EDTA, pH8.15	5 mM
PMSF	1 mM
Leupeptin	0.5 μg/ml

2.7.8 Solutions for estimating transfection efficiency

X-gal solution

X-gal (50mg/ml in dimethylformamide)	40 µl
0.5M $K_3Fe(CN)_6$	20 µl
0.5M $K_4Fe(CN)_6$	20 µl
1M $MgCl_2$	4 µl
1xPBS	1.916 ml

X-gal (50mg/ml in dimethylformamide) was added to the mixture just before use.

2.7.9 Reagents for HPLC

Substrate

BACE synthetic peptide substrate, EVKMDAEFR

(Acetyl-Glu-Val-Lys-Met-Asp-Ala-Glu-Phe-Arg-amide), prepared as 500 µM in 10% DMSO.

BACE synthetic Swedish mutation peptide substrate, SEVNLDAEFR

(Acetyl-Ser-Glu-Val-Asn-Leu-Asp-Ala-Glu-Phe-Arg-amide), prepared as 500 µM in 10% DMSO.

Cleavage peptide product, DAEFR

One peptide product of cleavage is (Asp-Ala-Glu-Phe-Arg-amide), prepared as 500 µM in 100% DMSO.

Sample mix (final volume of 50 µl) in 10% DMSO.

substrate (500 µM)	1 µl
sample	20 µl
assay buffer	29 µl

HPLC Buffer A

trifluoroacetic acid (TFA)	0.1%

The desiring volume was filled with nanopure water. The solution was filtered.

HPLC Buffer B

TFA	0.1%
Acetonitrile	80%

The remaining volume was filled with nanopure water. The solution was filtered in 0.22 µm filter.

2.7.10 Reagents for fluorometric assays

BACE fluorogenic Swedish mutation substrate, FS-1

(NH2-Arg-Glu(EDANS)-Glu-Val-Asn-Leu-Asp-Ala-Glu-Phe-Lys(DABCYL)-Arg-COOH) which was custom synthesized from SynPep (Dublin, CA, USA) and prepared

as 500 μM in 100% DMSO.

BACE fluorogenic wild-type substrate, FS-2 (N-acetyl-Arg-Glu(EDANS)-Val-Lys-Met-Asp-Glu-Phe-Arg-Lys(DABCYL)-Arg-amide), which was custom synthesized from Molecular Probes (Eugene, OR, USA) and prepared as 500 μM in 100% DMSO.

2.7.11 Reagents for Immunohistochemistry

Paraformaldehyde solution

paraformaldehyde	4%
sucrose	5%

The solution was made up to desired volume by PBS. The solution was incubated at 60°C for 20 minutes to solubilize paraformaldehyde.

Chapter 3 Results

Chapter 3

Results

3.1 Expression of BACE in *E.coli*

3.1.1 Cloning of truncated human and mouse BACE into pRSET

The cDNA for human BACE without the transmembrane and pre region, prohBACE (refer to Fig. 3-1A) was amplified by PCR techniques from human brain cDNA (in pCMV.SPORT purchased from BRL) using forward primer (hBACE_517F) and reverse primer (hBACE_R1833) (The primer sequences were shown in Appendix A2). A PCR product of about 1.3kb was amplified and extracted from gel by the QIAquick Gel Extraction Kit.

The cDNA for human BACE without transmembrane, pre and pro region, nohBACE (refer to Fig. 3-1A) was amplified by PCR techniques from human brain cDNA (in pCMV.SPORT purchased from BRL) using forward primer (hBACE_589F) and reverse primer (hBACE_R1833). Fragment of about 1.2kb were amplified and extracted from gel by the QIAquick Gel Extraction Kit (Fig. 3-1A).

The cDNA of mouse BACE without the transmembrane, pre and pro region, designated as nomBACE, was amplified by RT-PCR using total mouse brain RNA as

template. The forward primer (mBACE_147F) and reverse primer (mBACE_R1382). A PCR fragment of about 1.2kb was amplified and the amplified DNA was extracted from gel by the QIAquick Gel Extraction Kit.

The cDNA of nohBACE and prohBACE were subcloned into vector pRSETA (Invitrogen, the plasmid map was shown in Appendix A1-4) at the EcoRI and XhoI sites (Fig. 3-1A). The cDNA of nomBACE was subcloned into vector pRSETB at the EcoRI and NheI sites (Fig. 3-1B). The plasmids were purified by High Pure Plasmid Isolation Kit (Roche) and DNA sequencing was performed using T7 sequencing primer. The results from DNA sequencing showed that prohBACE in vector pRSETA (designated as prohBACE-pRSETA) and nohBACE in vector pRSETA (designated as nohBACE-pRSETA) had 98% similarity with the published human BACE mRNA sequence (GenBank Accession number AF190725) while nomBACE in vector pRSETB (designated as nomBACE-pRSETB) had 95% similarity with the published mouse BACE mRNA sequence (GenBank Accession number AF190726). After ensuring the nohBACE, prohBACE and nomBACE had successively been cloned into pRSET vector, the constructed plasmids were transformed into *E.coli* strain, BL21(DE3)LysS, which is specially designed for expression.

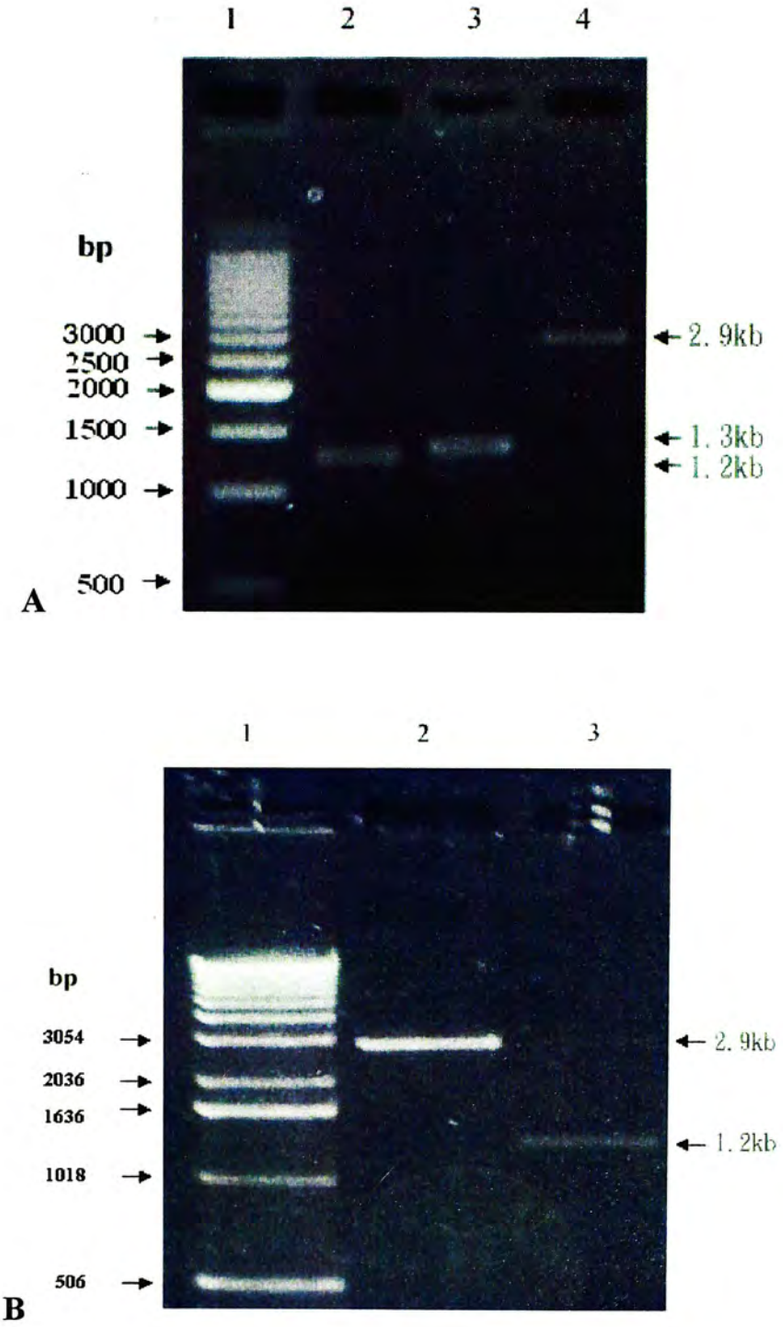

Fig. 3-1 (A) Digestion product of inserts (nohBACE and prohBACE) and vector (pRSETA) by restriction enzyme EcoRI and XhoI and was run in 1% agarose gel. Lane1. 500 bp marker. Lane 2. nohBACE cDNA of about 1.2kb. Lane 3. prohBACE cDNA of about 1.3kb. Lane 4. pRSETA of about 2.9kb. (B) Digestion product of insert, nomBACE and vector (pRSETB) by restriction enzyme EcoRI and NheI and was run in 1% agarose gel. Lane 1. 1 kb marker. Lane 2. Digested pRSETB of about 2.9kb as indicated by the marker. Lane 3. nomBACE gene of about 1.2kb as indicated by the marker.

3.1.2 Expression of BACE in BL21(DE3)LysS cells

3.1.2.1 Expression of truncated mouse and human BACE in BL21(DE3)LysS cells using conventional method

nomBACE, prohBACE and nohBACE were expressed in *E.coli* strain, BL21(DE3)LysS cells by induction of 0.4 mM IPTG (refer to section 2.2.1), the results were shown in Fig. 3-2A and Fig. 3-2B respectively. There was no apparent induction of mouse and human BACE when compared the expression profiles of the uninduced and induced cells. Much attempt had been tried to express the proteins, such as changing the concentration of IPTG, time of induction, expression of different clones (data not shown). However, no progress had been made. Finally, a plasmid stability test had been done, as described in section 2.2.10. According to the test, for stable plasmid, a very small proportion of cells will survive in LB plate with IPTG and almost all cells will survive in LB plate with antibiotics. However, the result of test showed a large number of cells survived in LB plate with IPTG and very few colonies survived in the LB plate with antibiotics. This proved the plasmids transformed were unstable or cDNAs transformed were toxic.

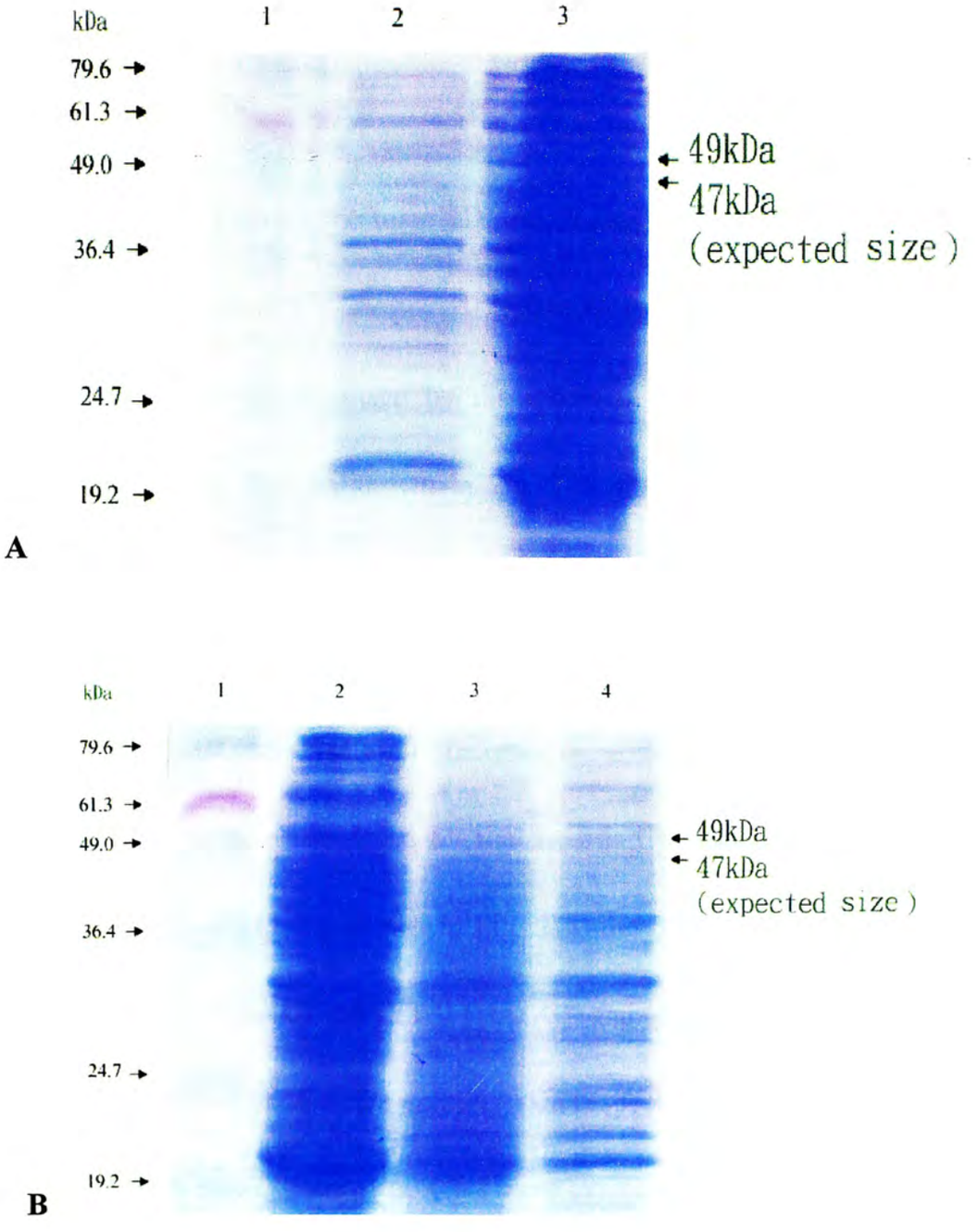

Fig. 3-2 Coomassie blue stained 15% SDS-PAGE gel of the expression of the mouse and human BACE protein using the pRSET expression vector by convention method. (A) Lane 1: Protein molecular weight markers (Invitrogen). Lane 2: induction of BL21(DE3)LysS cells transformed with nomBACE-pRSETB by 0.4 mM IPTG. Lane 3: no induction of BL21(DE3)LysS cells transformed with nomBACE-pRSETB. (B) Lane 1: Protein molecular weight markers (Invitrogen). Lane 2: uninduced BL21(DE3)LysS cells transformed with nohBACE-pRSETA. Lane 3: induction of BL21(DE3)LysS cells transformed with prohBACE-pRSETA by 0.4mM IPTG. Lane 4: induction of BL21(DE3)LysS cells transformed with nohBACE-pRSETA by 0.4mM IPTG.

3.1.2.2 Expression of truncated mouse and human BACE in BL21(DE3)LysS cells using modified method

In order to express the toxic cDNAs, the expression method was modified as described in section 2.2.2. BL21(DE3)LysS cells transformed with nomBACE-pRSETB was expressed by the modified method. The expression was induced by 0.4 mM IPTG. As shown in Fig. 3-3, there was no apparent induction when compared the expression profiles of the uninduced cells and induced cells.

BL21(DE3)LysS cells transformed with nohBACE-pRSETA and prohBACE-pRSETA were expressed by the modified method. The expression was induced by 0.4 mM IPTG. As shown in Fig. 3-4, the bacterial extracts from clones transformed with prohBACE-pRSETA (lane 3) and nohBACE-pRSETA (lane 4) over-expressed proteins of ~49 kDa and ~47 kDa respectively which was absent from the control (lane 2). The expressed proteins were extracted in inclusion body of *E.coli* using buffer B with 8M urea or buffer D with 6 M guanidine HCl. The proteins were refolded by rapid dilution in 10 fold buffer B or 60 fold buffer D. The proteins were purified by running His-tag binding column and eluted in buffer B with 0.8 M urea or buffer D with 0.1 M guanidine HCL with 200 mM imidazole. For detailed experiment methods above, refer to section 2.2. The results are shown in Fig. 3-5.

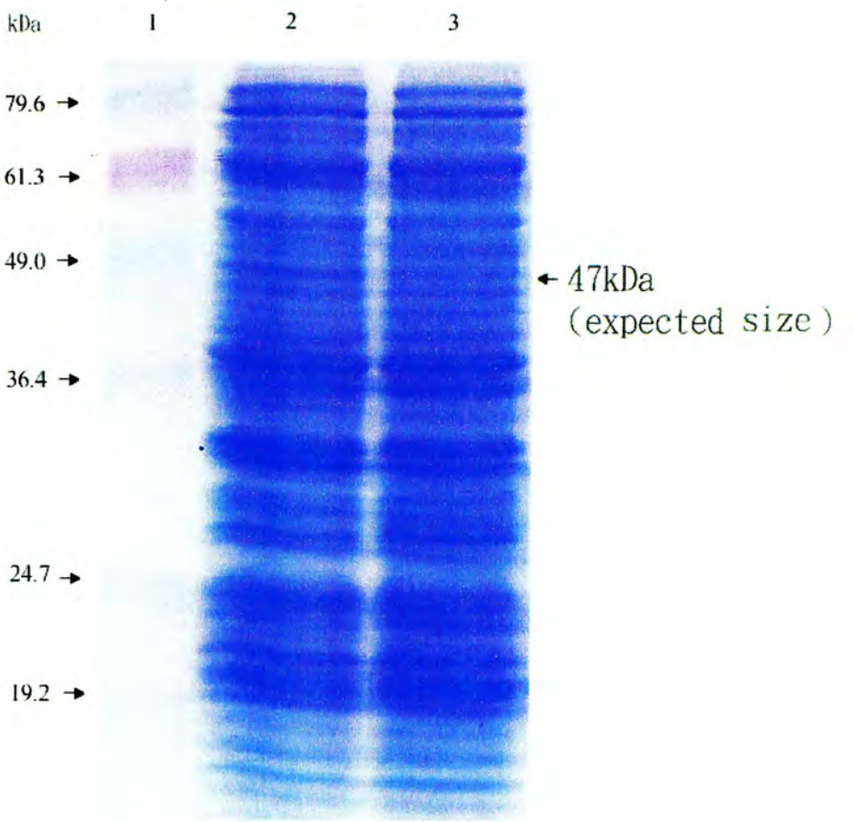

Fig. 3-3 Coomassie blue stained 15% SDS-PAGE gel showing the lack of expression of the mouse BACE protein using the pRSETB expression vector. Lane 1: Protein molecular weight markers (Invitrogen). Lane 2: cell lysates from BL21(DE3)LysS cells transformed with nomBACE-pRSETB without IPTG induction. Lane 3: cell lysates from BL21(DE3)LysS cells transformed with nomBACE-pRSETB with 0.4 mM IPTG induction.

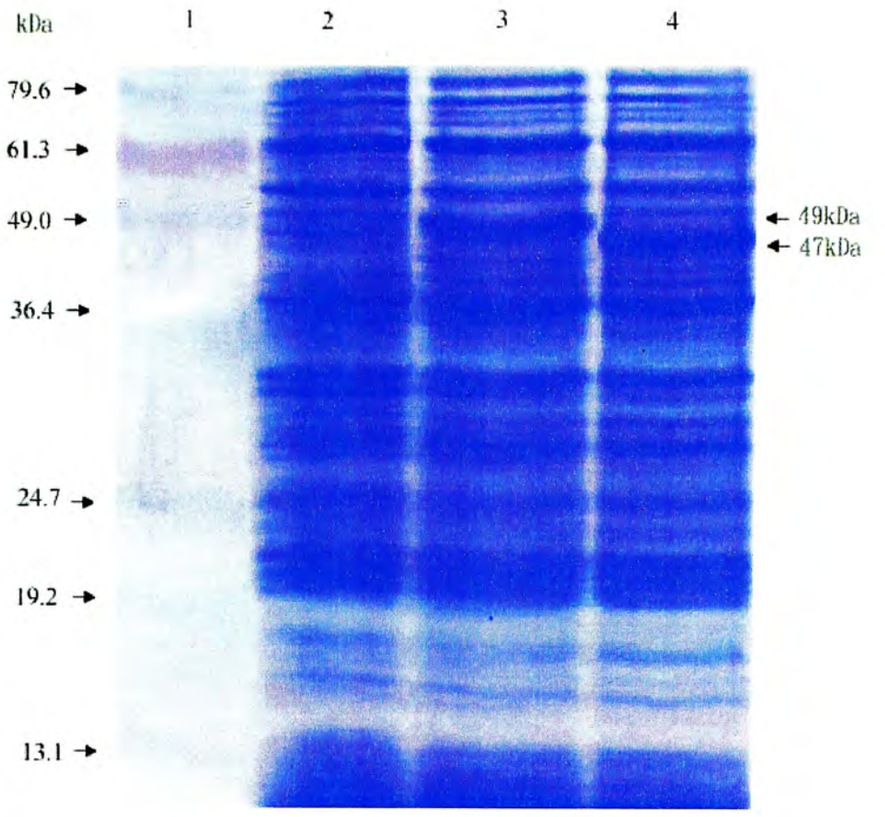

Fig. 3-4 Coomassie blue-stained 15% SDS-PAGE of *E.coli* cell lysates expressed with human BACE. Lane 1: Protein molecular weight markers (Invitrogen). Lane 2: cell lysates from BL21(DE3)LysS cells transformed with prohBACE-pRSETA without IPTG induction. Lane 3: cell lysates from BL21(DE3)LysS cells transformed with prohBACE-pRSETA with 0.4 mM IPTG induction. Lane 4: cell lysates from BL21(DE3)LysS cells transformed with nohBACE-pRSETA with 0.4 mM IPTG induction. Arrows indicated the specific protein bands with molecular sizes consistent with the predicted sizes of the recombinant BACE.

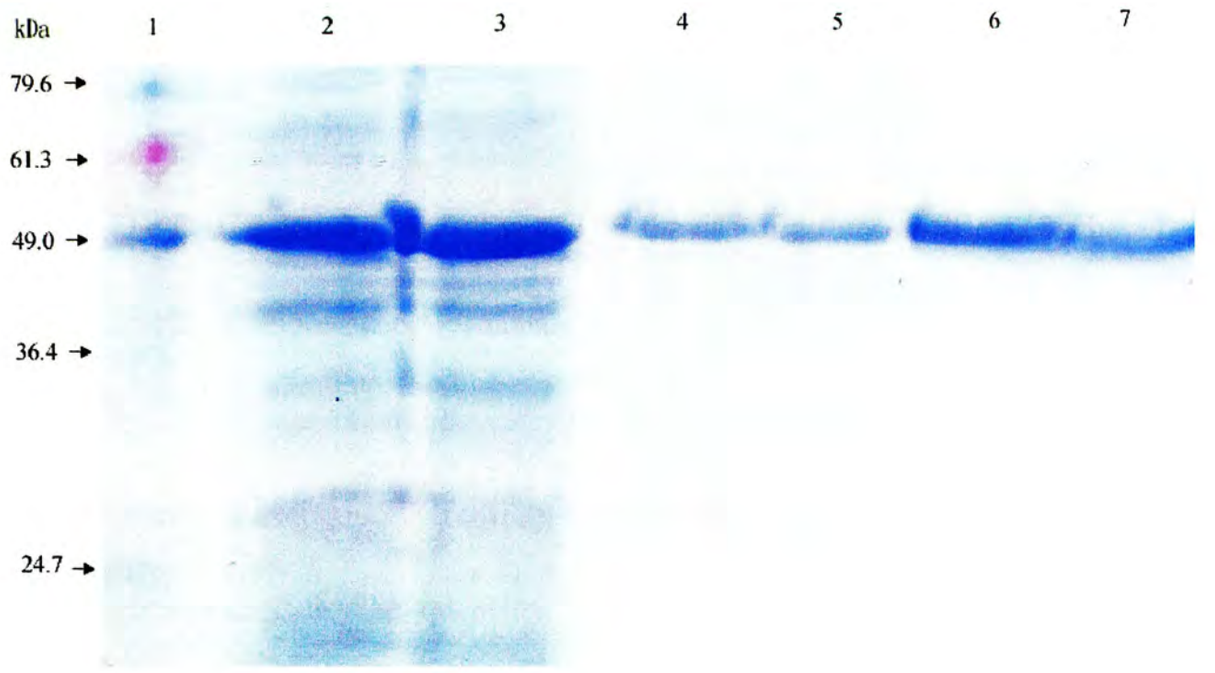

Fig. 3-5 Coomassie blue stained 15% SDS-PAGE of purified inclusion bodies from *E.coli* cell lysates overexpressed with prohBACE and nohBACE protein. Lane 1. Protein molecular weight markers (Invitrogen). Lane 2. extract of inclusion body from BL21(DE3)LysS cells transformed with plasmid prohBACE-pRSETA. Lane 3. extract of inclusion body from BL21(DE3)LysS cells transformed with plasmid nohBACE-pRSETA. Lane 4. prohBACE solublized in 0.8 M urea. Lane5. nohBACE solublized in 0.8 M urea. Lane 6. prohBACE solublized in 0.1 M guanidine HCl. Lane 7. nohBACE solublized in 0.1 M guanidine HCl.

3.1.3 Analysis of BACE activity of purified recombinant proteins

3.1.3.1 Fluorometric analysis

The BACE activity was measured by the use of a fluorometric assay based on the principle of fluorescence resonance energy transfer (FRET). It is based on a distance-dependent interaction between the electronic excited states of two dye molecules in which excitation is transferred from a donor molecule, the flurorophore to an acceptor molecule, the quencher. The longer the distance, the larger the fluorescence reading. The peptide contains both fluorophore and quencher at both ends and upon hydrolysis of the substrate by BACE, the quenching effect is abolished and the fluorescence increases in parallel to the level of hydrolysis (Ermolieff *et al.*, 2000).

The fluorophore used was 2-aminoethyl amino-naphthalene-1-sulfonic acid, EDANS with maximum absorption in wavelength of 335nm and maximum emission in wavelength of 493 nm. The quencher used was 4-dimethylaminophenylazo benzoic acid, DABCYL with maximum absorption in wavelength of 453 nm. The chemical structures of EDANS and DABCYL were shown in A3. Two substrates were used (refer to section 2.7.10). One synthetic peptide, (NH_2-RE(EDANS)EVNLDAEFK(DABCYL)R-COOH), FS-1, was derived from the APP of "Swedish mutation" (SEVNL/DAEFR) with BACE cleavage site (marked by

a slash). The other synthetic peptide,

(NH_2-RE(EDANS)VKMDEFAK(DABCYL)R-amide), FS-2 was derived from the wild type APP (SEVKM/DAEFR) with BACE cleavage site (marked by a slash).

The activity of purified nohBACE and prohBACE extracted in urea and guanidine HCL were analysed by the fluorescence assay using method described in section 2.5. Controls were prepared in which all proteins were boiled in 98°C for 30 minutes.

The fluorescence readings were changed to concentration of fluorophore released by the equation of $y = 0.57x + 6.48$ in the regression line of the standard curve in Fig. 3-6. No activity had been detected in the controls as shown by no increase in fluorescence reading. Comparing Fig. 3-7A and Fig. 3-7B, all proteins preparations had higher activity towards FS-1 than FS-2; Proteins extracted in guanidine HCl had higher activity towards both substrates than those extracted in urea; nohBACE had higher activity towards both substrates than prohBACE. Activity of enzyme stopped when it reach incubation time of 4 hours. 2 μg of samples were added in each assay. As shown in Fig. 3-7A, nohBACE extracted in guanidine HCl, prohBACE extracted in guanidine HCl, nohBACE extracted in urea and prohBACE extracted in urea had BACE activity of about 19.91, 15.22, 8.11 and 0.72 nmol/mg/hr towards FS-1 respectively. In Fig. 3-7B, nohBACE extracted in guanidine HCl,

prohBACE extracted in guanidine HCl, nohBACE extracted in urea and prohBACE extracted in urea had BACE activity of 8.78, 8.02, 1.81 and 1.12 nmol/mg/hr towards FS-2 respectively.

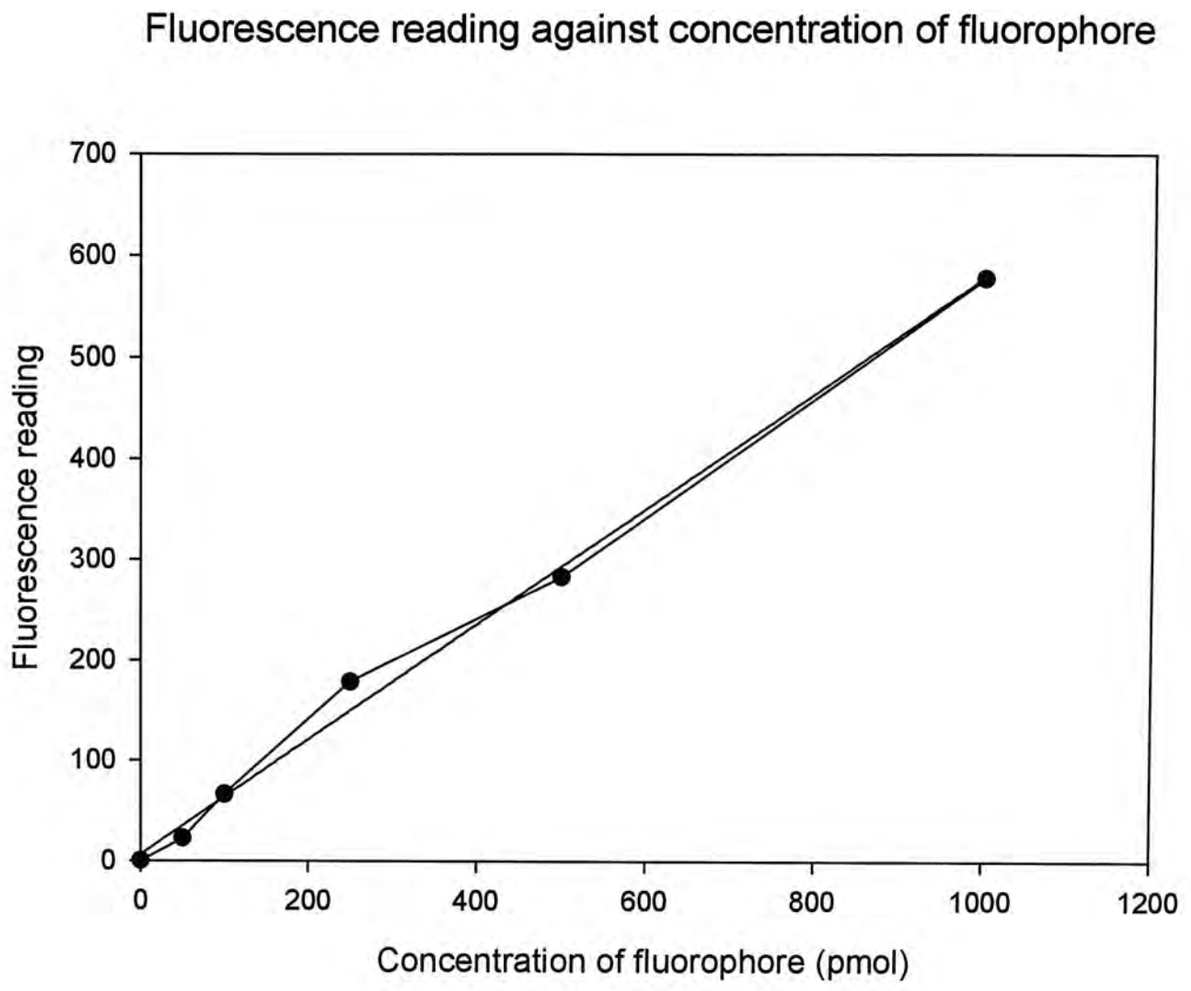

Fig. 3-6 Standard curve of EDANS fluorescence (Molecular Probes). Various concentration of EDANS was dissolved in assay buffer (section 2.7.7). The curve with fluorescence intensity (excitation 350 nm and emission 490 nm) against concentration of fluorophore, EDANS added (black circles). The regression was drawn in black solid line and with equation of $y = 0.57x + 6.48$.

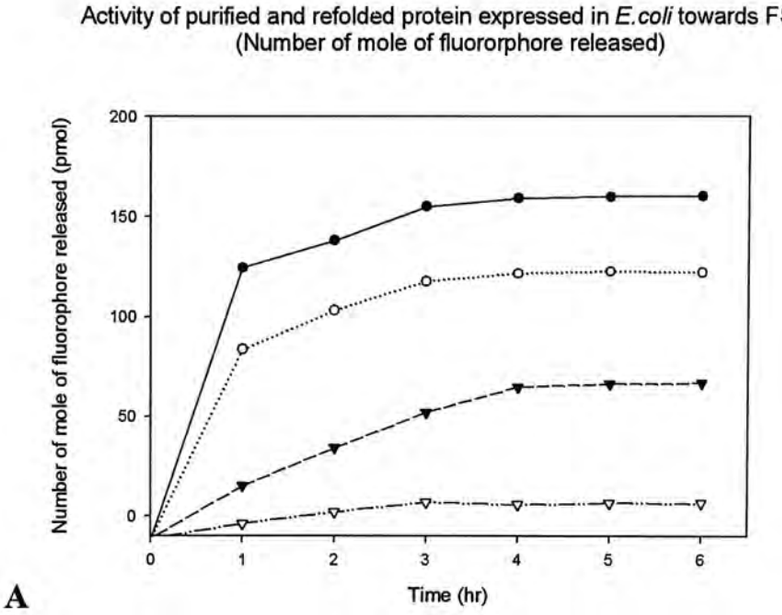

A

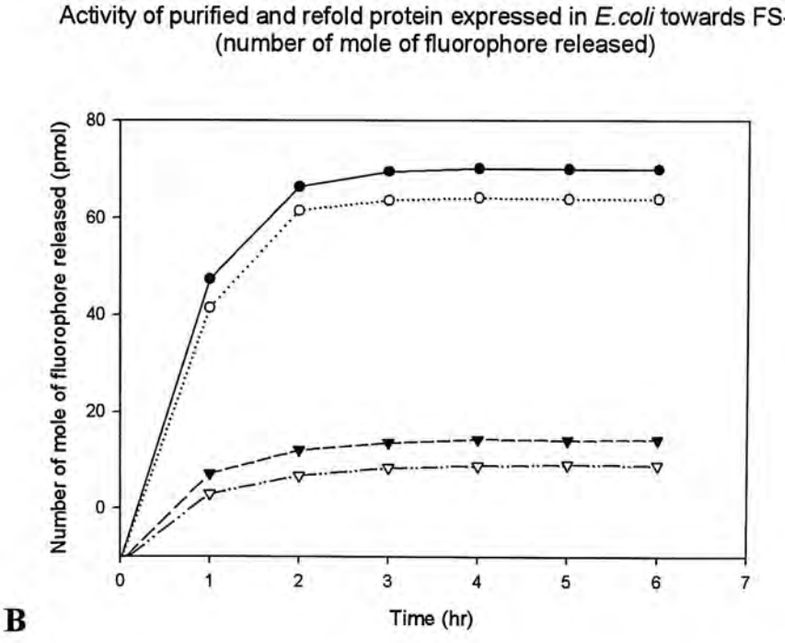

B

Fig. 3-7 BACE activity of partially purified protein towards 10 μM FS-1 (A) and 10 μM FS-2 (B) was measured by fluorometric method. Activity was measured in terms of number of mole of fluorophore released as calculated according to the standard curve of EDANS in Fig. 3-6. Four different samples were assayed. nohBACE purified and refolded protein extracted in 6M guanidine HCl (closed circles); prohBACE purified and refolded protein extracted in 6M guanidine HCl (open circles); nohBACE purified and refolded protein extracted in 8M urea (closed triangle); prohBACE purified and refolded protein extracted in 8M urea (open triangle).

3.2 Expression of BACE in mammalian cells

3.2.1 Cloning of full length mouse and human BACE into pCDNA3, pCDNA4HisMax

The cDNA encoding the full coding sequence of mouse BACE was amplified by RT-PCR using total mouse brain RNA as template. The forward primer (mBACE_423F) and reverse primer (mBACE_1940R) were synthesized according to the published sequence(GenBank Accession number AF190726). Consistent with the predicted size of mouse BACE cDNAs, a DNA fragment of about 1.6kb was amplified and the amplified DNA was extracted from gel by the QIAquick Gel Extraction Kit.

By similar approach, the cDNA encoding the full coding sequence of human BACE was amplified from human brain cDNA (in pCMV.SPORT purchased from BRL) using forward primer (hBACE_448) and reverse primer (hBACE_1946R) were synthesized according to the published sequence(GenBank Accession number AF190725). Consistent with the predicted size of human BACE cDNAs, a DNA fragment of about 1.6kb was amplified and the amplified DNA was extracted from gel by the QIAquick Gel Extraction Kit.

The cDNAs were first cloned into vector pBluescript KS II- (Stratagene, the

plasmid map was shown in Appendix A1-1) at restriction site between EcoRI and XhoI (Fig. 3-8A and Fig. 3-8B). After confirming the identities of BACE by partial DNA sequencing of positive clones, the cDNA of mouse BACE was subcloned into mammalian expression vectors, pCDNA3 (Invitrogen, the plasmid map was shown in Fig. A1-2) and pCDNA4HisMaxC (Invitrogen, the plasmid map was shown in Fig. A1-3). The cDNA of human BACE was subcloned into vectors pCDNA3 and pCDNA4HisMaxA. The plasmids were purified by High Pure Plasmid Isolation Kit (Roche). The recombinant plasmids were further confirmed by DNA sequencing using T3 and T7 sequencing primers. The results from DNA sequencing showed that mBACE in vector pCDNA3 (designated as mBACE-pCDNA3) and vector pCDNA4HisMaxC (designated as mBACE-pCDNA4HisMaxC) had 99% similarity with the published mouse BACE mRNA sequence (GenBank Accession number AF190726), while the human BACE in vector pCDNA3 (designated as hBACE-pCDNA3) and pCDNA4HisMaxA (designated as hBACE-pCDNA4HisMaxA) had 98% similarity with the published human BACE mRNA (GenBank Accession number AF190725).

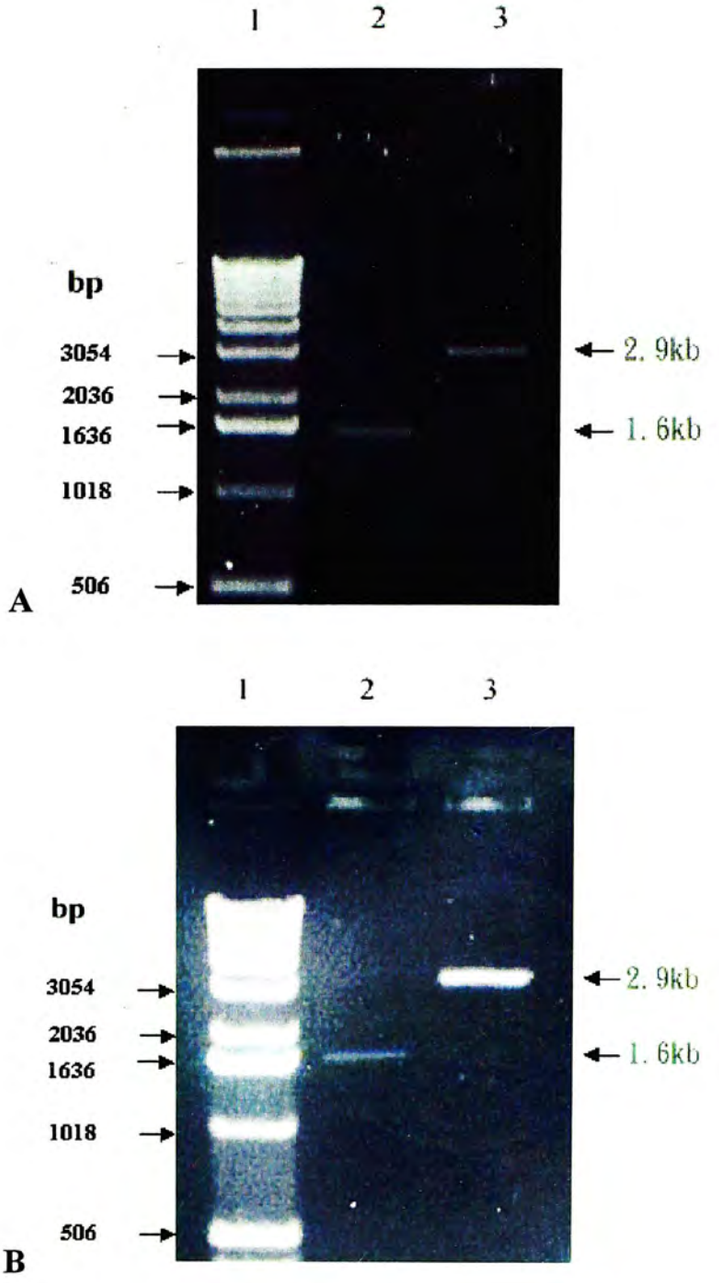

Fig. 3-8 (A) Digestion product of insert, total mouse BACE and vectors (pBluescript KS II-) by restriction enzyme EcoRI and XhoI and was run in 1% agarose gel. Lane 1. 1 kb marker. Lane 2. Digested mBACE of about 1.6kb as indicated by the marker. Lane 3. Digested pBluescript KS II- of about 2.9kb as indicated by the marker. (B) Digestion product of insert, hBACE and vector, pBluescript KS II- by restriction enzyme EcoRI and XhoI and was run in 1% agarose gel. Lane 1. 1kb marker. Lane 2. Digested total human BACE gene of about 1.6kb as indicated by the marker. Lane 3. Digested pBluescript KS II- of about 2.9kb as indicated by the marker.

3.2.2 Transient transfection

The constructed mBACE-pCDNA3, mBACE-pCDNA4HisMaxC, hBACE-pCDNA3 and hBACE-pCDNA4HisMaxA were transiently transfected into mammalian cell line, Chinese hamster ovary (CHO) cells using Lipofectamine transfection method, as described in section. 2.3.1.

The transfection efficiency was estimated by calculating the percentage of stained cells, which has β-galactosidase activity, in CHO cells transfected with pCDNA4HisMax*lacZ* using the same method as in section 2.3.2. The result was shown in Fig. 3-9. About 20% of cells were transfected. No transfection efficiency test was carried out on vector pCDNA3 as there is no lacZ gene provided for the vector.

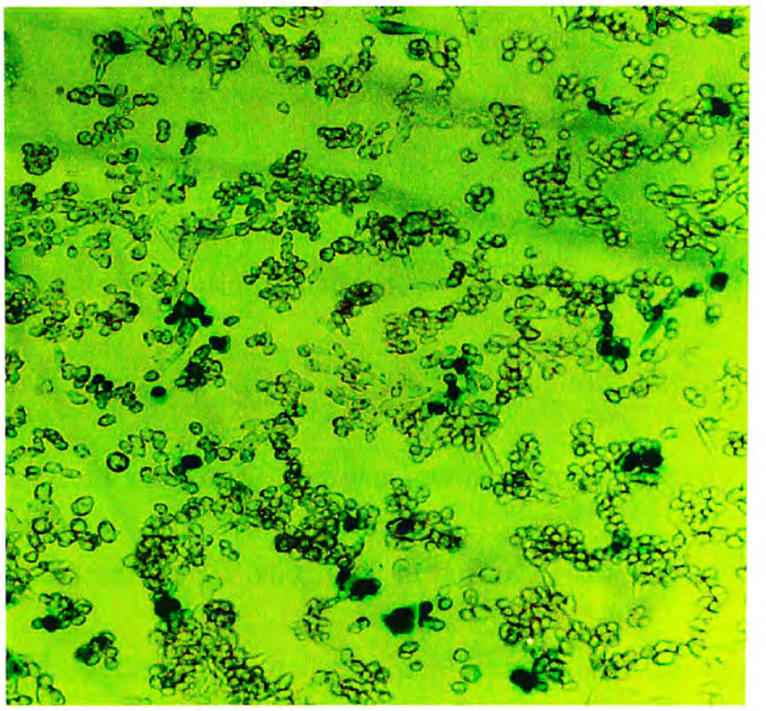

Fig. 3-9 The transfection efficiency of pCDNA4HisMax was estimated by β-galactosidase activity under 200 x light microscope. CHO cells transiently transfected with plasmid pCDNA4HisMax*lacZ*.

3.2.2.1 Western blot analysis

The membrane extracts were obtained from the transiently transfected cells, as described in section 2.3.4. To determine the expression of BACE in the transiently transfected cells, Western blotting was performed. Western blotting was carried out with two polyclonal antibodies, hBACE122 and hBACE485 separately, according to section 2.2.9. Sensitivity of hBACE485 was low as signals will only be detected after incubation of 4 hours with BCIP and NBT in buffer 3. hBACE485 binded to BACE expressed with high specificity, as no other non-specific binding was detected in Fig. 3-10B. No signal was detected in the untransfected cells, and weak protein band with molecular weight approximately 54 kDa were detected in cells transfected with mBACE-pCDNA3, mBACE-pCDNA4HisMaxC, hBACE-pCDNA3 and hBACE-pCDNA4HisMaxA. And a relatively strong signal was detected in cells transfected with mBACE-pCDNA4HisMaxC. However, there was no signal at all when using hBACE122 (result not shown).

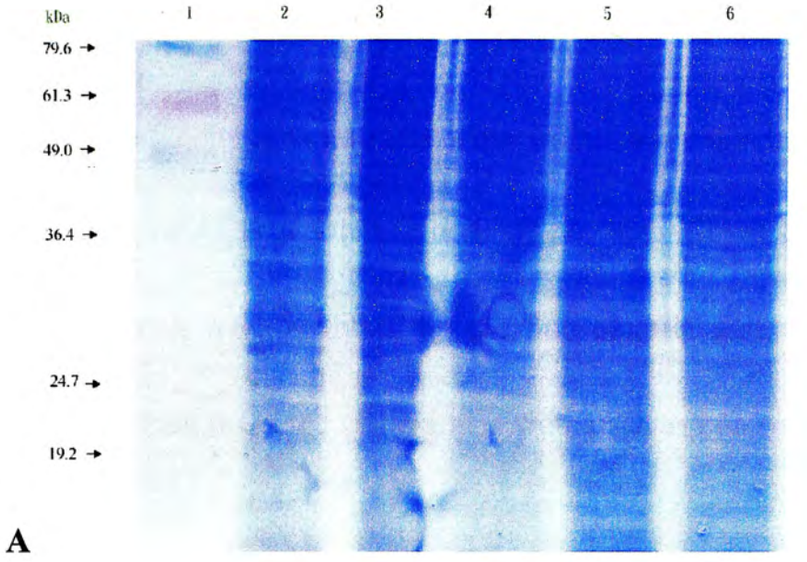

A

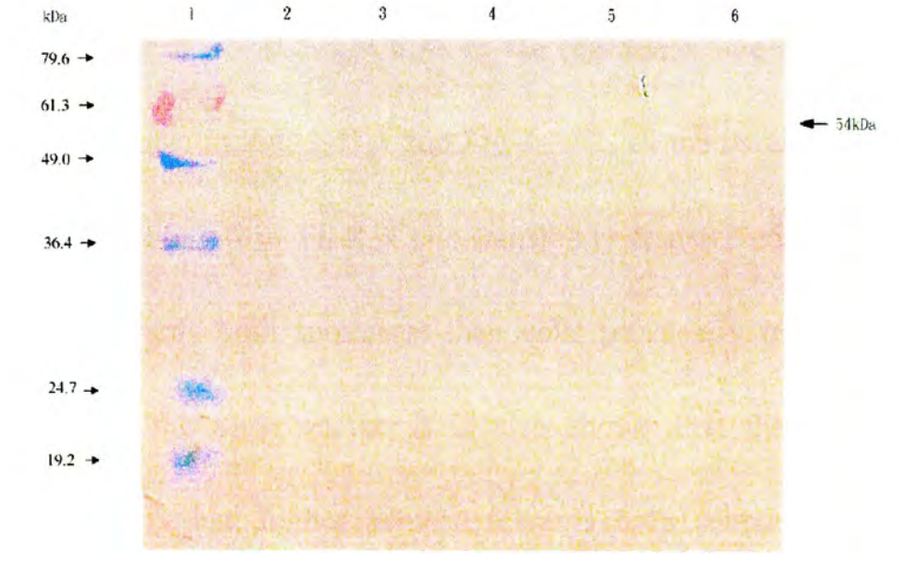

B

Fig. 3-10 Western blot analysis on membrane extracts of CHO cells transiently transfected with mBACE or hBACE in mammalian expression vectors with hBACE485 antibody. Membrane extracts obtained from transiently transfected cell lines were separated in SDS-PAGE (A) and were transferred to a PVDF membrane for Western blot analysis (B). Lane 1. Protein molecular weight markers (Invitrogen). Lane 2. Untransfected cells. Lane 3. Cells transiently transfected with hBACE-pCDNA3. Lane 4. Cells transiently transfected with hBACE-pCDNA4HisMaxA. Lane 5. Cells transiently transfected with mBACE-pCDNA3. Lane 6. Cells transiently transfected with mBACE-pCDNA4HisMaxC. A faint immunoreactive protein of 54 kDa was detected as indicated.

3.2.2.2 Fluorometric analysis

The activity of membrane extracts from cells transiently transfected with mBACE-pCDNA3, mBACE-pCDNA4HisMaxC, hBACE-pCDNA3 and hBACE-pCDNA4HisMaxA were analysed by the fluorometric assay using method described in section 2.5. Untransfected cell extracts were used as control.

The fluorescence readings were changed to concentration of fluorophore released by the equation of $y = 0.57x + 6.48$ in the regression line of the standard curve in Fig. 3-6. As shown in Fig. 3-11A and Fig 3-11B, all membrane extracts had higher activity towards FS-1 than FS-2; Cells transiently transfected with mBACE had higher activity towards both substrates than cells transiently transfected with hBACE constructed in the same vector, it is also shown that the constructs in pCDNAHisMax generally had higher activity towards both substrates than cells transiently transfected in constructs of pCDNA3. There were activity from the membrane extracts of untransfected cells. The activity in terms of concentration of fluorophore released due to the transfected genes only were obtained by deducting the activity of transfected cells by those of untransfected cells in each time intervals. 2 μg of samples were added in each assay. In Fig. 3-11A, membrane extracts of cells transiently transfected with mBACE-pCDNA3, hBACE-pCDNA3, mBACE-pCDNA4HisMaxC and hBACE-pCDNA4HisMaxA had BACE activity of

about 6.01, 1.64, 8.00 and 5.30 nmol/mg/hr towards FS-1 respectively. In Fig. 3-11B, membrane extracts of cells transiently transfected with mBACE-pCDNA3, hBACE-pCDNA3, mBACE-pCDNA4HisMaxC and hBACE-pCDNA4HisMaxA had BACE activity of about 2.07, 1.84, 3.12 and 0.08 nmol/mg/hr towards FS-2 respectively.

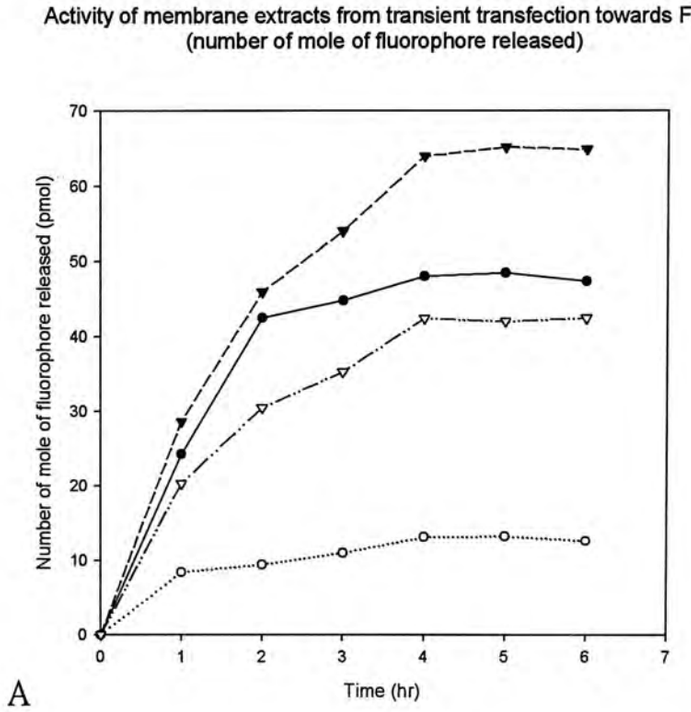

A

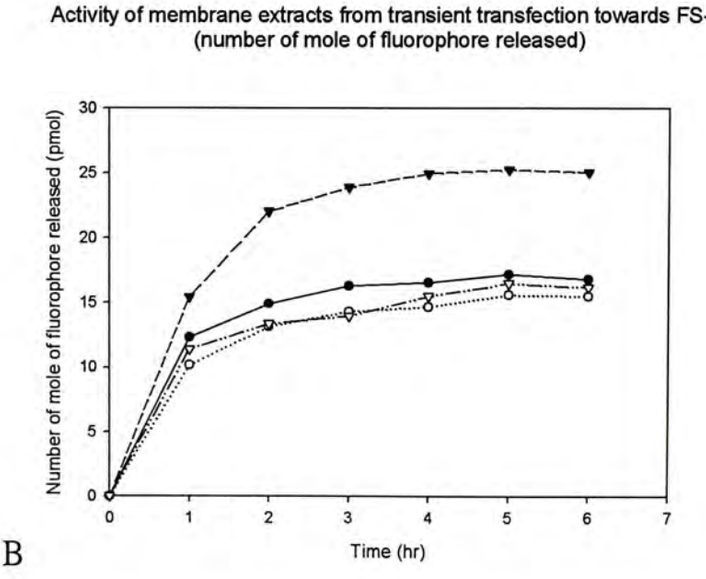

B

Fig. 3-11 BACE activity of membrane extracts from cells transfected with various mammalian expression vectors towards 10 μM FS-1 (A) and 10 μM FS-2 (B) was measured by fluorometric method. Activity was measured in terms of number of mole of fluorophore released as calculated according to the standard curve of EDANS in Fig. 3-6. Four different samples were assayed. Membrane extracts obtained from cells transfected with mBACE-pCDNA3 (closed circles), hBACE-pCDNA3 (open circles), mBACE-pCDNA4HisMaxC (closed triangles) and hBACE-pCDNA4HisMaxA (open triangles).

3.2.2.3 HPLC

The fluorometric analysis only determined the rate of cleavage of substrate deriving from Swedish mutation or wild type peptide. In order to determine the cleavage was correctly cleaved at NL site, analytical HPLC was performed. Two peptides substrates and one peptide product were used (refer to section 2.7.9). One synthetic peptide, SEVNLDAEFR, was derived from the APP of "Swedish mutation" (SEVNL/DAEFR) with BACE cleavage site (marked by a slash). The other synthetic peptide, EVKMDAEFR, was derived from the wild type APP (SEVKM/DAEFR) with BACE cleavage site (marked by a slash). As seen from cleavage of above, one common cleavage product, DAEFR, was also synthesized.

HPLC was performed as section 2.4. The three peptides were run in the HPLC as standard as shown in Fig. 3-12. Swedish mutation peptide substrate, SEVNLDAEFR was eluted in 15.7 minutes. Wild type peptide substrate, EVKMDAEFR was eluted in 15.1 minutes. Common product of cleavage, DAEFR was eluted in 12.1 minutes.

Three samples will be analysed, membrane extracts from untransfected cells; membrane extracts from cells transiently transfected with mBACE-pCDNA3 and membrane extracts from cells transiently transfected with

mBACE-pCDNA4HisMaxC. A control was set up for each sample, and was treated similarly as those of samples unless they were heated for 30 minutes before incubation with substrates. 2 μg of samples were added in each assay. And two peptide substrates, SEVNLDAEFR and EVKMDAEFR were incubated with the samples and their controls.

No product peak of DAEFR at 12.1 minutes were observed in the 12 HPLCs with the exception of incubation of SEVNLDAEFR with membrane extracts from cells transfected with mBACE-pCDNA4HisMaxC as shown in Fig. 3-13L. This result suggested that only cDNA of mBACE in pCDNA4HisMaxC had transient BACE activity.

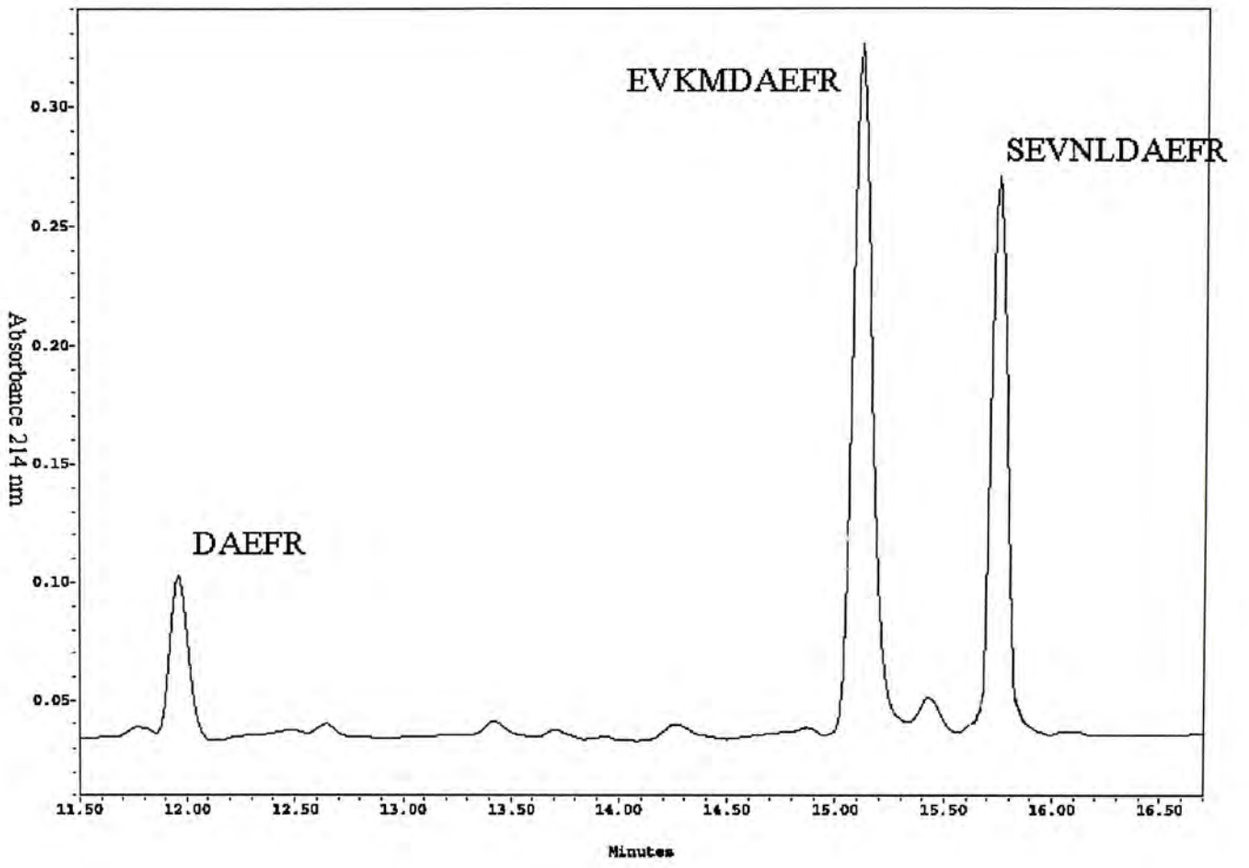

Fig. 3-12 HPLC chromatography of peptides used as BACE substrates and their cleaved product. The peptide substrates were EVKMDAEFR (wild type substrate) eluted at 15.1 minutes; SENVLDAEFR (Swedish mutation substrate) eluted at 15.7 minutes and their cleavage product, DAEFR eluted at 12.1 minutes.

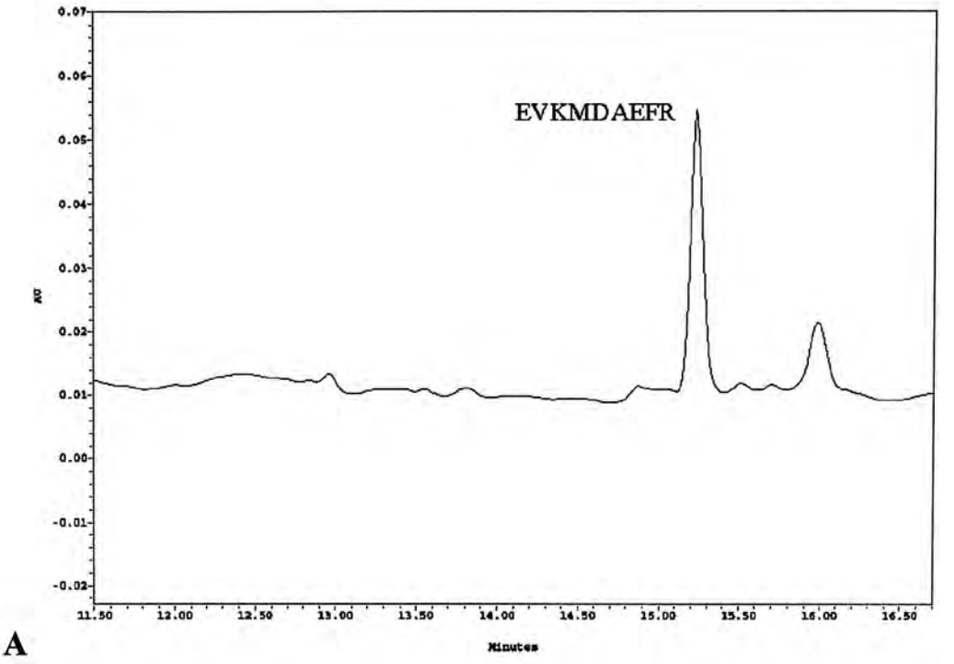

A

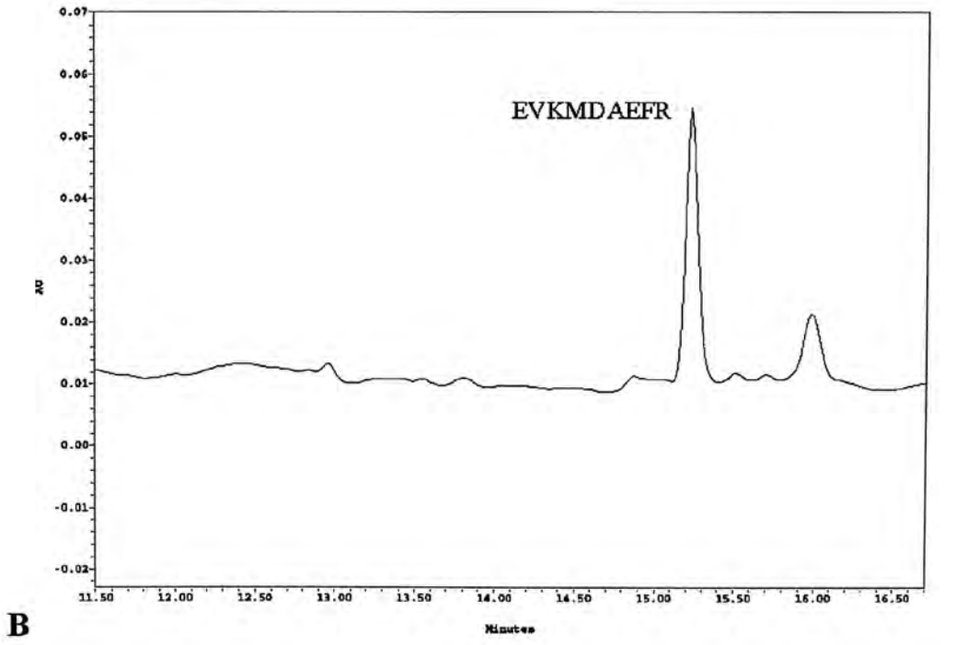

B

Fig. 3-13 Chromatograms of RP-HPLC assay. 10 μM peptide substrate and 2 μg sample were mixed in assay buffer. The reaction was stopped by boiling and storing in –20°C. (A) Membrane extracts from untransfected cells were boiled for 30 minutes before incubating with substrate EVKMDAEFR. (B) Membrane extracts from untransfected cells incubating with substrate EVKMDAEFR.

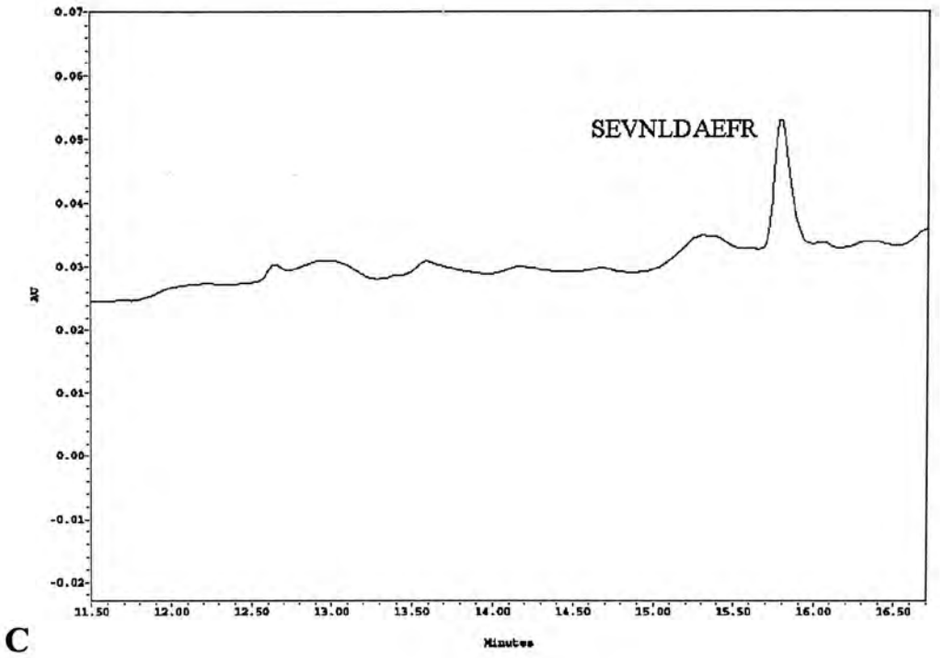

C

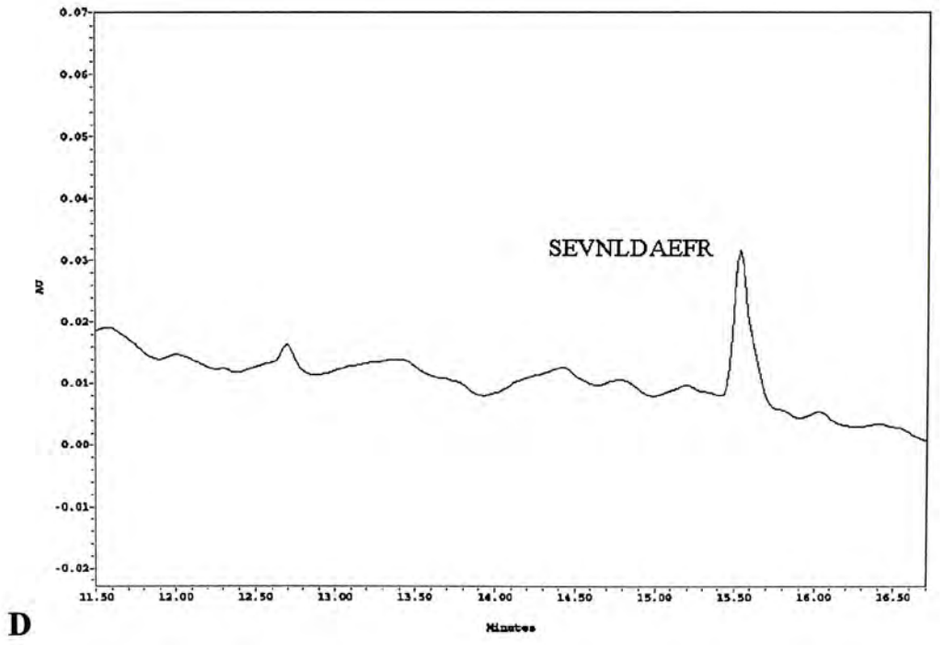

D

Fig. 3-13 (C) Membrane extracts from untransfected cells were boiled for 30 minutes before incubating with substrate SEVNLDAEFR. (D) Membrane extracts from untransfected cells incubating with substrate SEVNLDAEFR.

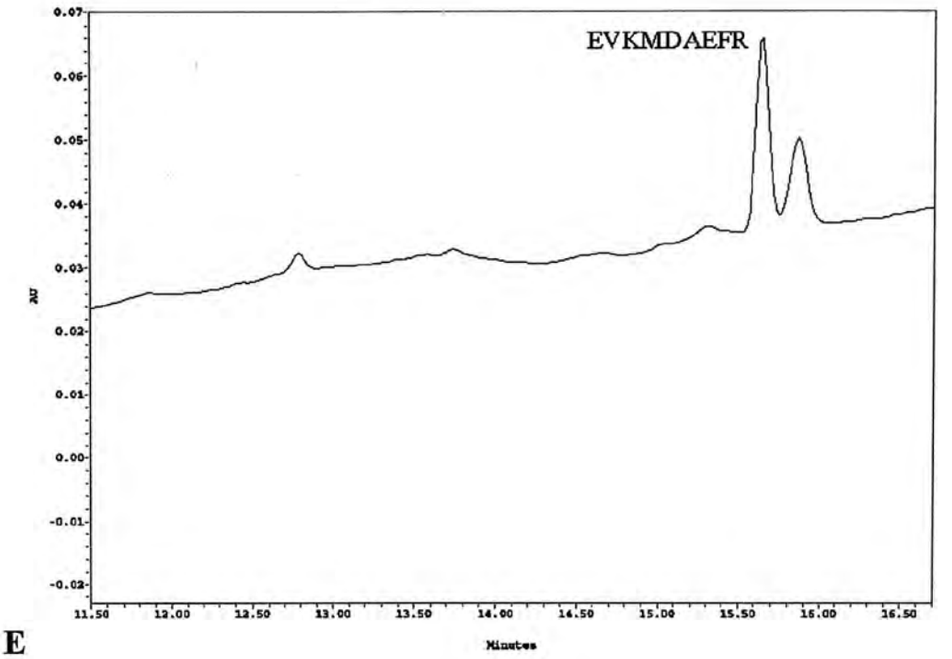

E

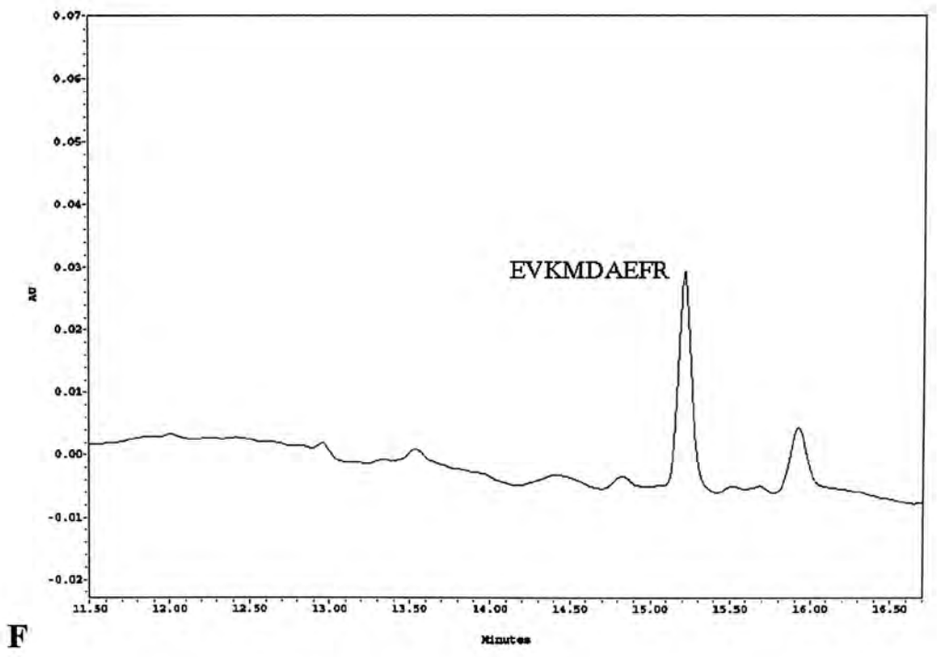

F

Fig. 3-13 (E) Membrane extracts from cells transiently transfected with mBACE-pCDNA3 were boiled for 30 minutes before incubating with substrate EVKMDAEFR. (F) Membrane extracts from cells transiently transfected with mBACE-pCDNA3 incubating with substrate EVKMDAEFR.

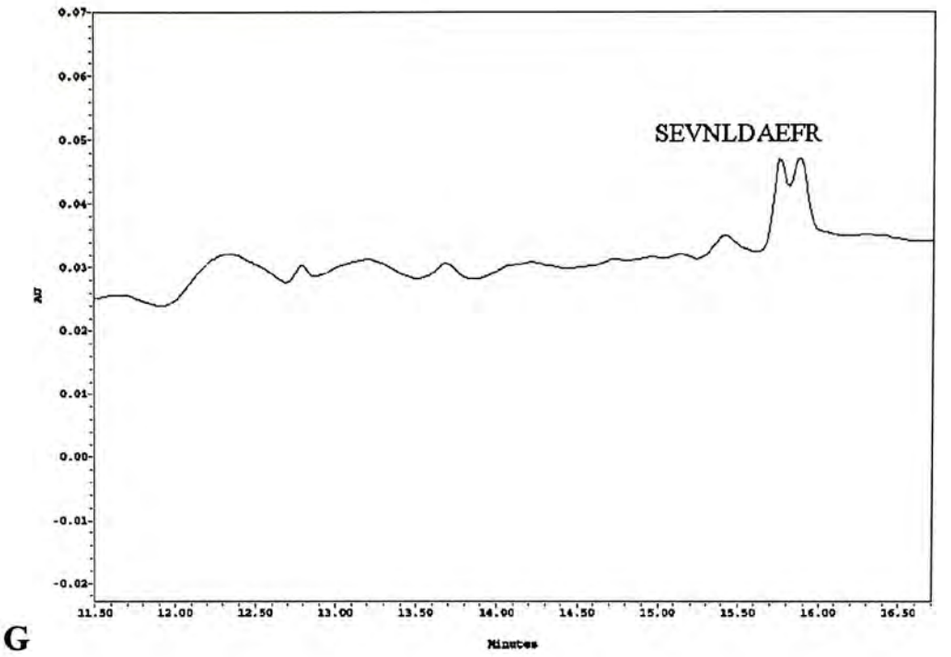

G

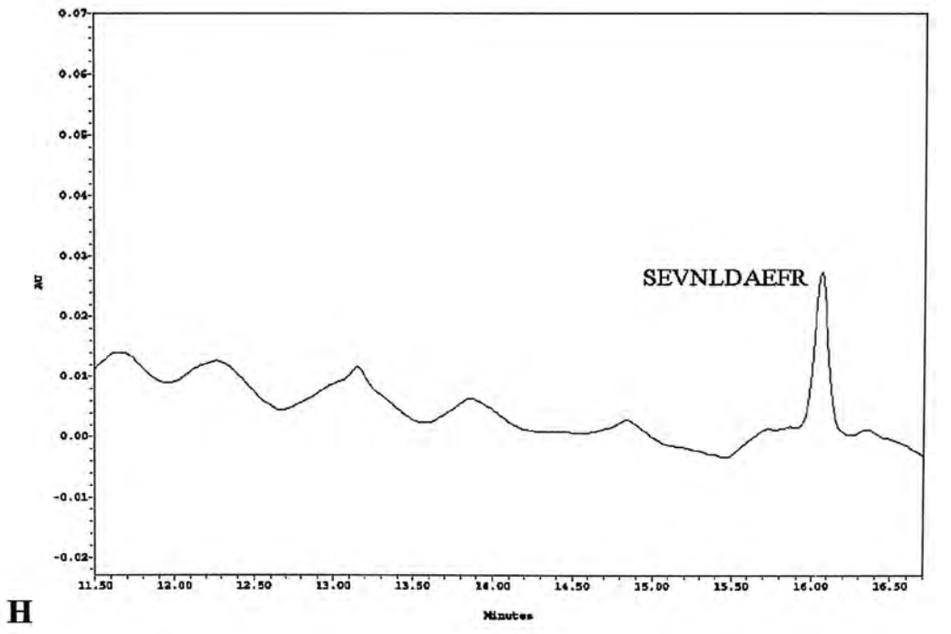

H

Fig. 3-13 (G) Membrane extracts from cells transiently transfected with mBACE-pCDNA3 were boiled for 30 minutes before incubating with substrate SEVNLDAEFR. (H) Membrane extracts from cells transiently transfected with mBACE-pCDNA3 incubating with substrate SEVNLDAEFR.

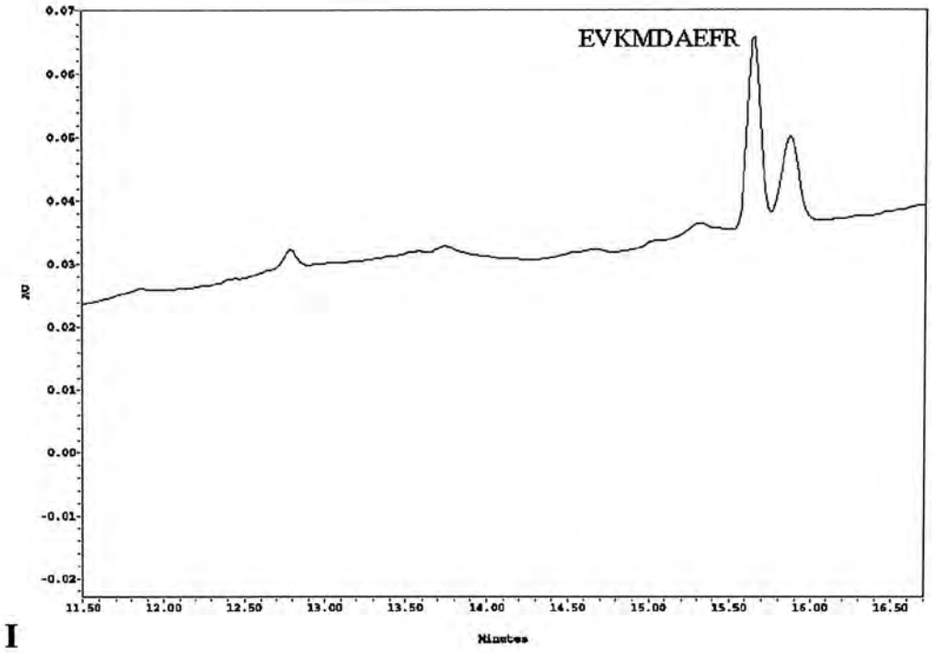

I

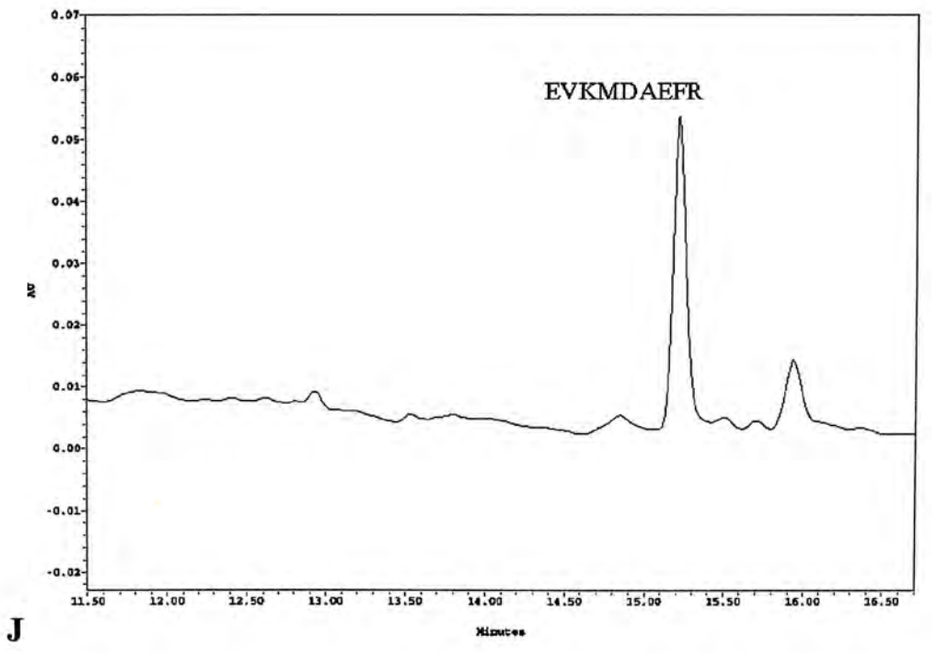

J

Fig. 3-13 (I) Membrane extracts from cells transiently transfected with mBACE-pCDNA4HisMaxC were boiled for 30 minutes before incubating with substrate EVKMDAEFR. (J) Membrane extracts from cells transiently transfected with mBACE-pCDNA4HisMaxC incubating with substrate EVKMDAEFR.

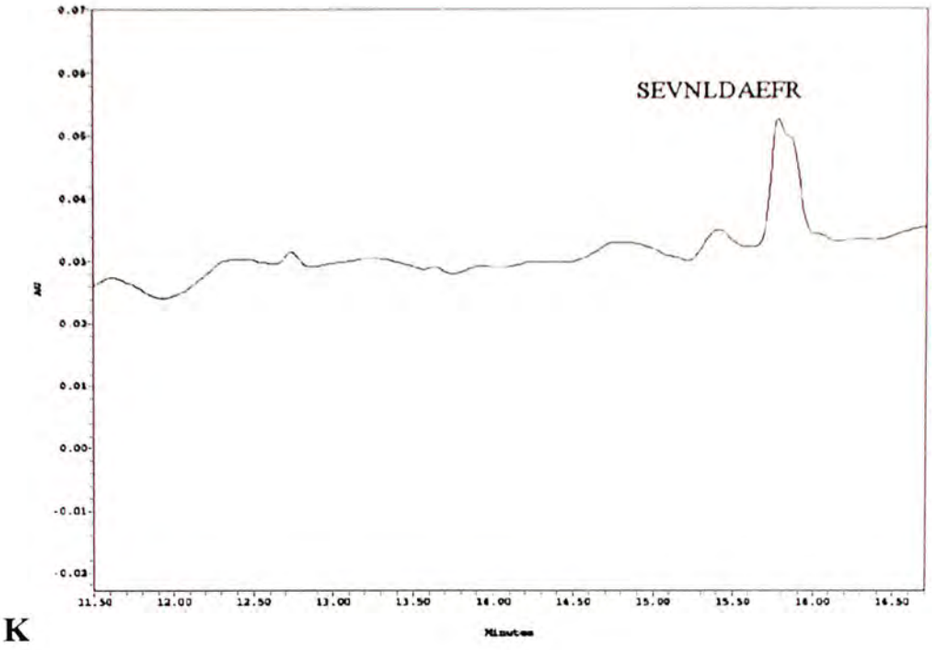

K

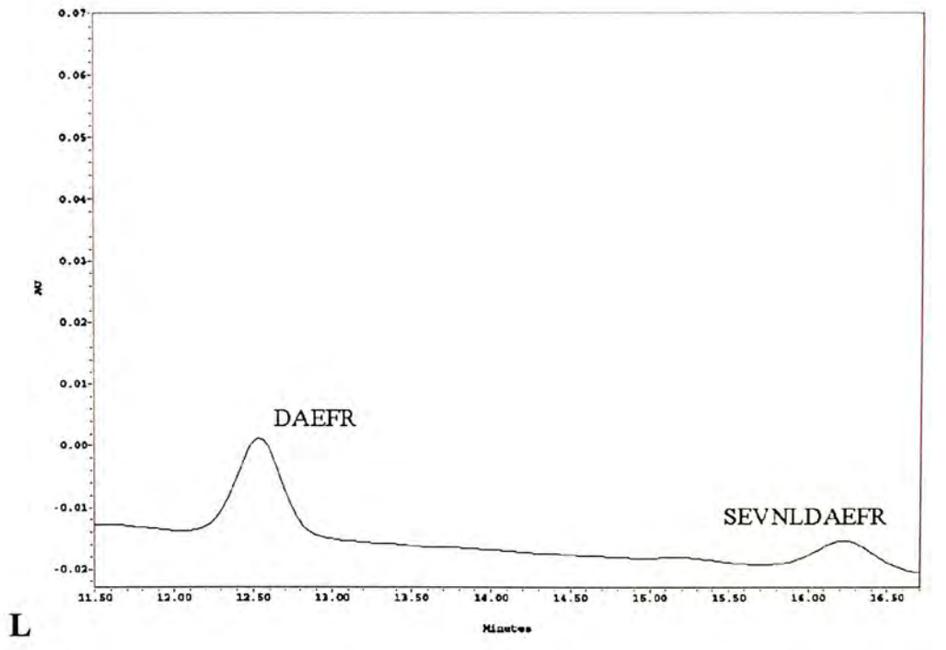

L

Fig. 3-13 (K) Membrane extracts from cells transiently transfected with mBACE-pCDNA4HisMaxC were boiled for 30 minutes before incubating with substrate SEVNLDAEFR. (L) Membrane extracts from cells transiently transfected with mBACE-pCDNA4HisMaxC incubating with substrate SEVNLDAEFR.

3.2.3 Stable transfection

As from the result of the Western blotting, fluorometric and HPLC analysis, the transient transfection of CHO cell line did not express BACE significantly as compared to controls. Hence, efforts had been made to develop CHO cells stably transfected with mBACE-pCDNA3 and hBACE-pCDNA3.

pCDNA3 contains neomycin resistance gene for selection of stable transfectants in mammalian cells against antibiotics, geneticin G418. Generation of stable transfected cell lines were transiently transfected with mBACE-pCDNA3 and hBACE-pCDNA3 as described in section 2.3.1, then the cells that stably transfected with plasmids were selected by antibiotics, geneticin G418, as described in section 2.3.3.

3.2.3.1 Western blot analysis

To determine the expression of BACE in the stably transfected cell lines, Western blotting was carried out with polyclonal antibody, hBACE485, according to section 2.2.9. Sensitivity of hBACE485 was low as signals will be detected after incubation of 4 hours with BCIP and NBT in buffer 3. hBACE485 binded to BACE expressed with high specificity, as no other non-specific binding was detected in Fig. 4.7B. No signal was detected in the untransfected cells, and strong signals of about 61 kD and 55 kD were detected in cells stably transfected with mBACE-pCDNA3 and hBACE-pCDNA3 respectively.

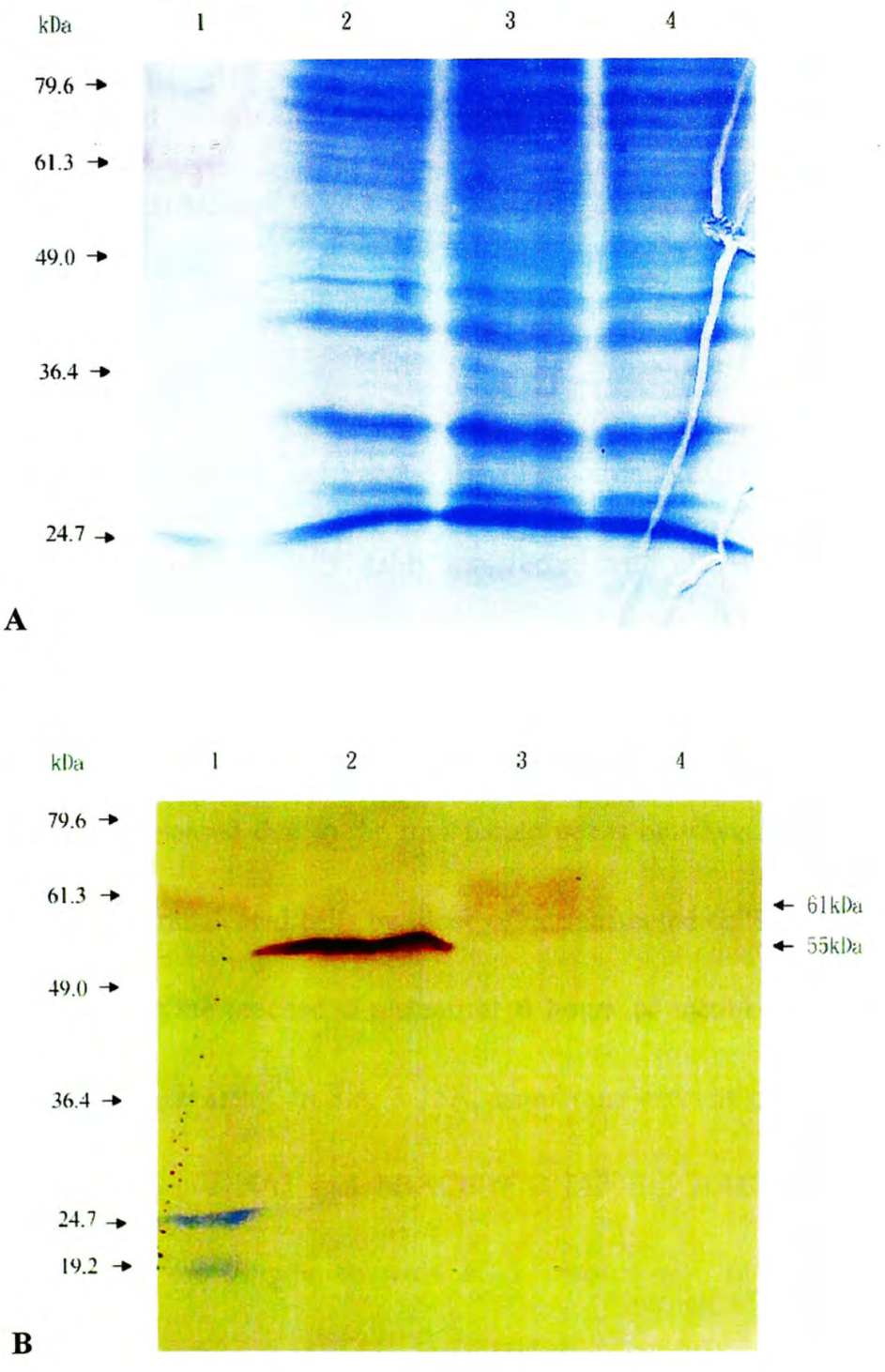

Fig. 3-14 Recognition of BACE gene on cells stably transfected with mBACE or hBACE gene by primary antibody hBACE485 in Western blotting. Membrane extracts obtained from stably transfected cell lines were separated in SDS-PAGE (A) and were transferred to a PVDF membrane for Western blot analysis (B) Lane 1. Protein molecular weight markers (Invitrogen). Lane 2. Cells stably transfected with hBACE-pCDNA3. Lane 3. Cells stably transfected with mBACE-pCDNA3. Lane 4. Untransfected cells.

3.2.3.2 Fluorometric analysis

The activity of membrane extracts from cells stably transfected with mBACE-pCDNA3 and hBACE-pCDNA3 were analysed by the fluorometric assay using method described in section 2.5.

As shown in Fig. 3-15A and Fig 3-15B, all membrane extracts had higher activity towards FS-1 than FS-2; Cells stably transfected with mBACE had higher activity towards both substrates than cells stably transfected with hBACE. There were activity from membrane extract of untransfected cells. The activity in terms of number of mole of fluorophore released due to the transfected genes only were obtained by deducting the activity of transfected cells by those of untransfected cells in each time intervals. Activity of enzyme reached a plateau at 4 hours of incubation. 2 μg of samples were added in each assay. In Fig. 3-15A, membrane extracts of cells stably transfected with mBACE-pCDNA3 and hBACE-pCDNA3 had BACE activity of about 23.25 and 16.06 nmol/mg/hr towards FS-1 respectively. In Fig. 3-15B, membrane extracts of cells stably transfected with mBACE-pCDNA3 and hBACE-pCDNA3 had BACE activity of about 10.58 and 8.29 nmol/mg/hr towards FS-2 respectively.

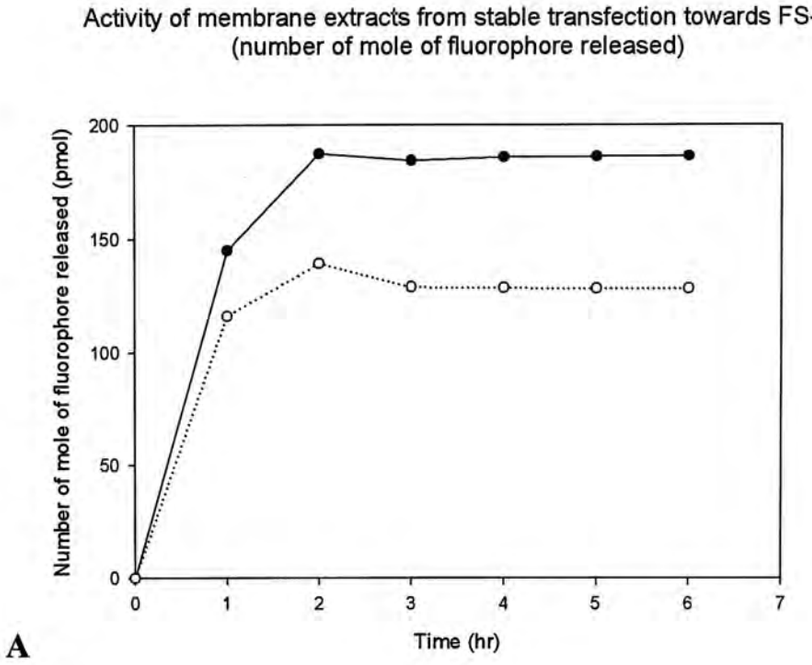

A

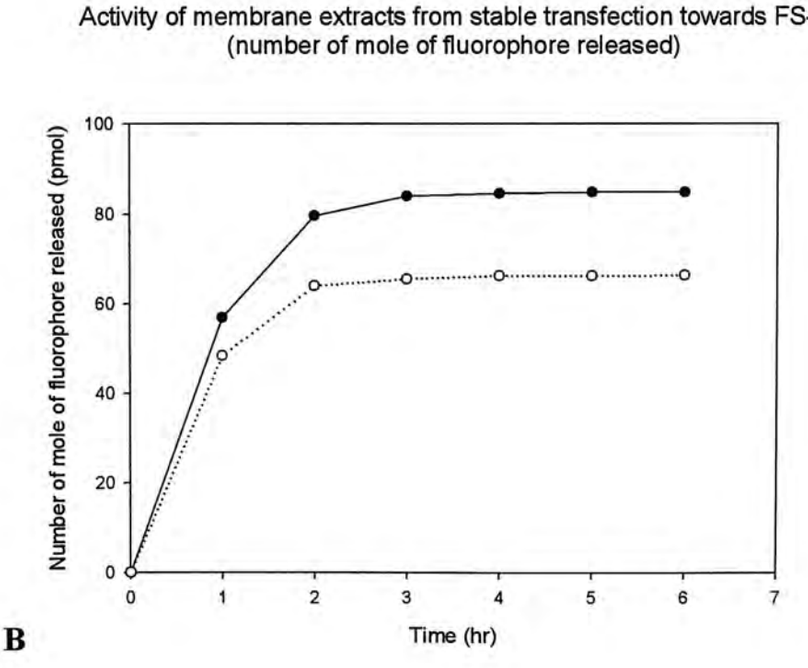

B

Fig. 3-15 BACE activity of membrane extracts from cells transfected with mBACE and hBACE in vector pCDNA3 towards 10 μM FS-1 (A) and 10 μM FS-2 (B) was measured by fluorometric method. Activity was measured in terms of number of mole of fluorophore released as calculated according to the standard curve of EDANS in Fig. 3-6. Two different samples were assayed. Membrane extracts obtained from cells stably transfected with mBACE-pCDNA3 (closed circles), hBACE-pCDNA3 (open circles).

3.2.3.3 HPLC

HPLC was performed as described in section 2.4. Three samples were analysed, membrane extracts from untransfected cells, cells stably transfected with mBACE-pCDNA3 and hBACE-pCDNA3. A control was set up for each sample, and was treated similarly as those of samples unless they were heated for 30 minutes before incubation with substrates. 2 μg of samples were added in each assay. And two peptide substrates, SEVNLDAEFR and EVKMDAEFR were incubated with the samples and their controls.

No product peak of DAEFR at 12.1 minutes was observed in the membrane extracts from untransfected cells either in the samples or boiled controls towards both substrates, as shown in Fig. 4.9A-D. No product peak of DAEFR at 12.1 minutes was observed in the boiled control of membrane extracts from cells stably transfected with mBACE-pCDNA3 and hBACE-pCDNA3 towards both substrates, as shown in Fig. 3-16 E, G, I, K. However, product peak of DAEFR at 12.1 minutes and the substrate peaks reduced significantly were observed in membrane extracts from cells transfected with mBACE-pCDNA3 and hBACE-pCDNA3 towards both substrates, as shown in Fig. 3-16 F, H, J, L.

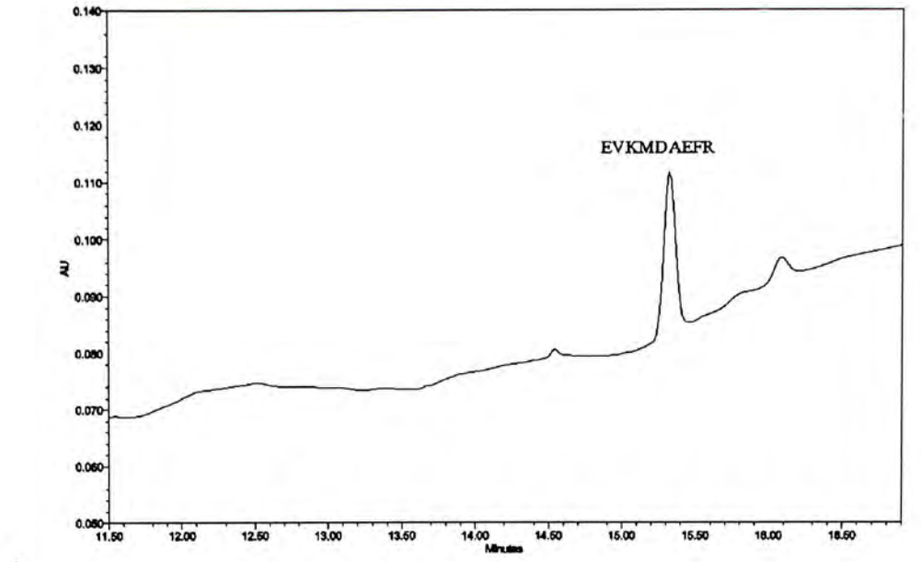

A

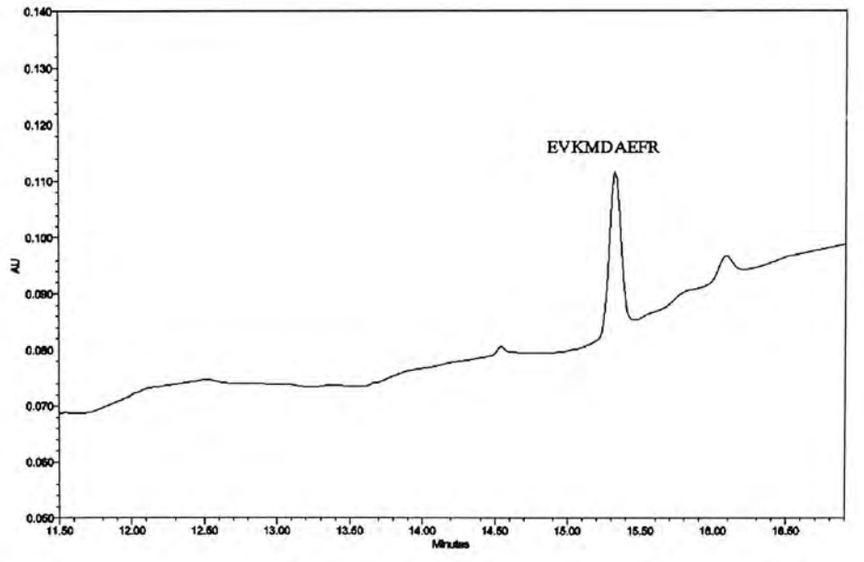

B

Fig. 3-16 Chromatograms of RP-HPLC assay. 10 μM peptide substrate and 2 μg sample were mixed in assay buffer. The reaction was stopped by boiling and storing in –20°C. (A) Membrane extracts from untransfected cells were boiled for 30 minutes before incubating with substrate EVKMDAEFR. (B) Membrane extracts from untransfected cells incubating with substrate EVKMDAEFR.

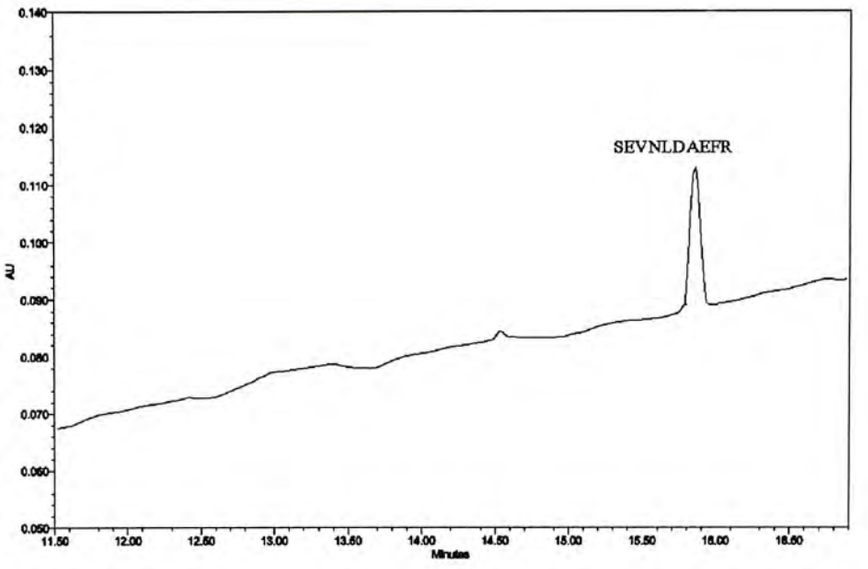

C

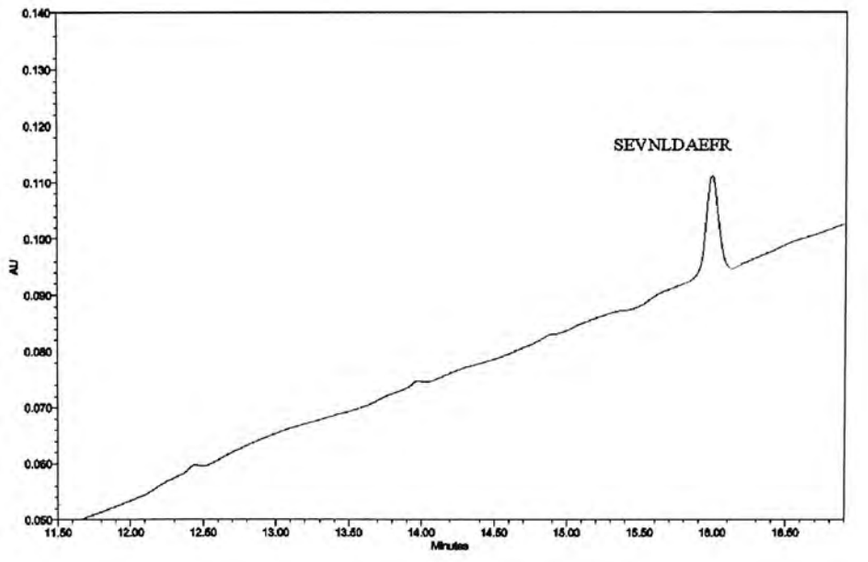

D

Fig. 3-16 (C) Membrane extracts from untransfected cells were boiled for 30 minutes before incubating with substrate SEVNLDAEFR. (D) Membrane extracts from untransfected cells incubating with substrate SEVNLDAEFR.

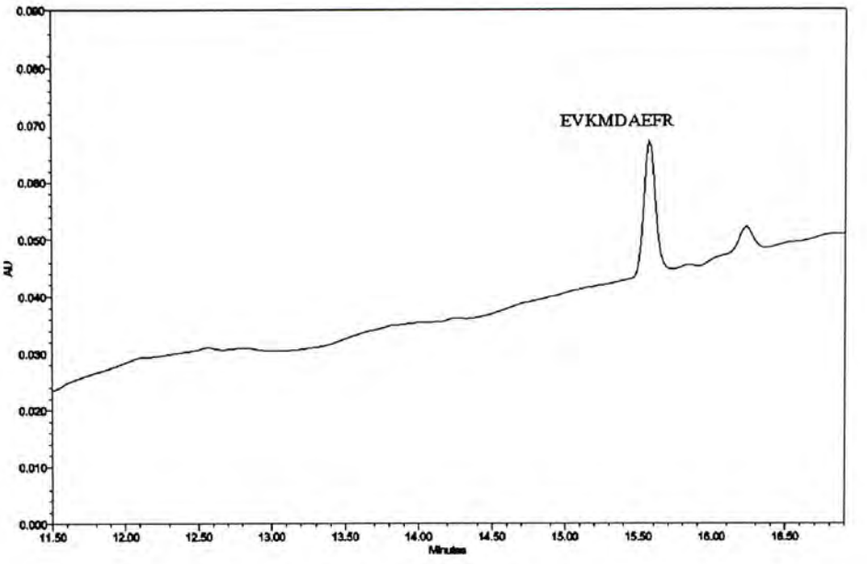

E

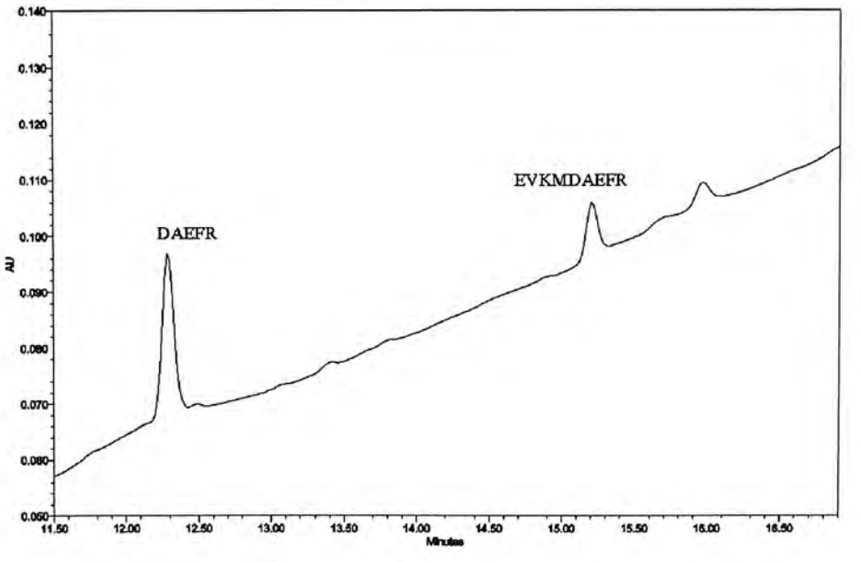

F

Fig. 3-16 (E) Membrane extracts from cells stably transfected with mBACE-pCDNA3 were boiled for 30 minutes before incubating with substrate EVKMDAEFR. (F) Membrane extracts from cells stably transfected with mBACE-pCDNA3 incubating with substrate EVKMDAEFR.

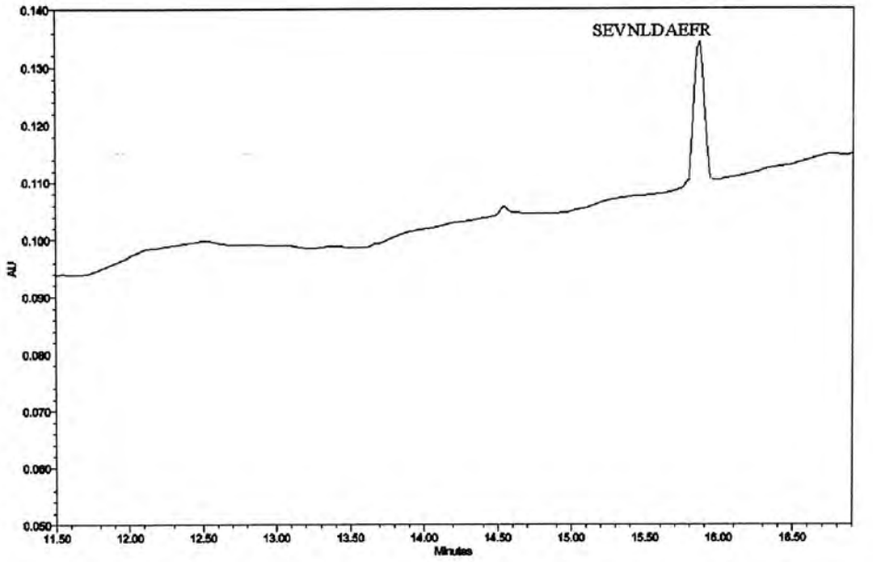

G

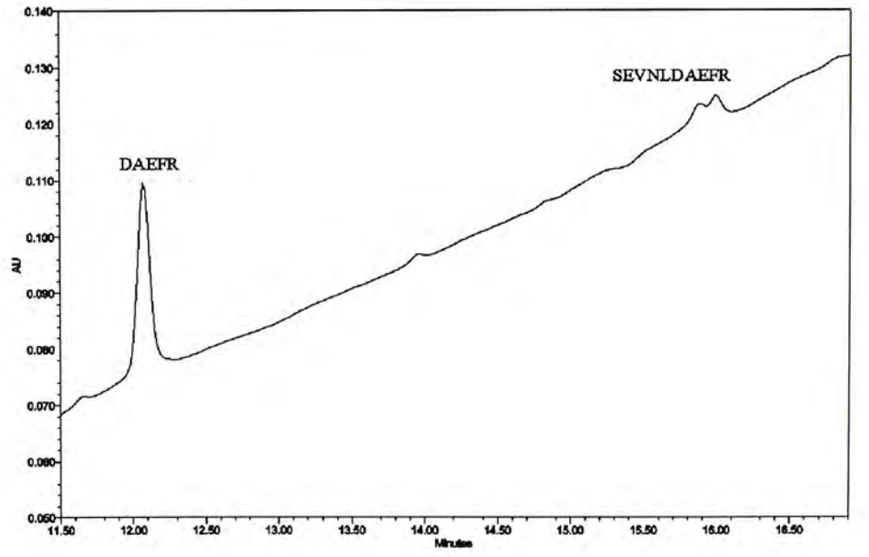

H

Fig. 3-16 (G) Membrane extracts from cells stably transfected with mBACE-pCDNA3 were boiled for 30 minutes before incubating with substrate SEVNLDAEFR. (H) Membrane extracts from cells stably transfected with mBACE-pCDNA3 incubating with substrate SEVNLDAEFR.

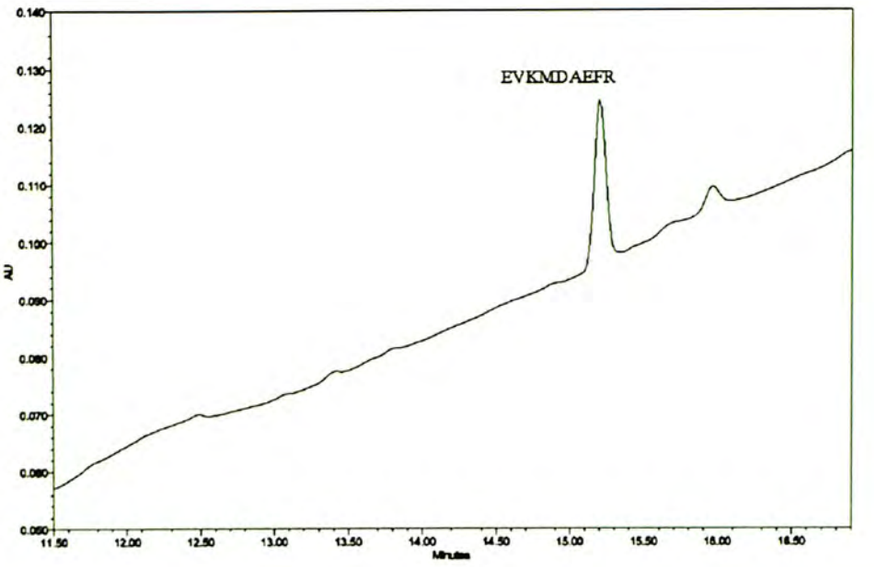

I

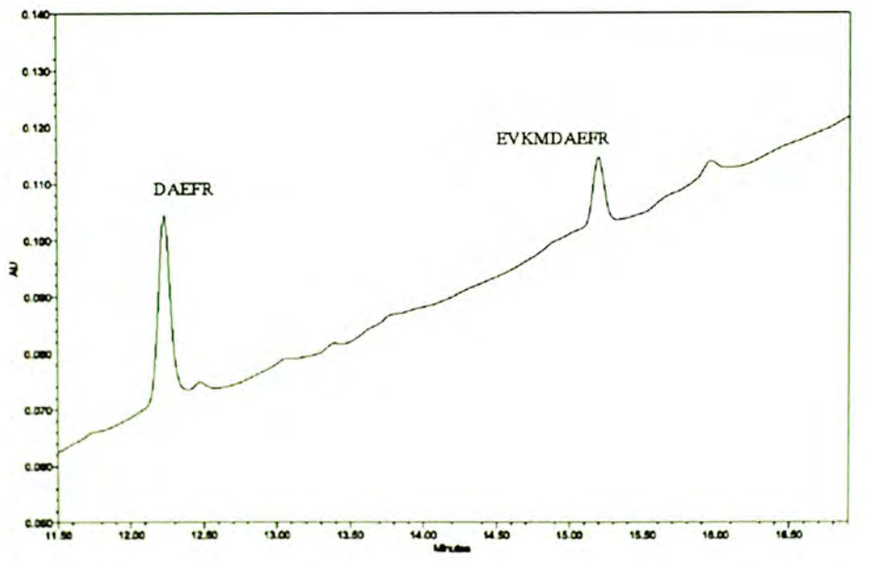

J

Fig. 3-16 (I) Membrane extracts from cells stably transfected with hBACE-pCDNA3 were boiled for 30 minutes before incubating with substrate EVKMDAEFR. (J) Membrane extracts from cells stably transfected with hBACE-pCDNA3 incubating with substrate EVKMDAEFR.

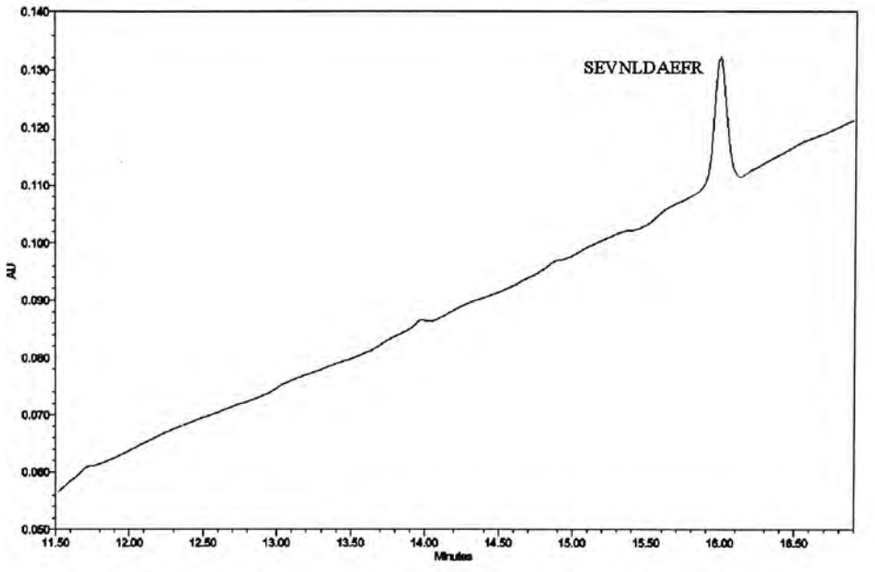

K

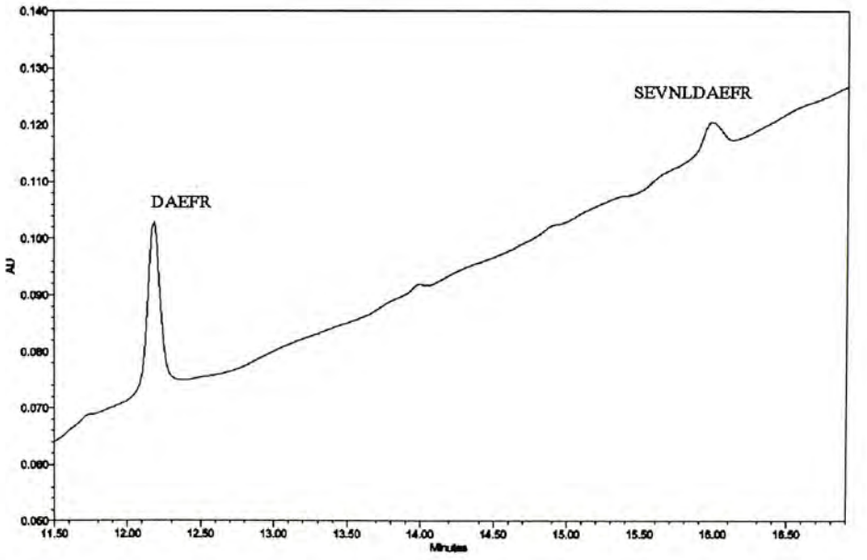

L

Fig. 3-16 (K) Membrane extracts from cells stably transfected with hBACE-pCDNA3 were boiled for 30 minutes before incubating with substrate SEVNLDAEFR. (L) Membrane extracts from cells stably transfected with hBACE-pCDNA3 incubating with substrate SEVNLDAEFR.

3.2.3.4 Immunohistochemistry

Polyclonal antibody hBACE485 purchased from ALEXIS was used as primary antibody used in immunohistochemistry. The cells were permealized with 0.1% triton X in PBS. Very few signals were detected in the untransfected cells, strong signals were detected in the cells stably transfected with mBACE-pCDNA3 and hBACE-pCDNA3, while stronger signals were detected in cells stably transfected with mBACE-pCDNA3. Most of cells had much stronger signals outside the nucleus.

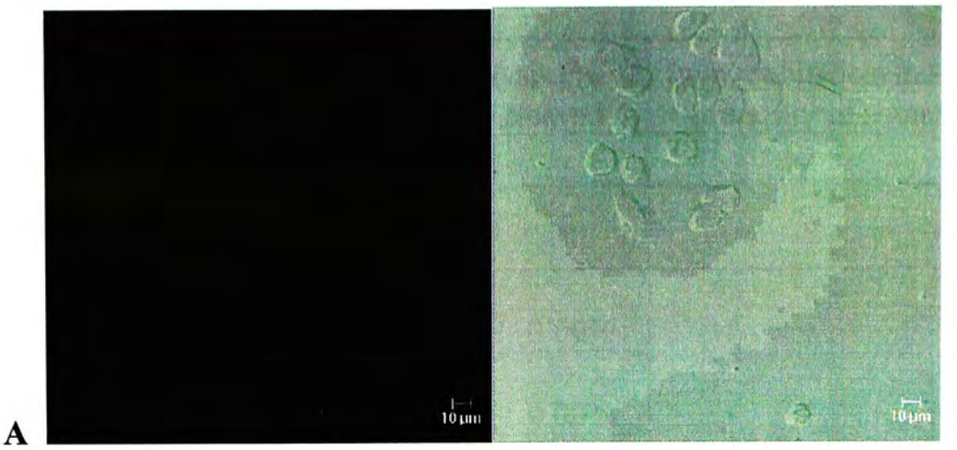

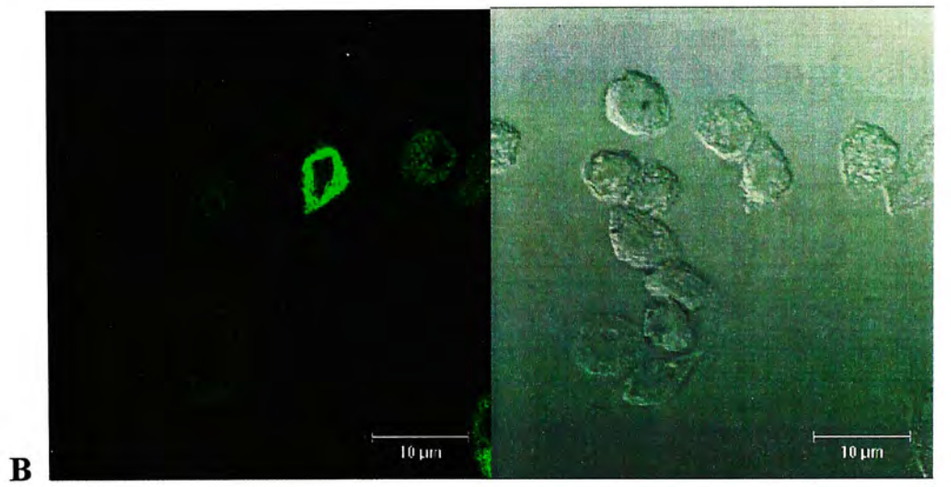

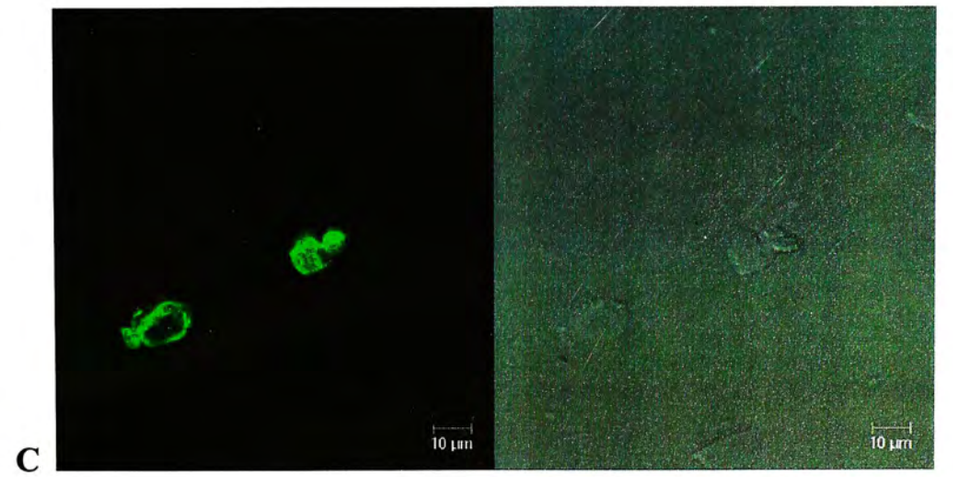

Fig. 3-17 Immunohistochemistry of BACE gene from (A) untransfected cells, (B) cells stably transfected with mBACE-pCDNA3 and (C) cells stably transfected with hBACE-pCDNA3 using hBACE485. The cells were unpermelised. Scale bar was 10 µM.

	Fluorometric analysis (nmol/mg/hr)		HPLC analysis (% of substrate cleaved)		Immunohistochemistry (intensity of signal)	Western Blot Analysis (intensity of signal)
	FS-1	FS-2				
Transiently transfected						
mBACE-pCDNA3	6.01	2.07	0.00%	0.00%		+
hBACE-pCDNA3	1.64	1.84	0.00%	0.00%		+
mBACE-pCDNA4HisMaxC	8.00	3.12	0.00%	0.00%		+
hBACE-pCDNA4HisMaxA	5.30	0.08	0.00%	60.00%	not applicable	+
Stably transfected						
mBACE-pCDNA3	23.25	10.58	66.67%	85.71%	+++++	+++
hBACE-pCDNA3	16.06	8.29	33.33%	81.82%	+++	+++++
E.coli. Expression						
urea						
nohBACE-pRSETA	8.11	1.81	not applicable			
prohBACE-pRSETA	0.72	1.12				
Guanidine HCL						
nohBACE-pRSETA	19.11	8.78	not applicable			
prohBACE-pRSETA	15.22	8.02				

* E.coli. expression was failed using vector nomBACE-pRSETB

Table 2 Summary of results of different assays using different vectors transformed and transfected into *E.coli* cells, BL21(DE3)LysS and mammalian cells, CHO cells respectively

Chapter 4 Discussions

Chapter 4

Discussion

Based on the sequencing results, the cloned BACE cDNAs have discrepancy with the published sequences, such as nomBACE and nohBACE had 95% and 98% identity with the reported sequences. The discrepancy was due to the wrong interpretations of computer, for example, some repeated signals, like CCCC, the computer may recognize it as CCC. The signals generated from the computer was checked manually using the program "chromas", the identity of sequences with the reported sequences were confirmed to 100% before transforming into BL21(DE3)LysS for expression, so as to avoid frameshift and wrongly encoded sequences occur.

In this study, the truncated forms of BACE without the transmembrane and C-terminal domains were demonstrated to be functionally expressed in prokaryotic expression system. Two constructs of BACE cDNAs were designed: one construct cDNA lacked of the coding sequence of the putative pre-domain; whereas the other lacked the pre- and pro-domain. ProhBACE and nohBACE had molecular size of 49 and 47 kDa as shown in SDS-PAGE in Fig. 3-4. According to analysis of protein size by SWISS-PROT, prohBACE and nohBACE protein had molecular weight of 48.78 and 46.14 kDa respectively. The size of protein expressed matched with the protein

size determined.

Using fluorometric analysis, Ermolieff *et al.* (2000) has determined the activity of BACE protein expressed from BL21(DE3) cells. Using synthetic Swedish mutation substrate, the activity of nohBACE was about 3.75 fold of that of prohBACE. Using synthetic wild-type substrate, the activity of nohBACE was about 1.60 fold of that of prohBACE. In this study, using synthetic Swedish mutation substrate, FS-1, the activity of nohBACE was about 2.27 fold of that of prohBACE. Using synthetic wild-type substrate, FS-2, the activity of nohBACE was about 1.90 fold of that of prohBACE. Comparing the result of Ermolieff et al. (2000) with ours, two similarity were found. First, the enzyme activity of BACE without the pro-domain (nohBACE) was higher than the one with the pro-domain (prohBACE). Secondly, the catalytic activity of both nohBACE and prohBACE towards FS-1 were higher than FS-2. The next two paragraphs will discuss the two similarity in details.

Like other aspartic proteases, the pro-domain blocks the entrance to the respective active-site clefts (James and Sielecki, 1986; Hartsuck *et al.*, 1992; Moore *et al.*, 1995). Likewise, it has previously been suggested that BACE is synthesized as zymogen with an inactive form containing the pro-domain (Bennett *et al.*, 2000; Haniu *et al.*, 2000). The lower catalytic activity of proHBACE suggested that the conformation of its pro domain exists in two equilibrium forms: one with the active

site 'open' and other with the active site 'closed' by virtue of a propeptide blockade (Ermolieff *et al.*, 2000). The catalytic activity of nohBACE was higher than prohBACE towards FS-1 and FS-2. This can be explained by the removal of the pro domain, leading to the formation of constitutively active enzyme.

The catalytic activity of both nohBACE and prohBACE towards FS-1 were higher than FS-2. This is consistent with the finding that BACE cleave synthetic peptides mimicking Swedish mutation APP than those peptides mimicking wild type APP (Vassar *et al.*, 1999; Yan *et al.*, 1999; Ermolieff *et al.*, 2000). The partial sequence of FS-2, which mimic wild type peptide, was EVKM*DA. Mutations of KM to NL at P2-P1, resulting EVNL*DA, the so-called Swedish mutation, were present in FS-1. These residues were labeled P4-P3-P2-P1/P1'-P2' in standard protease nomenclature with cleavage between P1 and P1' marked by *. In the models of BACE with APP-derived substrates as shown in Fig. 4-1, both the P1 leucine residue and P1 methionine residue on FS-1 and FS-2 make good hydrophobic contacts with Leu91, Tyr132 and Ile179. In FS-2, the P2 lysine makes a salt-bridge with BACE at Asp379. However, in FS-1, The P2 Asparagine can hydrogen bond to BACE Arg296, which hydrogen bonds to the P1' Asp (Sauder *et al.*, 2000). Having a more stable enzyme-substrate complex in FS-1 may account for the higher tendency of cleavage by BACE. Also various data showed that BACE has specificity for a hydrophobic residue at P1 (Sauder *et al.*, 2000).

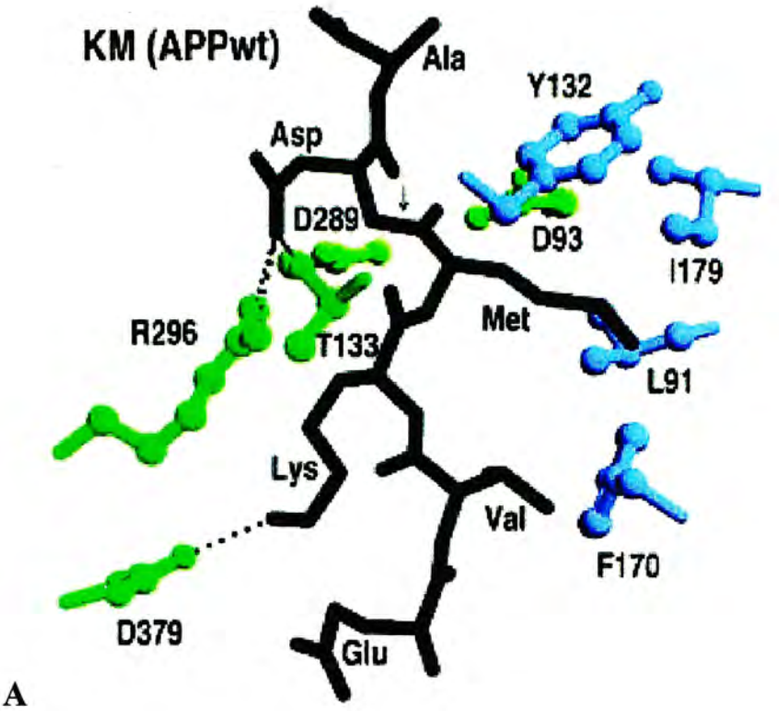

A

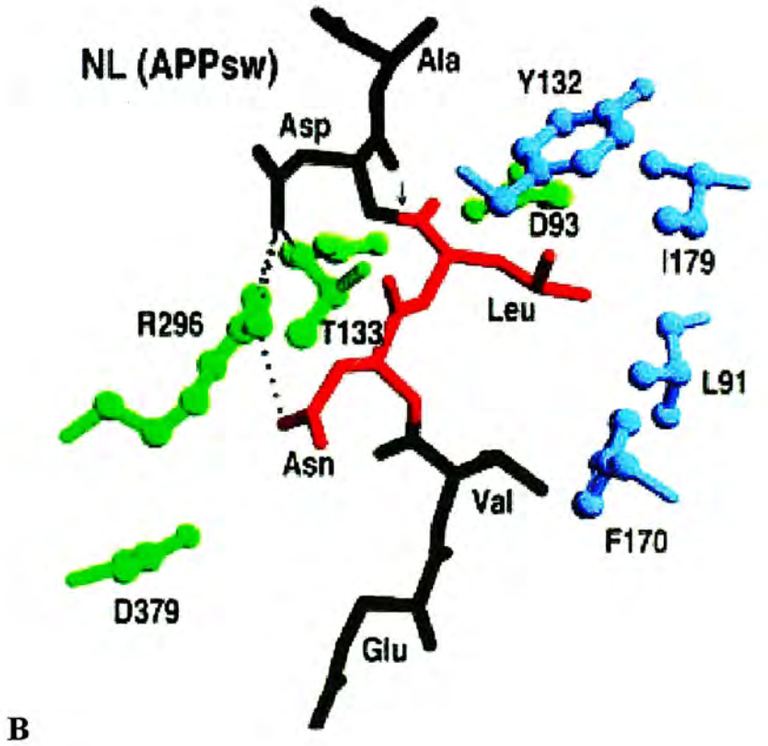

B

Fig. 4-1 Models of BACE with APP-derived substrates. (A) Wild-type substrate 592-597 of APP 695 (GenBank accession CAA312830.1) with sequence EVKM*DA with cleavage of the M-D peptide bond, indicated by an arrow. (B) Swedish mutation substrate with P2-P1 sequence of Asn-Leu (red) in place of wild-type Lys-Met (sequence EVNL*DA) (Sauder *et al.*, 2000).

Activity of protein purified and refolded in 0.1M guanidine HCl was higher than those in 0.8M urea. However this may not be the case, as guanidine HCl and urea, which are denaturing agent, still present in the solution. In order to make a comparison of the activity of protein extracted in guanidine HCl and urea, all the denaturing agent should be removed.

There had been difficulty in expressing truncated mouse and human BACE protein in BL21(DE3)LysS cells. After cloning of truncated mBACE and hBACE cDNAs into vector pRSETB and pRSETA respectively, much attempt had been tried to express the proteins using conventional method using different conditions, such as changing the concentration of IPTG, duration of induction, expression of different clones. However, no protein was successfully expressed. Finally, a plasmid stability test had been done to determine the level of toxic effect of target gene expression on bacterial growth, as described in section 2.2.10. According to the test, for stable plasmid, growth is prevented for any cells that have both the inducible gene for T7 RNA polymerase and a functional target plasmid. However, growth of cells that lack plasmid or mutants that have lost the ability to express target DNA is not prevented. Hence, less than 2% of cells will survive in LB plate with IPTG, less than 0.01% of cells will survive in LB plate with IPTG and antibiotics and almost all cells will survive in LB plate with antibiotics (Studier *et al.*, 1990). The result of test showed a large number of cells survived in LB plate with IPTG and very few colonies survived

in the LB plate with antibiotics. This proved the plasmids transformed were unstable or the genes were toxic.

If the gene whose product is toxic to the host cells is cloned in the plasmid. The level of expression may be such that the plasmid can be maintained but growth of the cells is impaired; segregation of cells lacking plasmid may also be increased because of decreased copy number or for other reasons. In this situation, cells that lack the plasmid can rapidly overgrow the culture whenever selective antibiotic is lacking. In the conventional method, the BL21(DE3)LysS cells were allowed to grow overnight in the presence of ampicillin before induction, a considerable amount of β-lactamase was secreted into the medium even if it became substantially overgrown by cells that lack plasmid. Subcultures were then grown from dilutions of 200 folds into fresh ampicillin-containing medium. However, enough β-lactamase was present in the saturated culture that, even at this dilution, enough remains to destroy all of the ampicillin before the cells that lack plasmid can be killed (Studier *et al.*, 1990). Therefore, the subculture will grow completely in the absence of selection. This explained why no protein was expressed after induction of 0.4 mM IPTG for 3 hours.

Hence, expression method was modified, as shown in section 2.2.2, in which bacterial culture were grown from picking of colonies from agar plate until OD_{600} of 0.2-0.6. Then the cells were centrifuged immediately so as to remove the old

medium containing secreted β-lactamase. The subcultures were grown with 1600 dilution in fresh medium containing ampicillin until OD_{600} of 0.2-0.6 so as to ensure the colonies bearing plasmids transformed were properly selected by ampicillin. Then the cells were centrifuged and induced for expression by 0.4 mM IPTG in the presence of ampicillin.

Using the modified method, nohBACE and prohBACE were successfully expressed. However, nomBACE was failed to express. The nomBACE was cloned into vector pRSETB while nohBACE and prohBACE were cloned into vector pRSETA. The difference between vector pRSETA and pRSETB was frameshifting of one amino acid in multiple cloning sites for expression of protein in suitable reading frame. Hence, using these two different vectors should not account for failure of expression for nomBACE. One possible reason may be due to the deletion of T7 gene 10 sequence in pRSETB during cloning. The cDNA of nomBACE was cloned into pRSETB at the EcoRI and NheI sites. Digestion of pRSETB by the two enzymes caused the deletion of T7 gene 10 sequence. T7 gene 10 sequence is a transcript stabilizing sequence gene 10 of phage T7. T7 gene 10 sequence increases the translational efficiency (Olins *et al.*, 1988; Olins and Rangwala, 1989) and stabilizes the mRNA (Sprengart *et al.*, 1996).

The HPLC and fluorometric analysis were done in assay buffer in pH 4.8,

refer to section 2.5, 2.6 and 2.7.7, as the activity of BACE was highest in pH of 4 to 5 (Lin *et al.*, 1999; Sinha *et al.*, 1999; Vassar *et al.*, 1999; Yan *et al.*, 1999). Leupeptin (serine/cysteine proteinase inhibitor) and PMSF (serine/cysteine proteinase inhibitor) were included in assay buffer in performing HPLC and fluorometric analysis, as BACE was not inhibited by these inhibitors (Sinha *et al.*, 1999). With these protease inhibitors, the cleavage of substrate by other enzymes could be significantly reduced.

In mammalian cells, BACE is synthesized as proBACE in the endoplasmic reticulum (ER) and then moves to the *trans*-Golgi network (TGN) where it rapidly loses its pro-domain due to cleavage by proprotein convertase (PC) (Huse *et al.*, 2000; Xiang *et al.*, 2000; Benjannet *et al.*, 2001) and furin or a furin-like proprotein convertase in mammalian cells (Bennett *et al.*, 2000; Shi *et al.*, 2001). Then BACE become mature after *N*-glycosylation (Vassar *et al.*, 1999; Bennett *et al.*, 2000; Walter *et al.*, 2000), especially on the catalytic ectodomain (Bodendorf *et al.*, 2001; Charlwood *et al.*, 2001). Because of *N*-glycosylation, the molecular mass of BACE expressed in human was greater than expected, and our results showed that the hBACE and mBACE expressed in stably cell lines were 55 and 61kDa which is larger than hBACE protein with transmembrane region but without pro-domain (51kDa).

In the immunohistochemistry of CHO cells stably transfected with mBACE-pCDNA3 and hBACE-pCNDA3, very few signals were detected in the

untransfected cells, much higher signals were detected in cells stably transfected with mBACE-pCDNA3 and hBACE-pCNDA3. Most of signals were detected in the cell membrane and cytoplasm. This was consistent with the results that BACE being membrane anchoring enzyme and present in secretory pathway, Golgi apparatus, *trans*-Golgi network (TGN), secretory vesicles and endosomes (Vassar *et al.*, 1999; Benjannet *et al.*, 2001; Walter *et al.*, 2001)

Membrane extracts from cells stably transfected by hBACE-pCDNA3 and mBACE-pCDNA3 preferentially cleaved the β-secretase site from the Swedish mutation over wild-type APP in fluorometric analysis as shown in Fig. 3-15, and cleaved at the expected position of substrates used in HPLC as BACE as shown in Fig. 3-16. These were consistent with the results of other groups (Vassar *et al.*, 1999; Yan *et al.*, 1999). In the fluorometric analysis, untransfected cells also had activity towards FS-1 and FS-2 implied that untransfected cells had expression of BACE, this may be due to the fact that most peripherial tissue had low levels of expression of BACE (Vassar *et al.*, 1999).

In transient transfection, expression of BACE in vector pCDNA4HisMax was higher than that of pCDNA3. Both pCDNA4HisMax and pCDNA3 contain cytomegalovirus (CMV) as promoter for expression. However, pCDNA4HisMax contains a QBI SP 163 translational enhancer for increased levels of recombinant

protein expression through ribosome recruitment and a cap-independent translational mechanism (Stein *et al.*, 1998). Moreover, presence of a large hairpin loop with a stability of 115 kcal/mol within the multiple cloning region (between BamHI and NotI) in pCDNA3, which likely inhibits translation (Kozak, 1989). Even expression of BACE in vector pCDNA4HisMax was better, stable cell lines using vector pCDNA4HisMax were not developed as antibiotic zeocin was required to develop stable cell line with vector pCDNA4HisMax. At that time, there was no zeocin in our laboratory and making new order of it consumes time. Because of time constraint, only cell lines with vector pCDNA3 were generated.

The expression of mBACE was better than hBACE in CHO cells as shown by fluorometric analysis in Fig. 3-11 and Fig. 3-15, immunohistochemistry in Fig. 3-17. Even mBACE had 93% sequence identity with hBACE. One possible explanation was that Chinese Hamester Ovary (CHO) cells was a mouse cell line, the cellular processing of mBACE in CHO cells make the protein more functional. If that is the case, a reverse situation may occur if mBACE and hBACE were expressed in human cell lines, such as Human Embryonic Kidney (HEK) 293 cells.

Using RP-HPLC, Vassar *et al.* (1999) has demonstrated that hBACE protein purified from stably transfected 293T cells had activity of 9 nmol/min/mg against 30 μM synthetic wild-type peptide with sequence

TTRPGSGLTNIKTEEISEVKMDAEFRHDK(dnp)G in a 50 µl assay. Their activity was 60 fold of that of membrane extracts from CHO cells stably transfected with hBACE-pCDNA3 (8.29 nmol/hr/mg) that we have performed. The difference may be due to the fact that the expressed hBACE protein in membrane extract has not been purified yet.

In order to develop a screening assay of inhibitor of BACE, a better expression system and a more sensitive assay method were employed. *E.coli* system was chosen to express protein for developing screening assay for inhibitor of BACE as *E.coli* can produce larger quantity of protein in a relatively short time that mammalian cells. nohBACE extracted in guanidine HCl will be used to screen for inhibitor of BACE as nohBACE had higher activity than prohBACE and nohBACE had higher activity when extracted in guanidine HCl than those extracted in urea. Fluorometric analysis will be employed as assay method to screen inhibitor of BACE as fluorometric analysis was able to analyze large amount of samples in a shorter time and was more sensitive that HPLC analysis.

References

References

Acquati, F., Accarino, M., Nucci, C., Fumagalli, P., Jovine, L., Ottolenghi, S., and Taramelli, R. (2000) The gene encoding DRAP (BACE2), a glycosylated transmembrane protein of the aspartic protease family, maps to the down critical region. *FEBS Lett.* **468:** 59-64.

Alzheimer's disease research center, ADRC, 2000. Available at http://www.alzresearch.org/

Alzheimer A. (1907) Ueber eine eigenartige Erkrankung der Hinirnde. *Allg Z. Psychiat* **46:** 146-148

Anderton, B.H., Brion, J.P., Couck, A.M., Davis, D.R., Gallo, J.M., Hanger, D.P., Ladhani, K., Latimer, D.A., Lewis, C., and Lovestone, S. (1995) Modulation of PHF-like tau phosphorylation in cultured neurons and transfected cells. *Neurobiol. Aging* **16:** 389-397.

Arrasate, M., Perez, M., Armas-Portela, R., and Avila, J. (1999) Polymerization of tau peptides into fibrillar structures. The effect of FTDP-17 mutations. *FEBS Lett.* **446:** 199-202.

Baker, D., Shiau, A.K., and Agard, D.A. (1993) The role of pro regions in protein folding. *Curr. Opin. Cell Biol.* **5:** 966-970.

Barrow, C.J. and Zagorski, M.G. (1991) Solution structures of beta peptide and its constituent fragments: relation of amyloid depostition. *Science* **253:** 179-182.

Bayer, A.J. (1999) The molecular basis and genetic determinants of Alzheimer's disease. *Clinical Gerontology* **9:** 297-304.

Benjannet, S., Elagoz, A., Wickham, L., Mamarbachi, M., Munzer, J.S., Basak, A., Lazure, C., Cromlish, J.A., Sisodia, S., Checler, F., Chretien, M., and Seidah, N.G. (2001) Post –translational processing of β -secretase (β -amyloid –converting enzyme) and its ectodomain shedding. *J. Biol. Chem.* **276:** 10879-10887.

Bennett, B.D., Babu-Khan, S., Loeloff, R., Louis, J.-C., Curran, E., Citron, M., and Vassar, R. (2000) Expression Analysis of BACE2 in Brain and Peripheral Tissues. *J. Biol. Chem.* **275:** 21099-21106.

Bodendorf, U., Fischer, F., Bodian, D., Multhaup, G., and Paganetti, P. (2001) A splice variant of beta-secretase deficient in the amyloidogenic processing of the

amyloid precursor protein. *J.Biol. Chem.* **276:** 12019-12023.

Borchelt, D.R., Thinakaran, G., Eckman, C.B., Lee, M.K., Davenport, F., Ratovitsky, T., Prada, C.M., Kim, G., Seekins, S., Yager, D., Slunt, H.H., Wang, R., Seeger, M., Levey, A.I., Gandy, S.E., Copeland, N.G., Jenkins, N.A., Price, D.L., Younkin, S.G., and Sisodia, S.S. (1996) Familial Alzheimer's disease-linked presenilin 1 variants elevate $A\beta_{1\text{-}42/1\text{-}40}$ ratio *in vitro* and *in vivo*. *Neuron* **17:** 1005-1013.

Braak, H. and Braak, E. (1998) Evolution of neuronal changes in the course of Alzheimer's disease. *J. Neural Transm.* **105:** 127-140.

Braak, E., Braak, H., and Mandelkow, E.M. (1994) A sequence of cytoskeleton changes related to the formulation of neurofibrillary tangles and neuropil threads. *Acta Neuropathol.* **87:** 554-567.

Bradford, M.M. (1976) A rapid and sensitive method for the quantitation of microgram quantities of protein utilizing the principle of protein dye binding. *Anal Biochem*. **72:** 248-254.

Bramblett, G.T., Goedert, M., Jakes, R., Merrick, S.E., Trojanowski, J.Q., and Lee, V.M. (1993) Abnormal tau phosphorylation at Ser396 in Alzheimer's disease

recapitulates development and contributes to reduced microtubule binding. *Neuron* **10:** 1089-1099.

Cai, X.-D., Golde, T.E., and Younkin, S.G. (1993) Release of excess amyloid β -protein from a mutant anyloid β-precursor. *Science* **259:** 514-516.

Castano, E.M., Ghiso, J., Prelli, F., Gorevic, P.D., Migheli, A., and Frangione, B. (1986) In vitro formation of amyloid fibrils from two synthetic peptides of different lengths homologous to Alzheimer's disease beta-protein. *Biochem. Biophys. Res. Commun.* **141:** 782-789.

Charlwood, J., Dingwall, C., Matico, R., Hussain, I., Johanson, K., Moore, S., Powell, D. J., Skehel, J. M., Ratcliffe, S., Clarke, B., Trill, J., Sweitzer, S., and Camilleri P. (2001) Characterization of the glycosylation profiles of Alzheimer's β-secretase protein Asp-2 expressed in a variety of cell lines. *J. Biol. Chem.* **276:** 16739-16748.

Chyung, A.S., Greenberg, B.D., Cook, D.G., Doms, R.W., and Lee, V.M. (1997) Novel beta-secretase cleavage of beta-amyloid precursor protein in the endoplasmic reticulum/intermediate compartment of NT2N cells. *J. Cell Biol.* **138:** 671-680.

Citron, M., Oltersdorf, T., Haass, C., McConlogue, L., Hung, A.Y., Seubert, P.,

Vigo-Pelfrey, C., Lieberburg, I., and Selkoe, D.J. (1992) Mutation of the beta-amyloid precursor protein in familial Alzheimer's disease increases beta-protein secretion. *Nature* **360:** 672-674.

D'Souza, I., Poorkaj, P., Hong, M., Nochlin, D., Lee, V.M., Bird, T.D., and Schellenberg, G.D. (1999) Missense and silent tau gene mutations cause frontotemporal dementia with parkinsonism-chromosome 17 type, by affecting multiple alternative RNA splicing regulatory elements. Proc. Natl. Acad. Sci. U.S.A. 96, 5598-5603.

Davies, P. and Maloney, A. J. (1976) Selective loss of central cholinergic neurons in Alzheimer's disease. *Lancet* **2**: 1403.

Dhavan, R. and Tsai, L.-H. (2001) A decade of cdk5. *Nat. Rev. Mol. Cell Biol.* **2:** 749-759.

Dovey, H.F., Chrysler, S.S., Lieberburg, I., Sinha, S., and Keim, P.S. (1993) Cells with a familial Alzheimer's disease mutation produce authentic beta-peptide. *Neuroreport* **4:** 1039-1042.

Embi, N., Rylatt, D.B., and Cohen P. (1980) Glycogen synthase kinase-3 from rabbit

skeletal muscle. Separation from cyclic-AMP-dependent protein kinase and phosphorylase kinase. *Eur. J. Biochem.* **107:** 519-527.

Ermolieff, J., Loy, J.A., Koelsch, G., and Tang, J. (2000) Proteolytic activation of recombinant Pro-memapsin 2 (Pro-β-secretase) studied with new fluorogenic substrates. *Biochemistry* **39:** 12450-12456.

Esiri. M.M. and Morris, J.H. (1997) The neuropathology of dementia. In. Cambridge university press. Cambridge, UK.

Farzan, M., Schnitzler, C.E., Vasilieva, N., Leung, D. and Choe, H. (2000) BACE2, a β-secretase homolog, cleaves at the β-site and within the amyloid- β region of the amyloid-β precursor protein. *Proc. Natl. Acad. Sci. USA* **97:** 9712-9717.

Forman, M.S., Cook, D.G., Leight, S., Doms, R.W. and Lee, V.M.-Y. (1997) Differential Effects of the Swedish Mutant Amyloid Precursor Protein on β-Amyloid Accumulation and Secretion in Neurons and Nonneuronal Cells. *J. Biol. Chem.* **272:** 32247-32253.

Glenner, G.G. and Wong, C.W. (1984) Alzheimer'disease: initial report of the purification and characterization of a novel cerebrovascular amyloid protein.

Biochemical and Biophysical Research Communications **120:** 885-890.

Goedert, M., Trojanowske, J.Q. and Lee, V. M.-Y. (1997) Tau protein and the neurofibrillary pathology of Alzheimer's disease. *Molecular Mechanisms of dementia*: 199-218.

Goldagaber, D., Lerman, M.I., and McBride, O.W. (1987) Characterization and chromosomal localization of a cDNA encoding brain amyloid of Alzheimer's Disease. *Science* **235:** 877-880.

Gotz, J., Chen, F., Dorpe, J.V., and Nitsch, R.M. (2001) Formation of neruofibrillary tangles in P301L tau transgenic mice induced by Aβ 42 fibrils. *Science* **293:** 1491-1495.

Grover, A., Houlden, H., Baker, M., Adamson, J., Lewis, J., Prihar, G., Pickering-Brown, S., Duff, K., and Hutton, M. (1999) 5' splice site mutations in tau associated with the inherited dementia FTDP-17 affect a stem-loop structure that regulates alternative splicing of exon 10. *J. Biol. Chem.* **274:** 15134-15143.

Grundke-Iqbal, I., Iqbal, K., Tung, Y.C., Quinlan, M., Wisniewske, H.M. and Binder, L.I. (1986) Abnormal phosphorylation of the microtubule-associated protein tau in

Alzheimer cytoskeletal pathology. *Proc. Natl. Acad. Sci. (USA)* **83:** 4913-4917.

Haass, C., Hung, A.Y., Selkoe, D.J., and Teplow, D.B. (1994) Mutations associated with a locus for familial Alzheimer's Disease result in alternative processing of amyloid β-protein precursor. *J. Biol. Chem.* **269:** 17741-17748.

Haniu, M., Denis, P., Young, Y., Mendiaz, E.A., Fuller, J., Hui, J.O., Bennett, B.D., Kahn, S., Ross, S., Burgess, T., Katta, V., Rogers, G., Vassar, R. and Citron, M. (2000) Characterization of Alzheimer's beta -secretase protein BACE. A pepsin family member with unusual properties. *J. Biol. Chem.* **275:** 21099-21106.

Hardy, J. and Allsop, D. (1991) Amyloid deposition as the central event in the aetiology of Alzheimer's disease. *Trends Pharmacol Sci* **12:** 383-388.

Hardy. J.A. and G.A. Higgins (1992) Alzheimer's disease: the amyloid cascade hypothesis. *Science* **256:** 184-185.

Hartsuck, J. A., Koelsch, G., and Remington, S. J. (1992) The high-resolution crystal structure of porcine pepsinogen. *Proteins.* **13:** 1-25.

Hemmings, B.A., Yellowees, D., Kernohan, J.C. and Cohen, P. (1981) Purification of

glycogen synthase kinase 3 from rabbit skeletal muscle. Copurification with the activating factor (FA) of the (Mg-ATP) dependent protein phosphatase. *Eur. J. Biochem.* **119:** 443-451.

Heutink, P. (2000) Untangling tau-related dementia. *Hum. Mol. Genet.* **9:** 979-986

Hughes K., Nikolakaki E., Plyte, S.E., Totty, N.F. and Woodgett, J.R. (1993) Modulation of the glycogen synthase kinase-3 family by tyrosine phosphorylation. *EMBO J.* **12:** 803-808.

Huse, J.T., Pijak, D.S., Leslie, G.J., Lee, V.M.-Y. and Doms, R.W. (2000) Maturation and endosomal targeting of β-Site amyloid precursor protein-cleaving enzyme. *J. Biol. Chem.*, **275:** 33729-33737.

Hussain, I., Powell, D., Howlett, D.R., Tew, D.G., Week, T.D., Chapman, C., Gloger, I.S., Murphy, K.E., Southan, C.D, Ryan, D.M., Smith, T.S., Simmons, D.L., Walsh, F.S., Dingwall, C. and Christie, G. (1999) Identification of a novel aspartic protease (Asp 2) as β-secretase. *Mol. Cell. Neurosci.* **14:** 419-427.

Imahori, K. and Uchida, T. (1997) Physiology and pathology of tau protein kinases in relation to Alzheimer's disease. *J. Biochem. (Tokyo)* **121:** 179-188.

Ishiguro, K., Kobayashi, S., Ormori, A., Takamatsu, M., Yonekura, S., Anzai, K., Imahori, K. and Uchida, T. (1994) Identification of the 23 kDa subunit of tau protein kinase II as a putative activator of cdk5 in bovine brain. *FEBS LETT.* **342:** 203-208.

James, M. N. and Sielecki, A. R. (1986) Molecular structure of an aspartic proteinase zymogen, porcine pepsinogen, at 1.8A resolution. *Nature* **319:** 33-38.

Jarrett, J.T., Berger, E.P. and Lansbury, P.T. (1993) The C-terminus of the beta protein is critical in amyloidgenesis. *Annals of the New York Academy of Sciences* **695:** 144-148.

Kang, J., Lemaire, H.G., Unterbeck, A., Salbaum, J.M., Masters, C.L., Multhap, G., Beyreuther, K., and Uller-Hill, B. (1987) The precursor of Alzheimer disease amyloid A4 protein resembles a cell surface receptor. *Nature* **325:** 733-736.

Khan, A. R. and James, M.N.G. (1998) Molecular mechanisms for the conversion of zymogens to active proteolytic enzymes. *Protein Sci.* **7:** 815-836.

Knops, J., Suomensaari, S., Lee, M., McConlogue, L., Serbert, P. and Sinha, S. (1995) Cell-type and amyloid precursor protein-type specific inhibition of A beta release by

bafilomycin A1, a selective inhibitor of vacuolar ATPase. *J. Biol. Chem.* **270:** 2419-2422.

Kozak, M. (1989) Circumstances and mechanisms of inhibition of translation by secondary structure in eukaryotic mRNAs. *Mol Cell Biol.* **9:** 5134-42.

Lee, G. (1993) Non-motor microtubule-associated proteins. *Curr. Opin. Cell Biol.* **5:** 88-94.

Lee, M.K., Slunt, H.H., Martin, L.J., Thinakaran, G., Kim. G., Gandy, S.E., Seeger, M., Koo, E., Price, D.L., and Sisodia, S.S. (1996) Expression of presenilin 1 and 2 (PS1 and PS2) in human and murine tissues. *J.Neurosci.* **16:** 7513-7525.

Lendon. C.L., Ashall., F. and Goate, A.M. (1997) Exploring the etiology of Alzheimer disease using molecular genetics. *Jama.* **277:** 825-831.

Levis J., Dennis W.D, Lin W., Louise C., Anthony C., Graham J., Yen S-H., Sahara N., Lisa S., Debra Y., Chris E., John H., Mike H., and Eileen M. (2001) Enhanced neurofibrillary degeneration in transgenic mice expressing mutant tau and APP. *Science* **293:** 1487-1491.

Levy-Lahad, E., Wijsman, E.M., Nemens, E., Anderson, L., Goddard, K.A., Weber, J.L., Bird, T.D., and Schellenberg, G.D. (1995) A familial Alzheimer's disease locus on chromosome 1. *Science* **269:** 970-973

Lew, J., Huang, Q.Q., Qi, Z., Winkfein, R.J., Aebersold, R., Hunt, T. and Wang, J.H. (1994) A brain-specific activator of cyclin-dependent kinase 5. *Nature* **371:** 423-426.

Lin, X., Koelsch, G., Wu, S., Downs, D., Dashti, A. and Tang, J. (2000) Human aspartic protease memapsin 2 cleaves the β-secretase site of β-amyloid precursor protein. *Proc. Natl. Acad. Sci. USA* **97:** 1456-1460.

Lorenzo, A. and Yanker, B.A. (1994) β-amyloid neurotoxicity requires fibril formation and is inhibited by Congo red. *PNAS USA* **91:** 12243-12247.

Lovestone S. and Reynolds C.H. (1997) The phosphorylation of tau: a critical stage in neurodevelopment and neurodegenerative processes. *Neuroscience* **78:** 309-324.

Lovestone S., Reynolds C.H., Latimer D., Davis D.R., Anderton B.H., Gallo J.M., Hanger D., Mulot S., Marquardt B., and Stabel S. (1994) Alzheimer's disease-like phosphorylation of the microtubule-associated protein tau by glycogen synthase kinase-3 in transfected mammalian cells. *Curr Biol.* **4:** 1077-1086.

Lu, M. and Kosik, K.S. (2001) Competition for microtubule-binding with dual expression of tau missence and splice isoforms. *Mol. Biol. Cell* **12:** 171-184.

Mallender, W.D., Yager, D., Onstead, L., Nichols, M.R., Eckman, C., Sambamurti, K., Kopcho, L.M., Marcinkeviciene, J., Copeland, R.A., and Rosenberry, T.L. (2001) Characterization of recombinant, soluble beta-secretase from an insect cell expression system. *Mol Pharmacol* **59:** 619-626.

Mandelkow E. and Mandelkow E.M. (1995) Microtubules and microtubule-associated proteins, *Curr. Opin. Cell Biol.* **7:** 72-81.

Masters, C.L., Simms, G., Weinman, N.A., Multhaup, G., McDonald, B.L., and Beyreuther, K. (1985). Amyloid plaque core protein in Alzheimer disease and Down syndrome. *Proc Natl Acad Sci (U S A)* **82:** 4245-4249.

Mattson, M.P., Cheng, B., Culwell, A. R., Esch, F. S., Lieberburg, I., and Rydel, R.E. (1993) Evidence for excitoprotective and intraneuronal calcium-regulating roles for secreted forms of the beta-amyloid precursor protein. *Neuron* **10:** 243-254.

Moore, S. A., Sielecki, A. R., Chernaia, M. M., Tarasova, N. I., and James, M. N.

(1995) Crystal and molecular structures of human progastricsin at 1.62 A resolution. *J. Mol. Biol.* **247:** 466-485.

Mudher, A. and Lovestone, S. (2002) Alzheimer's disease-do tauists and Baptists finally shake hands? *Trends in Neurosciences* **25:** 22-25.

Mullan, M. (1992) A pathogenic mutation for probably Alzheimer's disease in the APP gene at the N-terminus of beta-amyloid. *Nature Genet.* **1:** 345-347.

Mulot, S.F., Hughes K., Woodgett, J.R., Anderton, B.H. and Hanger D.P. (1994) PHF-tau from Alzheimer's brain comprises four species on SDS-PAGE which can be mimicked by in vitro phosphorylation of human rain tau by glycogen synthase kiinase-3 beta, *FEBS Lett.* **349:** 359-364.

Nagy, Z., Esiri, M.M., Jobst, K.A., Morris, J.H., King, E.M., McDonald, B., Litchfield, S., Smith, A., Barnetson, L., and Smith, A.D. (1995) Relative roles of plaques and tangles in the dementia of Alzheimer's disease: correlations using three sets of neuropathological criteria. *Dementia* **6:** 21-31.

Neve, R.L. and Robakis, N.K. (1998) Alzheimer's disease: a re-examination of the amyloid hypothesis. *Trends Neurosci.* **21:** 15-19.

Olins, P.O., Devine, C.S., Rangwala, S.H., and Kavka, K.S. (1988) The T7 phage gene 10 leader RNA, a ribosome-binding site that dramatically enhances the expression of foreign genes in *Escherichia coli*. *Gene* **73:** 227-235.

Olins, P.O. and Rangwala, S.H. (1989) A novel sequence element derived from bacteriophage T7 mRNA acts as an enhancer of translation of the *lacZ* gene in *Escherichia coli*. *J. Biol. Chem*. **264:** 16973-16976.

Oltresdorf, T., Fritz, L.C., Schenk, D.B., Lieberburg, I., Johnson-Wood, K.I., Beattie, E.C., Ward, P.J., Blaher, R.W., Dovey, H.F., and Sinha, S. (1989) The secreted form of the Alzheimer's amyloid precursor protein with the Kunitz domain is protease nexin-II. *Nature* **341:** 144-147.

Patrick, G.N., Zukerberg, L., Nikolic, M., de la Monte, S., Dikkes, P. and Tsai, L.H. (1999) Conversion of p35 to p25 deregulates cdk5 activity and promotes neurodegeneration. *Nature* **402:** 615-622.

Paudel, H.K., Lew, J., Ali, Z. and Wang, J.H. (1993) Brain proline-directed protein kinase phosphorylates tau on sites that are abnormally phosphorylated in tau associated with Alzheimer's paired helical filaments. *J.Biol. Chem.* **268:**

23512-23518.

Pei, J.J., Grundke-Iqbal, I., Iqbal, K., Bogdanovic, N., Winblad, B. and Cowburn, R.F. (1998) Accumulation of cyclin-dependent kinase 5 (cdk5) in neurons with early stages of Alzheimer's disease neurofibrillary degeneration. *Brain Res.* **797:** 267-277.

Pei, J.J., Tanaka, T., Tung, Y.C., Braak, E., Iqbal, K. and Grundke-Iqbal I. (1997) Distribution , levels, and activity of glycogen synthase kinase-3 in the Alzheimer disease brain, *J. Neuropathol. Exp. Neurol.* **56:**70-78.

Perez, M., Lim, F., Arrasate, M., and Avila, J. (2000) The FTDP-17-linked mutation R406W abolishes the interaction of phosphorylated tau with microtubules. *J. Neurochem.* **74:** 2583-2589.

Perry, E. K., Tomlinson, B. E., Blessed, G., Bergmann, K., Gibson, P. H. and Perry, P. H. (1978) Correlation of cholinergic abnormalities with senile plaques and mental test scores in senile dementia. *Br. Med. J.* **2**: 1457-1459.

Pike, C.J., Burdick, D., Walencewicz, A.J., Glabe, C.G. and Cotman, C.W. (1993) neurodegeneration induced by beta-amyloid peptides in vitro: the role of peptide assembly state. *Journal of Neuroscience* **13:** 1676-1687.

Price, D.L. and Sisodia, S.S. (1998) Mutant genes in familial Alzheimer's disease and transgenic models. *Annu. Rev. Neurosci.* **21:** 497-505.

Rawlings, N. D. and Barrett, A. J. (1995) Families of aspartic peptidases, and those of unknown catalytic mechanism. *Methods Enzymol.* **248:** 105-120.

Rizzu, P., Joosse, M., Ravid, R., Hoogeveen, A., Kamphorst, W., Van-Swieten, J.C., Willemsen, R., and Heutink, P. (2000) Mutation-dependent aggregation of tau protein and its selective depletion from the soluble fraction in brain of P301L FTDP-17 patients. *Hum. Mol. Genet.* **9:** 3075-3082.

Robakis, N.K., Lahiri, D.K., Brown, H.R., Rubenstein, R., Mehta, B., Wisniewski, H., and Goller, N. (1988). Expression studies of the gene encoding the Alzheimer's Disease and Down Syndrome amyloid peptide. Disorders of the Developing Nervous System: changing views on their origins, diagnoses and treatments. New York, Alan, R., *Liss.*: 183-193.

Sauder, J.M., Arthur, J.W. and Dunbrack, R.L.J. (2000) Modeling of substrate specificity of the Alzheimer's disease amyloid precursor protein beta-secretase. *J Mol Biol.* **300:** 241-8.

Saunders, A.M., Strittmatter, W.J., Schmechel, D., George-Hyslop, P.H., Perick-Vance, M.A., Joo, S.H., Rosi, B.L., Gusella, J.F., Crapper-MacLachlan, D.R., and Alberts, M.J. (1993) Association of apolipoprotein E allele epsilon 4 with late-onset familial and sporadic Alzheimer's disease. *Neurology* **43:** 1467-1472.

Selden S.C. and Pollard T.D. (1983) Phosphorylation of microtubule-associated proteins regulates their interaction with actin filaments. *J. Biol. Chem.* **258:** 7064-7071.

Sherrington, R., Rogaev, E.I., Liang, Y., Rogaeva, E.A., Levesque, G., Ikeda, M., Chi, H., Lin, C., Li, G., and Holman, K. (1995) Cloning of a gene bearing missense mutations in early-onset familial Alzheimer's disease. *Nature* **375:** 754-760.

Shi, X-P., Chen, E., Yin, K-C., Na, S., Garsky, V.M., Lai, M-T., Li, Y-M., Plathchek, M., Register, R.B., Sardana, M.K., Tang, M-J., Thiebeau. J., Wood, T., Shafer, J.A. and Gardell, S.J. (2001) The Pro domain of β-secretase does not confer strict zymogen-like properties but does assist proper folding of the protease domain. *J.Biol. Chem.* **276:** 10366-10373.

Shirurba, R.A., Ishiguro K., Takahashi, M., Sato K., Spooner E.T., Mercken, M.,

Yoshida R., Wheelock, T.R., Yanagawa, H., Imahori K. and Nixon R.A. (1996) Immunocytochemistry of tau phosphoserine 413 and tau protein kinase I in Alzheimer pathology. *Brain Res.* **737:** 119-132.

Sinha, S., Anderson, J.P., Barbour, R., Basi, G.S., Caccavello, R., Davis, D., Doan, M., Dovey, H.F., Frigon, N., Hong, J., Jacobson-Croak, K., Jewett, N., Keim, P., Knops, J., Lieberburg, I., Power, M., Tan, H., Tatsuno, G., Tung, J., Schenk, D., Seubert, P., Suomersaari, S.M., Wang, S., Walker, D., Zhao, J., McConlogue, L. and John, V. (1999) Purification and cloning of amyloid precursor protein [beta]-secretase from human brain. *Nature* **402:** 537-540.

Smith, R.P., Higuchi, D.A., and Broze, G.J. (1990) Platelet coagulation factor Xia-inhibitor, a form of Alzheimer amyloid precursor protein. *Science* **248:** 1126-1128.

Sprengart, M.L., Fuchs, E., and Porter, A.G. (1996) The downstream box: an efficient and independent translation initiation signal in *Escherichia coli*. *EMBO*. **15:** 665-674.

St. George-Hyslop, Haines, P., Rogaev, J., Mortilla, E., Vaula, M., Pericak-Vance, G., Foncin, M., Montesi, J.-F., Bruni, M., Sorbi, A., Rainero, S., Pinessi, I., Pollen, L., Polinsky, D., Nee, R., Kennedy, L., Macciardi, J., Rogaeva, F., Liang, E., Alexandrova,

Y., Lukiw, N., Schlumpf, W., and Tanzi, K.R. (1992) Genetic evidence for a novel familial Alzheimer's disease locus on chromosome 14. *Nature Genet.* **2:** 330-334.

Stein, I., Itin, A., Einat, P., Skaliter, R., Grossman, Z., and Keshet, E. (1998) Translation of vascular endothelial growth factor mRNA by internal ribosome entry: implications for translation under hypoxia. *Mol Cell Biol.* **18:** 3112-3119.

Strittmatter, W.J., Weisgraber, K.H., Huang, D.Y., Schemechel, D., Saunders, A.M., and Roses, A.D. (1993) Binding of human liporpotein E to synthetic amyloid beta peptide: isoform-specific effects and implications for late onset AD. *PNAS, USA*, **90:** 8098-8102.

Strooper, B.D., Saftig, P., Craessaerts K., Vanderstichele H., Guhde, G., Annaert, W., Figura, K.V., and Leuven, F.V. (1998) Deficiency of presenilin-1 inhibits the normal cleavage of amyloid precursor protein. *Nature* **391:** 387-390.

Studier, F.W., Rosenberg, A.H., Dunn, J.J. and Dubendorf, J.W. (1990) Use of T7 RNA polymerase to direct expression of cloned genes. *Methods Enzymol.* **185:** 60-89.

Suzuki, N., Cheung, T.T., Cai, X.D., Odaka, A., Otvos, L., Eckman, C.J., Golde, T.E. and Younkin, S.G. (1994) An increased percentage of long amyloid beta protein

secreted by familial amyloid beta protein precursor (beta APP717) mutants. *Science* **264:** 1336-1340.

Tanzi, R.E., Gusella, J.F., Watkins, P.C., Bruns, G.A.P., St George-Hyslop, P.H., and Van Keuren, M.L. (1987) Amyloid β-protein gene: cDNA, mRNA distribution and genetic linkage near the Alzheimer locus. *Science*, **235:** 880-884.

Tsai, L.H., Delalle, I., Caviness, V.S.J., Chae, T. and Harlow, E. (1994) p35 is a neural-specific regulatory subunit of cyclin-dependent kinase 5. *Nature*, **371:** 419-423.

Tucker, R.P. (1990) The roles of microtubule-associated proteins in brain morphogenesis. *Brain Res. Rev.* **15:** 101-120.

Van Broeckhoven, C., Backhovens, H., Cruts, M., De Winter, G., Bruyland, M., Cras, P., and Martin, J.-J. (1992) Mapping of a gene predisposing to early-onset Alzheimer's disease to chromosome 14q24.3. *Nature Genet.* **2:** 335-339.

Vassar, R., Bennett, B.D., Babu-Khan, S., Kahn, S., Mendiaz, E.A., Denis, P., Teplow, D.B., Ross, S., Amarante, P., Loeloff, R., Luo, Y., Fisher, S., Fuller, J., Edenson, S., Lile, J., Jarosinski, M.A., Biere, A.L., Curran, E., Burgess, T., Louis, J-C., Collins, F.,

Treanor, J., Rogers, G. and Citron, M. (1999) β-Secretase cleavage of Alzheimer's amyloid precursor protein by the transmembrane aspartic protease BACE. *Science* **286:** 735-741.

Walter, J., Fluhrer, R., Hartung, B., Willem, m., Kaether, C., Capell, A., Lammich, S., Multhaup, G. and Haass, C. (2000) Phosphorylation regulates intracellular trafficking of β-secretase. *J.Biol. Chem.* **276:** 14634-14641.

Weisgraber, K. H., Roses, A.D., and Strittmatter, W.J. (1994) The role of apolipoprotein E in the nervous system. *Curr. Opin. Lipidology* **5:** 110-116.

Whitehouse, P. J., Price, D. L., Struble, R. G., Clark, A. W., Coyle J. T. and Delong. M. R. (1982) Alzheimer's dosease and senile dementia: Loss of neurons in the basal forebrain. *Science* **215:** 1237-1239.

Wolfe, M.S., Weiming, X., Ostaszewski, B.L., Thekla, S. D., Kimberly, W.T., and Selkoe, D.J. (1999) Two transmembrane aspartates in presenilin-1 required for presenilin endoproteolysis and γ-secretase activity. *Nature* **398:** 513-517.

Wood, J.G., Mirra, S.S., Pollock, N.J., and Binder, L.I. (1986) Neurofibrillary tangles of Alzheimer disease share antigenic determinants with the axonal

microtubule-associated protein tau. *Proc. Natl. Acad. Sci. (USA)* **83:** 4040-4043.

Xiang, Y., Molloy, S.S., Thomas, L. and Thomas, G. (2000) The PC6B cytoplasmic domain contains two acidic clusters that direct sorting to distinct *trans*-Golgi network/endosomal compartments. *Mol. Biol. Cell* **11:** 1257-1273.

Yamaguchi H., Ishiguro K., Uchida T., Takashima A., Lemere C.A and Imahori K. (1996) Preferential labeling of Alzheimer neurofibrillary tangles with antisera for tau protein kinase (TPK) I/glycogen synthase kinase-3 beta and cyclin-dependent kinase 5, a component of TPK II. *Acta. Neuropathol. (Berl.)* **92:** 232-241.

Yan, R., Bienkowski, M.J., Shuck, M.E., Miao, H., Tory, M.C., Pauley, A.M., Brashler, J.R., Stratman, N.C., Mathews, W.R., Buhl, A.E., Carter, D.B., Tomasselli, A.G., Parodi, L.A., Heinrikson, R.L. and Gurney, M.E. (1999) Membrane-anchored aspartyl protease with Alzheimer's disease β-secretase activity. *Nature* **402:** 533-537.

Yamazaki, T. and Ihara, Y. (1998) Effects of specific protease inhibitors on amyloid beta-protein 42 secretion. *Neurobiol Aging* **19:** S77-9.

Yanker, B.A. (1996) Mechanisms of neuronal degeneration in Alzheimer's disease. *Neuron* **16:** 921-932.

Younkin, S.G. (1998) The role of A beta 42 in Alzheimer's disease. *J. Physiol (Paris)* **92:** 289-292.

Appendix

A1 Vector circle maps of pBluescript II-, pCDNA3, pCDNA4HisMax, pRSET

A2 Primer lists

A3 Chemical structure of fluorophore and quench used in fluorometric assay

Appendix

A1 Vector circle map

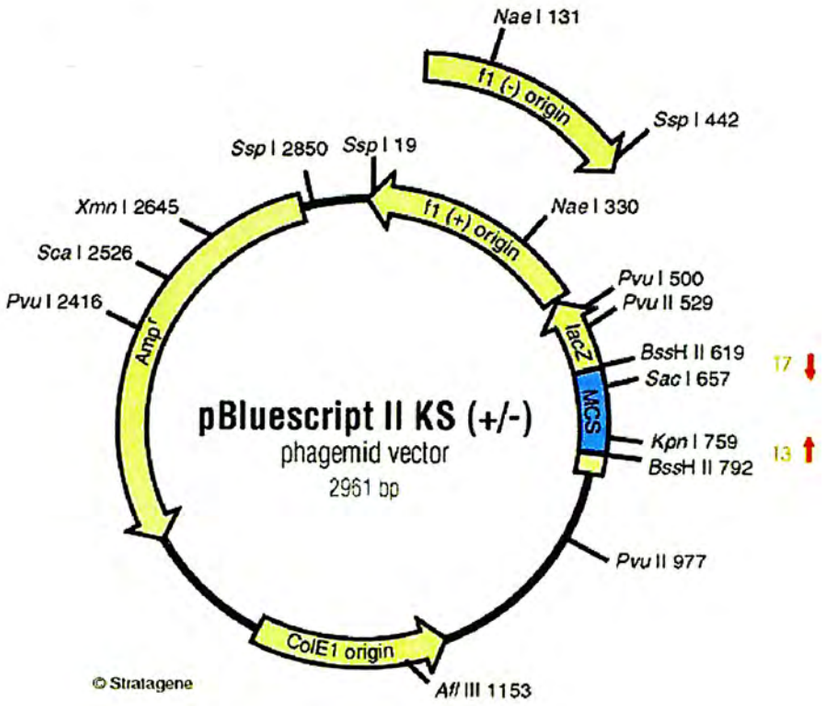

pBluescript II KS (+/–) Multiple Cloning Site Region (sequence shown 598–826)

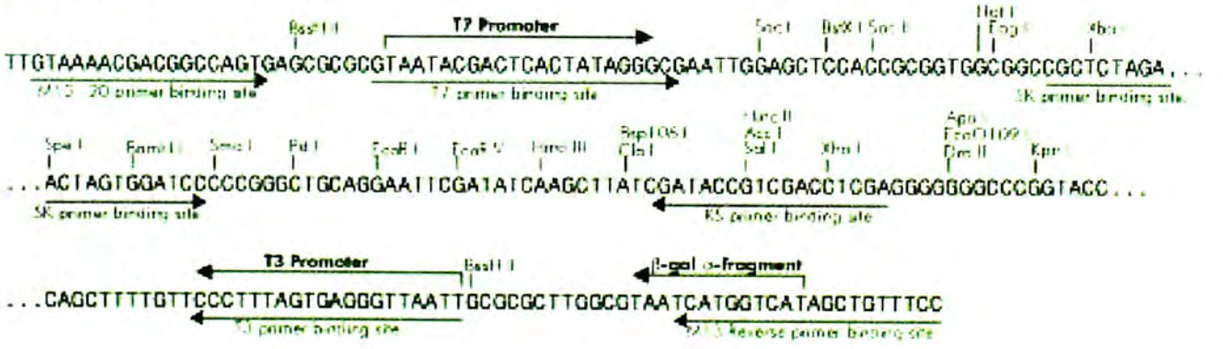

Fig. A1-1 Vector circle map of pBluescript KS II-

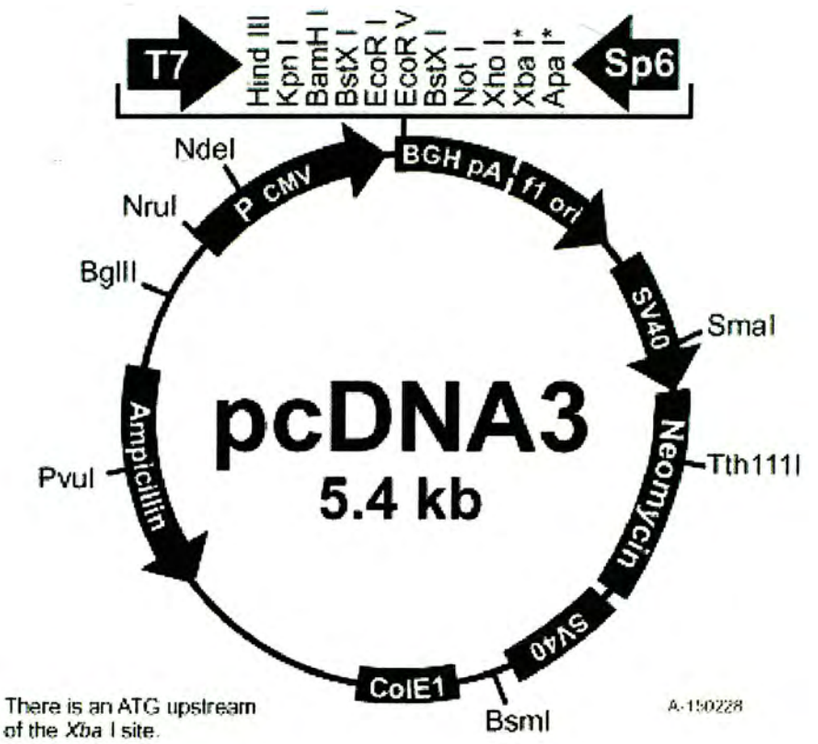

putative transcriptional start — T7 promoter

824 GCTAACTAGA GAACCCACTG CTTACTGGCT TATCGAAATT AATACGACTC ACTATAGGGA

Hind III — Kpn I — BamH I — Bst XI — Eco R I

884 GACCCAAGCT TGGTACCGAG CTCGGATCCA CTAGTAACGG CCGCCAGTGT GCTGGAATTC

Eco R V — Bst X I — Not I — Xho I — Xba I — Apa I

944 TGCAGATATC CATCACACTG GCGGCCGCTC GAGCATGCAT CTAGAGGGCC CTATTCTATA

Sp6 promoter

1004 GTGTCACCTA AATGCTAGAG CTCGCTGATC AGCCTCGACT GTGCCTTCTA GTTGCCAGCC

1064 ATCTGTTGTT TGCCCCTCCC CCGTGCCTTC CTTGACCCTG GAAGGTGCCA CTCCCACTGT

BGH polyA

1124 CCTTTCCTAA TAAAATGAGG AAATTGCAT

Fig. A1-2 Vector circle map of pCDNA3

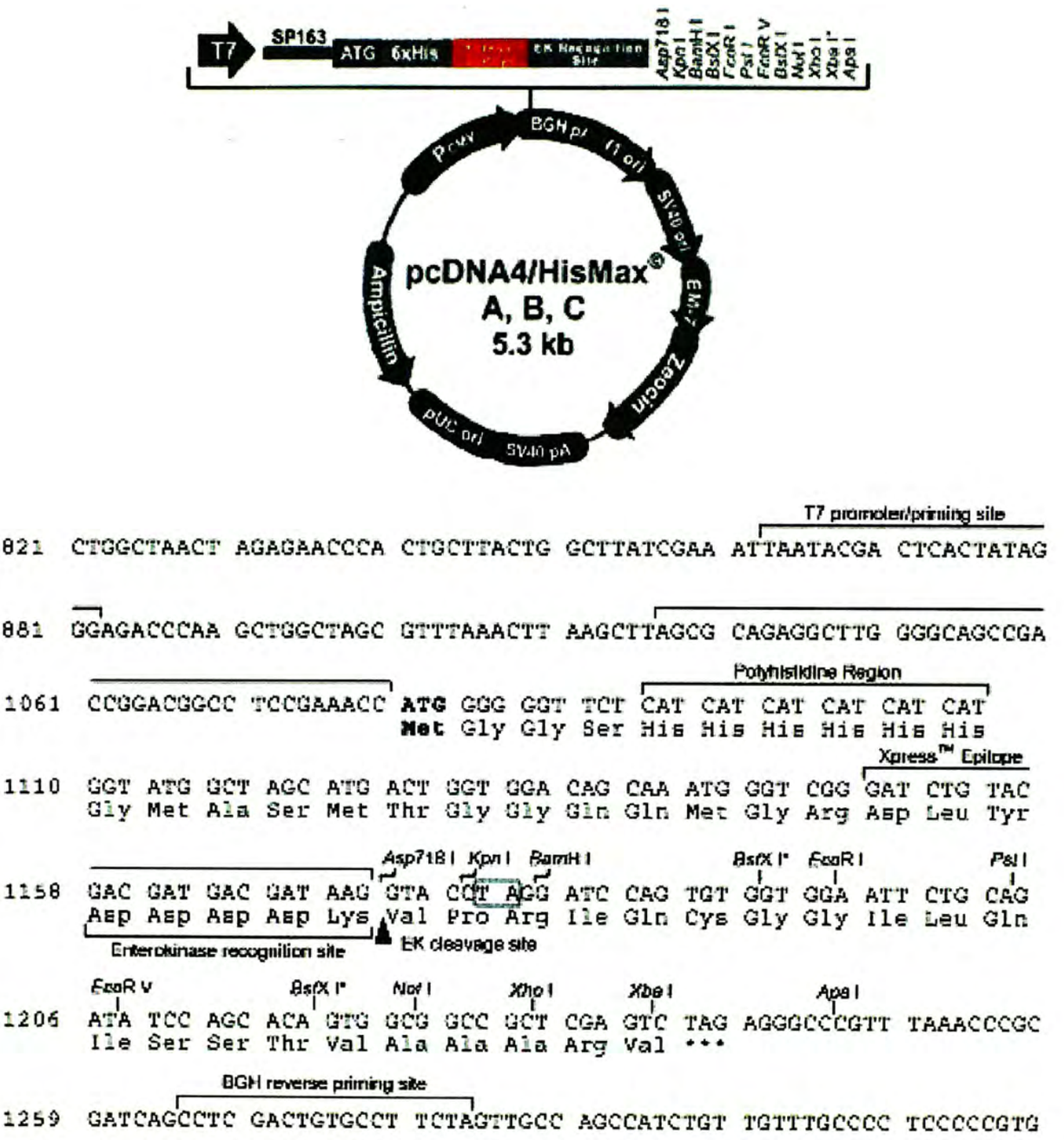

Fig. A1-3 Vector circle map of pCDNA4HisMax

Fig. A1-4 Vector circle map of pRSET

A2 Primer lists

1. Full length human BACE forward PCR primer with EcoRI site (hBACE_448F)

   5'-GTG AAT TCC CAC CAT GGC CCA AGC C-3'

2. pro hBACE forward PCR primer with XhoI site (hBACE_517F)

   5'-CGC TCG AGA CCC AGC ACG GCA TCC G-3'

3. nohBACE forward PCR primer with XhoI site (hBACE_589F)

   5'-GGC TCG AGA CCG ACG AAG AGC CCG-3'

4. prohBACE and nohBACE reverse PCR primer with EcoRI site (hBACE_R1833)

   5'-GCG AAT TCA ATA GGC TAT GGT CAT GAG-3'

5. Full length human BACE reverse PCR primer with XhoI site (hBACE_R1946)

   5'-GCC TCG AGG GCC TCC TCA CTT CAG CAG GG-3'

6. Full length mouse BACE forward PCR primer with EcoRI site (mBACE_423F)

   5'-GCG AAT TCC TCA CTA TGG CCC CGG-3'

7. Full length mouse BACE reverse PCR primer with XhoI site (mBACE_R1940)

   5'-GGC TCG AGG CCT CCT TAC TTC AGC AG-3'

8. nomBACE forward PCR primer with NheI site (mBACE_147F)

   5'-CTG GCT AGC GAG ACG GAC GAG GAA T-3'

9. nomBACE forward PCR primer with EcoRI site (mBACE_R1382)

   5'-GCG AAT TCT TAG GTC ATA AGT GTT GAC-3'

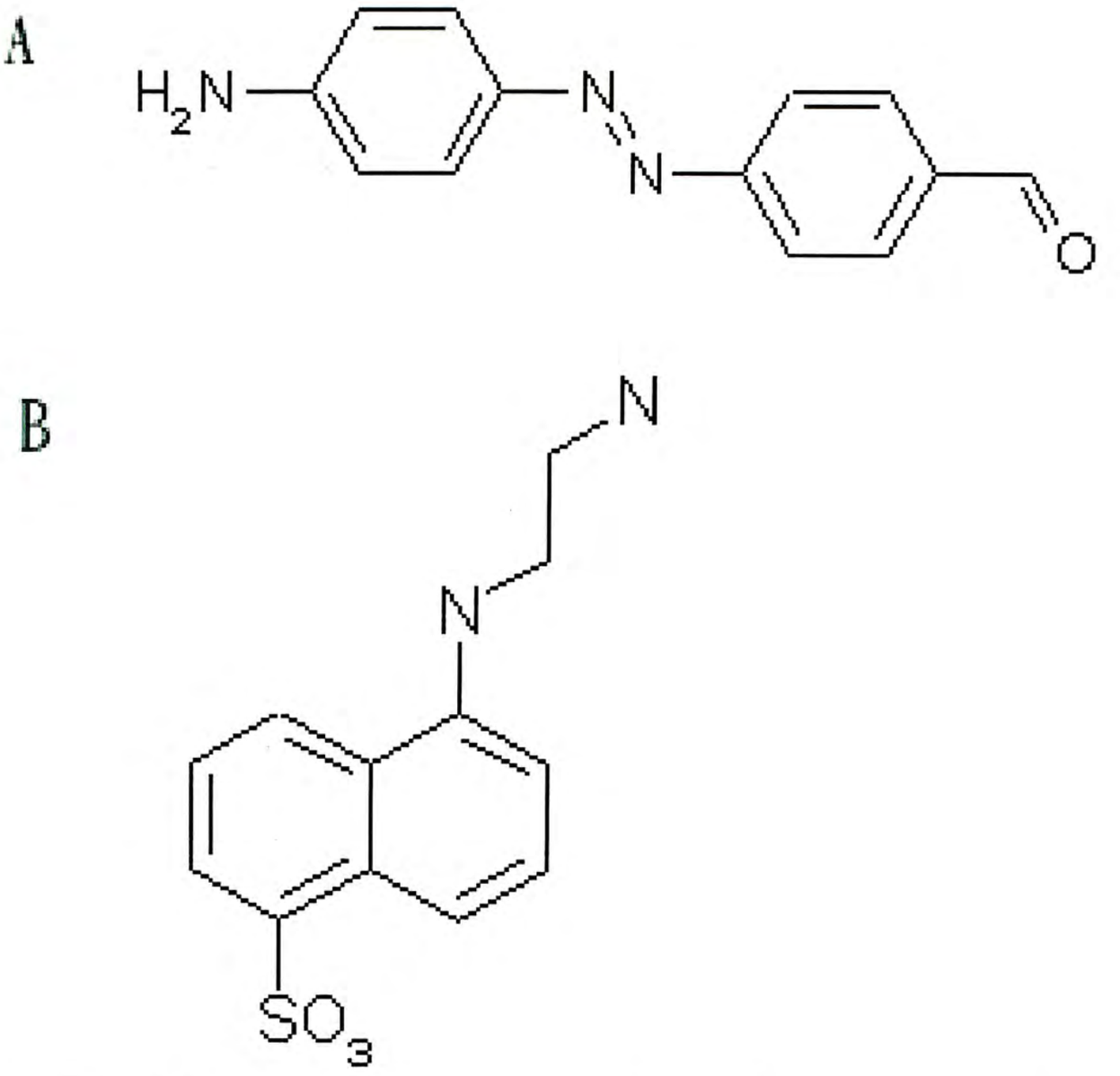

Fig. A3 Chemical structure of fluorophore and quench used in fluorometric assay. (A) Chemical structure of quench, DABCYL. (B) Chemical structure of fluorophore, EDANS.

CUHK Libraries
003955798